



UNIVERSITEIT VAN PRETORIA
UNIVERSITY OF PRETORIA
YUNIBESITHI YA PRETORIA

**Shape analysis of the zygoma to assess ancestry and sex variation
in modern South Africans**

by

Samantha Muller

Submitted in fulfilment of the requirements for the degree,

Master of Science (Anatomy)

In the

Faculty of Health Sciences

Department of Anatomy

University of Pretoria

2020

DECLARATION

University of Pretoria

DECLARATION OF ORIGINALITY

This document must be signed and submitted with every essay, report, project, assignment, dissertation and / or thesis.

Full names of student: **Samantha Muller**

Student number: **14048796**

Declaration:

I understand what plagiarism is and am aware of the University's policy in this regard. I declare that this **dissertation** (eg essay, report, project, assignment, dissertation, thesis, etc) is my own original work. Where other people's work has been used (either from a printed source, Internet or any other source), this has been properly acknowledged and referenced in accordance with departmental requirements. I have not used work previously produced by another student or any other person to hand in as my own. I have not allowed and will not allow anyone to copy my work with the intention of passing it off as his or her own work.

SIGNATURE OF STUDENT:



ABSTRACT

Skeletal remains exposed to an outdoor context are prone to post-mortem damage and fragmentation, making skeletal analysis difficult for the anthropologist. Research on ancestry and sex from isolated fragments of the cranium is necessary to improve identification of fragmented remains. The zygoma has proven to be more durable post skeletonization than other cranial bones, making research relevant into variation within the zygoma. Whilst the shape of the zygoma has been studied in a South African population using morphological, metric and geometric morphometric techniques, these studies did not include Indian South Africans. The Indian South African population comprises 2.6% of the total population but make up a larger proportion of the population in certain areas. For example, Indian South Africans comprise 7.4% of the population in Kwa-Zulu Natal and 2.9% in Gauteng. More specifically, Indian South Africans make up to 60% of the population in the suburb of Chatsworth with a further 91% of the population in sub-area of Arena Park, and 80% of the population in the Laudium suburb of Gauteng. Therefore, Indian South Africans must be included in anthropological studies attempting ancestry classifications. The purpose of the study was to assess the shape variation and projection of the zygoma attributable to sexual dimorphism and ancestral variation among South Africans, including Indian South Africans, using a geometric morphometric approach.

A sample of 400 three-dimensionally (3D) reconstructed models from head CT scans of black, coloured, white, and Indian South Africans were used with an equal sex and ancestry distribution. Eleven landmarks previously described in the literature were used for the analysis. Each landmark was used to depict the most prominent points on the outline of the zygoma. Additionally, semi-landmarks were placed along the curves of the zygoma. The landmarks and semi-landmarks were tested for observer repeatability and reliability using dispersion analysis and revealed that all landmarks were repeatable. Procrustes ANOVA revealed significant differences among the population groups and between the sexes for all population groups, except between coloured South African males and females. A pairwise post-*hoc* test revealed that white and Indian South Africans had the most similarities except for males, where coloured and Indian South Africans had the most similarities for landmarks.

Three interlandmark distances were created to assess the zygoma's projection. The ANOVA for the projection of the zygoma revealed significant differences for both sex and ancestry except for white South African males and females and males overall for the

zygomaticomaxillary length. The zygomaticomaxillary length (ZML) is defined as the maximum distance between the landmarks *zygoorbitale* and *zygomaxilare*. No significant differences were noted for female South Africans for the Superior Zygomatic Length which, is a measure of the maximum length of the superior margin of the zygoma (between *porion* and *zygoorbitale*; PorZygool). Further analysis of the zygoma's projection involved creating angles between the interlandmark distances. The ANOVA for the angles of projection revealed significant differences between sexes and populations, except for white and Indian South African males and females at *Angle1* (Angle at the intersection of ZML and *PorZygool*) and *Angle3* (the angle at the intersection of *PorZygool* and *PorZygool*) and black, coloured and Indian South African males and females at *Angle2* (the angle at the intersection of ZML and *PorZygool*).

The large amount of overlap amongst ancestry groups demonstrated substantial group similarities; however, differences were noted at the zygomaticomaxillary, zygomaticotemporal and frontomalar sutures. Overlap was also present between males and females, but on average, males were larger than females. Differences, such as a more inferior placement of the *zygoorbitale* landmark were noted at the inferior margin of the orbit specifically in females. Differences were also noted at the inferior margin of the orbit across all groups. Discriminant functions were created to assess the classifying ability of the shape of the zygoma. Results revealed low accuracies for ancestry classification for the shape and projection of the zygoma. However, higher accuracies were noted for sex classification for the shape and projection of the zygoma.

While results demonstrate shape variation of the zygoma, the classifying ability of the zygoma is precarious at best, and the use of the zygoma in a forensic context may not be an option. However, the differences observed can be taken into consideration during medical procedures such as zygomatic and infraorbital implants. Although landmark placements were reliable and repeatable, further analysis of the zygoma using a semi-automatic surface registration method along with different imaging techniques (MicroCT and CBCT scans) may assist in the data collection procedure and may potentially increase the accuracy of the results. Furthermore, the results of the current study highlight the need for the assessment of the effects of diet, climate, age, edentulism and symmetry on the shape of the zygoma.

Keywords: Zygoma, Sex, Ancestry, Indian South Africans, Geometric Morphometrics, Shape, Landmarks, Semi-Landmarks, Projection, Angles.

ACKNOWLEDGEMENTS

What a journey writing this thesis has been. The journey has been a rollercoaster that has taught me valuable lessons along the way. None of the research would have been possible without the numerous individuals who contributed both academically and emotionally. Thank you to my supervisors, Gabriele C Krüger and Leandi Liebenberg, for providing me with amazing support. Thank you for the endless random conversations, the inside jokes and for helping me calm down when I was overwhelmed. Thank you for imparting your knowledge and for always pushing me to be a better researcher. I will forever be grateful to you both. I would like to acknowledge and thank Dr Jean Dumoncel for his endless help with running my statistics and fixing problems along the way. None of my results would have been possible without your help and guidance and for that I thank you. I would also like to acknowledge the NRF for the generous funding awarded to me. A big thank you to my family for always supporting me, from my undergraduate years until this moment. Thank you for putting up with the stress that goes along with writing a thesis and for letting me vent my frustrations. Lastly, a huge thank you to the love of my life, Wesley Drew. Thank you for pushing me to keep going even when I did not want to, for dealing with the tears and frustration and for always encouraging me to ask for help. You are my rock, and I cannot thank you enough.

TABLE OF CONTENTS

DECLARATION	i
ABSTRACT.....	ii
ACKNOWLEDGEMENTS	iv
LIST OF TABLES	vii
LIST OF FIGURES	x
CHAPTER 1: INTRODUCTION	1
CHAPTER 2: LITERATURE REVIEW	5
2.1. The Concept of Race	5
2.2. Population History of South Africa.....	6
2.3. Anatomy and Ontogeny of the Zygoma.....	9
2.4. Sexual Dimorphism of the Cranium.....	11
2.5. Sexual Dimorphism of the Zygoma	13
2.6. Ancestral Variation of the Zygoma.....	15
2.7. Projection of the Zygoma.....	17
2.8. Geometric Morphometrics in Anthropology.....	21
2.9. Computed Tomography in Anthropology	22
CHAPTER 3: MATERIALS AND METHODS	24
3.1. Sample.....	24
3.2. Procedure.....	25
3.2.1. Model Processing, Landmark Placement and Data Preparation	25
3.3. Statistics	27
3.3.1. Intra- and Inter-observer Repeatability	27
3.3.2. Significance Test.....	28
3.3.3. Principal Components Analysis.....	28
3.3.4. Linear Discriminant Analysis	29

3.3.5. <i>Analysis of the Projection of the Zygoma</i>	30
CHAPTER 4: RESULTS	33
4.1. Intra- and Inter-observer Error	33
4.2. Sexual Dimorphism.....	34
4.3. Ancestral Variation	43
4.4. Projection of the Zygoma.....	56
4.4.1. <i>Interlandmark Distances</i>	56
4.4.2. <i>Angle of Projection</i>	60
CHAPTER 5: DISCUSSION.....	66
5.1. Shape Variation of the Zygoma	66
5.2. Forensic Application of the Zygoma.....	71
5.3. Future Recommendations.....	73
REFERENCES	78
APPENDIX.....	95
Appendix I.....	95
Appendix II	104

LIST OF TABLES

Table 3.1. Distribution and source of sample.	24
Table 4.1. Mean dispersion error (mm) of manual landmark placements.	33
Table 4.2. Mean dispersion error (mm) of semi-landmark placements.	33
Table 4.3. Mean dispersion error (mm) of individual manual landmark placements.	34
Table 4.4. Results of the Procrustes ANOVA test (1000 permutations) of the landmarks and semi-landmarks showing significant differences of the sex and ancestry of the zygoma. Bold p-values indicate significant differences.	34
Table 4.5. Results of the Procrustes ANOVA test (1000 permutations) demonstrating whether a significant degree of sexual dimorphism is present from the landmarks and semi-landmarks amongst the population groups for the zygoma. Bold p-values indicate significant differences.	35
Table 4.6. LDA classification matrix when estimating sex from landmarks. Bold indicates highest accuracy obtained.	42
Table 4.7. LDA classification matrix when estimating sex from semi-landmarks. Bold indicates highest accuracy obtained.	43
Table 4.8. Results of the Procrustes ANOVA test for landmarks and semi-landmarks showing significant differences between female and male of the zygoma. Bold p-values indicate significant differences.	43
Table 4.9. Results of the pairwise post-hoc test to assess where population differences occurred. Bold indicates largest values.	44
Table 4.10. Classification matrix for estimating ancestry using set landmarks. Bold indicates highest accuracy obtained.	54
Table 4.11. Classification matrix for estimating ancestry using semi-landmarks. Bold indicates highest accuracy obtained.	55
Table 4.12. A summary of the descriptive statistics for the three interlandmark distances comparing both ancestry and sex. n = number of individuals; SD = Standard deviation. .	56
Table 4.13. p-values for the ANOVA test showing significant differences of the interlandmark distances in combined sex and ancestry of the zygoma. Bold indicates significant differences.	57
Table 4.14. ANOVA results showing significant differences of the interlandmark distances between the population groups to test for sexual dimorphism of the zygoma. Bold indicates significant differences.	57

Table 4.15. p-values for the ANOVA test showing significant differences of the interlandmark distances between females and males of the zygoma. Bold indicates significant differences.	58
Table 4.16. Breakdown of group overlap for interlandmark distances based on ANOVA and Tukey’s HSD. B = Black; C = Coloured; W = White; I = Indian.	59
Table 4.17. Classification matrix for estimating sex from interlandmark distances. Bold indicates highest accuracy obtained.	59
Table 4.18. Classification matrix for estimating ancestry from interlandmark distances. Bold Indicates highest accuracy obtained.	60
Table 4.19. Angles of projection for ancestry when sexes were pooled and separated (°). Bold indicates largest mean.....	61
Table 4.20 Angles of projection for the sexes when populations were pooled (°).	61
Table 4.21. p-values for the ANOVA test showing significant differences of the angles in sex and ancestry. Bold indicates significant differences.	62
Table 4.22. ANOVA results showing significant differences of the angles of projection between the different population groups to test for sexual dimorphism. Bold indicates significant differences.....	62
Table 4.23. p-values for the ANOVA test showing significant differences of the angles of projection between females and males. Bold indicates significant differences.	62
Table 4.24. Breakdown of group overlap for angles of projection based on ANOVA and Tukey’s HSD. B = Black; C = Coloured; W = White; I = Indian.	63
Table 4.25. Classification matrix for estimating sex from angles of projection. Bold indicates highest accuracy obtained.....	64
Table 4.26. Classification matrix for estimating ancestry from the angles of projection. Bold indicates highest accuracy obtained.	65
Table A1. Landmarks used for the analysis.....	95
Table A2. Loadings associated with PC1 and PC2 for all landmarks to assess sexual dimorphism. Bold values indicate landmarks with the largest contribution.	96
Table A3. Loadings associated with PC1 and PC2 for all landmarks to assess sexual dimorphism of black South Africans. Bold values indicate landmarks with the largest contribution.....	97
Table A4. Loadings associated with PC1 and PC2 for all landmarks to assess sexual dimorphism of coloured South Africans. Bold values indicate landmarks with the largest contribution.....	98

Table A5. Loadings associated with PC1 and PC2 for all landmarks to assess sexual dimorphism of white South Africans. Bold values indicate landmarks with the largest contribution.....99

Table A6. Loadings associated with PC1 and PC2 for all landmarks to assess sexual dimorphism of Indian South Africans. Bold values indicate landmarks with the largest contribution..... 100

Table A7. Loadings associated with PC1 and PC2 for all landmarks to assess ancestral variation. Bold values indicate landmarks with the largest contribution. 101

Table A8. Loadings associated with PC1 and PC2 for all landmarks to assess ancestral variation of male South Africans. Bold values indicate landmarks with the largest contribution. 102

Table A9. Loadings associated with PC1 and PC2 for all landmarks to assess ancestral variation of female South Africans. Bold values indicate landmarks with the largest contribution. 103

LIST OF FIGURES

Figure 2.1. Post-natal growth of the Zygoma (superior view).....	10
Figure 2.2. Right zygoma indicating features.....	10
Figure 2.3. Image showing a normal zygoma, left, and an os japonicum, right.....	11
Figure 2.4. Vitek’s technique used to score zygomatic projection.....	19
Figure 2.5. Bass’s (1995) technique used to score zygomatic projection.....	19
Figure 3.1. Anterior (left) and lateral (right) views of the skull demonstrating the landmarks used.....	26
Figure 3.2. Lateral View of the skull showing the interlandmark distances taken to assess the projection of the zygoma.	31
Figure 3.3. Figure showing the angles between the interlandmark distances.....	32
Figure 4.1. PCA plot and wireframe graph (anterior view) depicting the mean shape between males and females (combined ancestry) for set landmarks.	36
Figure 4.2. PCA plot and wireframe graph (anterior view) depicting the mean shape between males and females (combined ancestry) for semi-landmarks.....	36
Figure 4.3. PCA plot and wireframe graph depicting the mean shape between black male and female South Africans for set landmarks.	37
Figure 4.4. PCA plot and wireframe graph depicting the mean shape between black male and female South Africans for semi-landmarks.....	37
Figure 4.5. PCA plot and wireframe graphs (anterior view) depicting the mean shape between coloured male and female South Africans for set landmarks.....	38
Figure 4.6. PCA plot and wireframe graphs(anterior view) depicting the mean shape between coloured male and female South Africans for semi-landmarks.	39
Figure 4.7. PCA plot and wireframe graphs (anterior view) depicting the mean shape between white male and female South Africans for set landmarks.....	40
Figure 4.8. PCA plot and wireframe graphs(anterior view) depicting the mean shape between white male and female South Africans) for semi-landmarks.	40
Figure 4.9. PCA plot and wireframe graphs (anterior view) depicting the mean shape between Indian male and female South Africans for set landmarks.....	41
Figure 4.10. PCA plot and wireframe graphs(anterior view) depicting the mean shape between Indian male and female South Africans) for semi-landmarks.....	41
Figure 4.11. PCA plot showing ancestral variation (sexes pooled; set landmarks left, semi-landmarks right).....	46

Figure 4.12. Wireframe graphs showing ancestral shape differences of the zygoma (sex combined; set landmarks left, semi-landmarks right).	47
Figure 4.13. PCA plot showing ancestral variation (males; set landmarks left, semi-landmarks right).	49
Figure 4.14. Wireframe graphs showing ancesral shape differences of the zygoma (males; set landmarks left, semi-landmarks right).	50
Figure 4.15. PCA plot showing ancestral variation (females; set landmarks left, semi-landmarks right).	52
Figure 4.16. Wireframe graphs showing ancestral shape differences of the zygoma (females; set landmarks left, semi-landmarks right).	53
Figure A1. Tukey’s HSD plots depicting statistically significant overlap between groups for ancestry when males and females were combined looking at PorZygoml (B = Black; C = Coloured; W = White; I = Indian).	104
Figure A2. Tukey’s HSD plots depicting statistically significant overlap between groups for ancestry when males and females were combined looking at ZML (B = Black; C = Coloured; W = White; I = Indian).	105
Figure A3. Tukey’s HSD plots depicting statistically significant overlap between groups for ancestry when males and females were combined looking at PorZygoool (B = Black; C = Coloured; W = White; I = Indian).	106
Figure A4. Tukey’s HSD plots depicting statistically significant overlap between groups for ancestry of male South Africans looking at PorZygoml (B = Black; C = Coloured; W = White; I = Indian).	107
Figure A5. Tukey’s HSD plots depicting statistically significant overlap between groups for ancestry of male South Africans looking at ZML (B = Black; C = Coloured; W = White; I = Indian).	108
Figure A6. Tukey’s HSD plots depicting statistically significant overlap between groups for ancestry of male South Africans looking at PorZygoool (B = Black; C = Coloured; W = White; I = Indian).	109
Figure A7. Tukey’s HSD plots depicting statistically significant overlap between groups for ancestry of female South Africans looking at PorZygoml (B = Black; C = Coloured; W = White; I = Indian).	110

Figure A8. Tukey’s HSD plots depicting statistically significant overlap between groups for ancestry of female South Africans looking at ZML (B = Black; C = Coloured; W = White; I = Indian).	111
112	
Figure A9. Tukey’s HSD plots depicting statistically significant overlap between groups for ancestry of female South Africans looking at PorZygoool (B = Black; C = Coloured; W = White; I = Indian).	112
Figure A10. Tukey’s HSD plots depicting statistically significant overlap between groups for ancestry when males and females were combined looking at Angle1 (B = Black; C = Coloured; W = White; I = Indian).	113
114	
Figure A11. Tukey’s HSD plots depicting statistically significant overlap between groups for ancestry when males and females were combined looking at Angle2 (B = Black; C = Coloured; W = White; I = Indian).	114
Figure A12. Tukey’s HSD plots depicting statistically significant overlap between groups for ancestry when males and females were combined looking at Angle3 (B = Black; C = Coloured; W = White; I = Indian).	115
116	
Figure A13. Tukey’s HSD plots depicting statistically significant overlap between groups for male South Africans when looking at Angle1 (B = Black; C = Coloured; W = White; I = Indian).	116
Figure A14. Tukey’s HSD plots depicting statistically significant overlap between groups for male South Africans when looking at Angle2 (B = Black; C = Coloured; W = White; I = Indian).	117
Figure A15. Tukey’s HSD plots depicting statistically significant overlap between groups for male South Africans when looking at Angle3 (B = Black; C = Coloured; W = White; I = Indian).	118
Figure A16. Tukey’s HSD plots depicting statistically significant overlap between groups for female South Africans when looking at Angle1 (B = Black; C = Coloured; W = White; I = Indian).	119
Figure A17. Tukey’s HSD plots depicting statistically significant overlap between groups for female South Africans when looking at Angle2 (B = Black; C = Coloured; W = White; I = Indian).	120

Figure A18. Tukey's HSD plots depicting statistically significant overlap between groups for female South Africans when looking at Angle3 (B = Black; C = Coloured; W = White; I = Indian). 121

CHAPTER 1: INTRODUCTION

The biological profile is an important aspect for biological anthropologists to estimate as the profile can help indicate a possible identity of a set of unknown remains (Klaes & Kenyhercz 2015). The biological profile involves the estimation of sex, stature, ancestry, and age-at-death (Spradley 2016a). However, the estimations of the parameters of the biological profile rely on the exploration and quantification of human skeletal variation within and among population groups and between the sexes (Krüger *et al.* 2018). In South Africa, identification of unknown individuals can become difficult as the unknowns may be illegal immigrants, have no identification documents, or be workers that have travelled from other provinces (Krüger *et al.* 2018). With these difficulties, alternative methods are being tested on the variation seen within the South African population to improve the estimation of the parameters of the biological profile and improve the identification of unknown persons (Krüger *et al.* 2018).

Mid-facial morphology has been the topic of much research in biological anthropology. For instance, nasal dimensions and climate have been strongly correlated and demonstrate differences among groups (Harvati & Weaver 2006). The zygoma plays a major role in cheek projection. The resultant cheek projection is a feature that has also been used to distinguish groups of people. A prominent cheek projection has been associated with Native American, and East Asian groups, and a limited projection of the cheek area has been associated with white North Americans (Gill *et al.* 1988; Stavrianos *et al.* 2012). Although cheek projection has been shown to have differences among population groups, the projection of the zygoma has not yet been explored, using more robust methodology, in a South African population and further research to quantify the differences in the zygomatic projection in the black, coloured, white and Indian South African populations is needed. Due to the inherent differences observed, the mid-face has also received a lot of attention in forensic anthropology focusing specifically on the estimation of ancestry. While most skeletal elements have been researched to explore sex and ancestry variations, the cranium is still the most commonly recovered skeletal element in forensic cases in South Africa, as the well-known shape makes it easily identifiable (Small *et al.* 2018). Fragmentary remains may also be recovered and further research on individual components of the cranium is needed and will have a significant forensic application.

The estimation of sex is an important parameter of the biological profile; however, a basic understanding of the genetic information that determines sex is important to understand skeletal

growth and sexual dimorphism. Furthermore, to describe any differences between males and females better, some terminology needs to be clarified. The term “gender” has often been used in past literature as a feature that can be estimated from skeletal remains. However, “gender” refers to a socially constructed designation of an individual. While the socially constructed designation is correlated to the biological features, in a modern society this can no longer be taken for granted (Walker & Cook 1998). In modern societies, multiple gender types exist that each have their own meaning, most of which do not correlate to the secondary sexual characteristics of the individual. The limited correlation of gender and physical appearance of an individual limits the use of “gender” to identify skeletal remains. Using the term “sex” is more descriptive, as it refers to the observable biological characteristics of an individual (Walker & Cook 1998).

The exploration of sexual dimorphism among modern black, coloured, and white South Africans has focused on size differences using multiple methodologies, such as morphological, morphoscopic and metric methods (Steyn & İşcan 1998; Krüger *et al.* 2015, 2017; Small 2016). Research on the sexual dimorphism of the skull has used morphological features or traditional landmarks, which are often not repeatable or limit the amount of shape variation that can be assessed because of the large error rates associated with the methodology (Monticelli & Graw 2008; Krüger *et al.* 2015; Muller 2018). Previous research on the sexual dimorphism of the zygoma, in particular, has used non-metric, metric and geometric morphometric methods. The geometric morphometric techniques used to assess the zygoma in previous studies, however, were not performed on a South African population or did not include Indian South Africans in the sample (Wilson-Taylor 2015; Tawha *et al.* 2020). Furthermore, the large error rates observed in studies of a morphoscopic and morphological nature warrant the exploration of a more repeatable and quantifiable approach to exploring shape variation in the zygoma among different populations of modern South Africans (Krüger *et al.* 2015; Muller 2018).

Similarly, the estimation of ancestry is required to evaluate the other parameters of the biological profile, such as stature, sex, and age-at-death (İşcan & Steyn 2013; Krüger *et al.* 2015). “Race” has traditionally been used to describe human variation. However, “race” is often associated with an effort to classify individuals into distinct groups based on typology, but the concept has been disputed as “race” is a consequence of more than just biological variation. Geographical background, cultural, and communal influences also play a role in the expression of human variation (White & Folkens 2005; L’Abbé *et al.* 2013a). The term ancestry is now used instead of “race” because the term allows for observable skeletal variation

to be linked to population groups and to move away from the negative connotation associated with the term “race”. In South Africa, individuals continue to classify themselves according to social race groups, for the purpose of redress in the post-*Apartheid* era (Posel 2001a; Liebenberg 2015). These social classifications are important when attempting to estimate ancestry from unknown remains.

The estimation of ancestry involves metric differences observed in the bones that are statistically linked to different population groups. Population groups of South Africa originate from different geographic locations where environmental and genetic contributions affected skeletal morphology; however, the metric differences observed today are also the result of endogamy following institutionalised racism and socio-political boundaries (L’Abbé *et al.* 2013a). Overlap between populations groups is expected as ancestry is a fluid concept due to variation within and amongst groups (Edgar & Hunley 2009).

Many ancestry estimation techniques presented in previous literature include either morphological descriptions of skeletal features or morphoscopic techniques, which involves the scoring of the expression of a certain feature or the scoring of a feature as present or absent (Hefner 2009; İşcan and Steyn 2013). While visual assessments of skeletal features are often used, osteometric and geometric morphometric (GM) techniques are often regarded as the more accurate of the methods as they are more repeatable and rely less on observer experience (Decker *et al.* 2011; Garvin & Ruff 2012; Spradley 2016a). To quantify the shape of the zygoma (the largest contributor to cheek projection), digitised landmarks can be used and assessed. Statistical analysis can determine whether sufficient variation is present in the zygoma, and whether the skeletal element can accurately estimate the ancestry of an unknown person. To assess ancestral variation of the zygoma among South Africans, a sample representative of the modern South African population is needed.

A lack of Indian South Africans in skeletal collections limits the exploration of variation among the South African populations. While Indian South Africans make up a small proportion of the total South African population (2.6%), in some Provinces and suburbs such as Kwa-Zulu Natal, the population consists of much larger proportions of Indian and Asian South Africans (7.4%; Statistics South Africa 2011). Furthermore, the suburb of Chatsworth comprises 60% Indian and Asian South Africans with a further 91% in Arena park, a sub area of Chatsworth (Frith 2011a, c). Laudium, a suburb in Gauteng comprises of 80% Indian and coloured South Africans (Frith 2011b). Additionally, a large proportion of South African Indians observe either

Hindu or Islamic religious practices and while the practices differ greatly between the two religions, one commonality is that remains of a decedent need to be returned to the family as soon as possible after death and may not be embalmed or modified, which includes accessioning the individual into skeletal collections (Burton & Underwood 2007; Mehta *et al.* 2015). Therefore, because of a lack of Indian South Africans in skeletal collections, this group has not yet been studied in South Africa and the lack of comparative samples for Indian South Africans makes accurately classifying individuals of Indian ancestry impossible.

While research on modern skeletons is possible in South Africa due to the vast number of skeletal collections available, many other countries have no modern skeletal collections to assess. However, in a South African context, Indian South Africans are an exception due to religious practices. To explore their populations, researchers of such countries have made use of several scanning modalities, such as computed tomography (CT), to study living individuals as research samples (Franklin *et al.* 2012, 2014; Decker *et al.* 2011; Mehta *et al.* 2014, 2015). The use of CT scans has many advantages and include that religious practices no longer affect samples because the individuals are still living. By making use of living individuals, the research samples are modern, not affected by secular trends, and represent the current population. Furthermore, the three-dimensional (3D) nature of reconstructed CT scans allows the skulls to be assessed for both size and shape using multiple techniques that include standard and non-standard linear measurements and geometric morphometrics (Dereli *et al.* 2018).

The aim of the study was to assess the shape variation of the zygoma using CT scans of modern black, coloured, white and Indian South Africans to provide more information on the current South African population and to help provide presumptive identifications for unknown individuals in forensic contexts. Additionally, the study also aimed to assess the variation in the zygoma's projection between the stated groups and sexes as a potential feature for assisting in the estimation of sex and ancestry. The aims were achieved by testing for significant differences between the shape of the zygoma among the population groups and between sexes as well as by testing for significant differences of the projection of the zygoma among the population groups and between sexes. The current study did not intend to discriminate between any population groups but aimed to assess the ancestral variation seen in the zygoma to aid in identification of individuals from skeletal remains.

CHAPTER 2: LITERATURE REVIEW

2.1. The Concept of Race

The concept of race has grown throughout the 20th century, influencing what is studied by anthropologists today. The term race was first introduced into society during the 15th century when the western world was discovered and classified individuals according to distinct characteristics such as skin colour, hair type, facial morphology and religion/culture (Brace 1995; McDowell 2012). However, the use of race brought about discrimination amongst groups as the concept was based on essentialism, biological determinism, and clades (Caspari 2003). The first classification system used to group individuals into distinct race groups was created by Linnaeus (1759), who grouped individuals into four main subspecies. The four subspecies were *Homo sapiens americanus*, *Homo sapiens africanus*, *Homo sapiens asiaticus*, and *Homo sapiens europeus* (Wheat 2009). Blumenbach then created a classification system in 1775 that comprised a single species called Caucasian. Blumenbach also described four other types called American, Mongolian, Ethiopian, and Malayan (Crawford 1868). However, the classification system did not take all human variation into account, and Blumenbach associated the variation with the mixing of the major groups (Crawford 1868).

By the 1800s, craniometric techniques were used to classify individuals into specific groups. Anders Retzius was considered the first to use craniometrics to calculate a cephalic index to classify individuals and coined the terms dolichocephalic and brachycephalic (Triarhou 2013). Dolichocephalic refers to a “long” skull where the breadth of the skull is less than 75% of the length of the skull. Brachycephalic refers to a “short” skull where the breadth of the skull is larger than 80% of the length (Crawford 1868). Cephalic indices have commonly been used to assess ancestral variation but have also been used to discriminate against groups by inferring intelligence and socioeconomic background from cranial size (Agarwal *et al.* 2014). Classifying individuals using discrete traits and univariate or bivariate craniometric techniques did not capture human variation in its entirety as it is a fluid concept and is present within and amongst populations (Edgar and Hunley 2009). Therefore, anthropologist moved from classifying according to discrete traits to a clinal view, where Livingstone (1962) argued that “there are no races, there are only clines” (Livingstone & Dobzhansky 1962, p. 279). Since then, a new view on the race concept has emerged and has been widely accepted by the anthropology community. The new view states that “there are no races, there are only populations” (Howells 1996, p. 103). The emerging view acknowledges that there is variation

within and amongst populations yielding massive overlap between groups and that the inherent variation is affected by language, culture, and geography (Edgar and Hunley 2009).

Gene flow and social boundaries have also affected the variation observed amongst populations, particularly in South Africa, where institutionalised racism during *Apartheid* led to segregation and a limitation on gene flow allowing for skeletal differences amongst the population groups (L'Abbé *et al.* 2013b). The field of anthropology has thus moved away from describing human variation as “race” and instead uses the term ancestry to describe any differences between individuals based on geographical origins (Ousley *et al.* 2009). However, anthropologists still estimate the ancestry of an individual, using statistics, to find out where the individual may have come from, thereby assisting in the identification process.

2.2. Population History of South Africa

The South African population was socially separated into race groups prior to the *Apartheid* era. However, the legal separation of groups only occurred once *Apartheid* began in 1948 and segregation was achieved by placing people into three major groups based on descent and physical characteristics described by the Population Registration Act 30 of 1950 (Posel 2001b). Individuals were divided into white, native (black), and coloured groups (non-white groups), where other groups such as Asians and Indians fell under either coloured or non-white South Africans (Posel 2001b). Individuals were classified during a census taken once the Population Registration Act 30 of 1950 was approved; however, the process did not come without issues. Officials conducting the census used subjectivity to group individuals. A classification could be appealed and changed if an individual thought that they were wrongly classified, but many people did not contest their classification (Posel 2001b). Individuals who did have their classification appealed did so to improve their living conditions and treatment as a racial hierarchy was present and certain races were treated better than others, such as white South Africans were treated better than black South Africans (Posel 2001b).

Midyear population statistics of South Africa for 2020 indicated the distribution of social race groups in South Africa. Black South Africans constituted the largest proportion of the population (80.8%), followed by coloured South Africans (8.8%), white South Africans (7.8%), and Indian South Africans and other Asian groups (2.6%) (Statistics South Africa 2020).

2.2.1. *Black South Africans*

The history of the black South African population dates to over 5000 years ago, where Bantu-speaking people from West Africa migrated to and finally settled in southern Africa during the first millennium AD (Newman 1995). Throughout the southward migration, the Bantu-speaking population further split into the cultural groups known throughout South Africa today, which include the Zulu, Swazi, Southern Sotho, Tswana, and Xhosa speaking groups (Newman 1995). Some gene flow occurred between the Bantu-speaking populations and the indigenous Khoi and San, but morphological and genetic differences are still noted between the populations (Herbert 1990; Liebenberg *et al.* 2015). Because of differences in environment as well as additional genetic components from the Khoi and San, black South Africans differ from their West African ancestors (Hiernaux 1966).

2.2.2. *Coloured South African's*

The South African coloured population established themselves during the late 19th century and is an admixed population group with ancestry that included genetic contributions from multiple parental groups such as the Khoi and San, Asian groups, European groups and Bantu-speaking groups (Adhikari 2005; de Wit *et al.* 2010; Patterson *et al.* 2010; Peterson *et al.* 2013). Indian, African and East Asian slaves were brought to the Cape Colony but could not keep their original identity. They married other slaves and the indigenous Khoi and San, leading to a group called the Cape Malays that kept this term until the *Apartheid* era where the group was renamed to coloured South Africans (Indian Council of World Affairs 2001).

The contribution of each parental group to the coloured population is highly sex-specific. For example, the Khoi and San contributed 60% of the total maternal genetic contribution, while Europeans contributed less than 5%. This is contrary to the paternal genetic contribution, where Europeans contributed over 32.5%, similar to the contribution of Khoi and San and Bantu-speakers combined (Quintana-Murci *et al.* 2010). The sex-specific genetic distribution indicates that the early European settlers interacted with the female Khoi and San about 350 years ago (Quintana-Murci *et al.* 2010). The complex distribution of the variation within the coloured South African population has made the population distinct yet somewhat similar to the other population groups within South Africa.

2.2.3. *White South Africans*

In 1652, Jan van Riebeeck arrived at the Cape of Southern Africa and started the colonisation of South Africa by giving settlers farm land and allowing them to become citizens (Beck 2000). The South African white population is dominated by Dutch ancestry along with other contributions from German, French and British populations (Thompson 2001; Greeff 2007). Since admixture occurred between the male settlers and the slaves in South Africa (Khoi and San, and Bantu-speaking South Africans), a proportion of the maternal genetic distribution of white South Africans is said to have been obtained from the Khoi and San and Bantu-speaking South Africans (Steyn & İşcan 1998; Greeff 2007).

2.2.4. *Indian South Africans*

The first Indians were brought to the South African Cape as slaves in 1653; however, a larger group of Indians from the eastern and southern parts of India only arrived in Natal after 1860 as indentured labourers to work on sugarcane farms (Bhat & Narayan 2010). The workers were given the option to return to India after their contracts ended. However, the majority of individuals had a better life in South Africa than the poverty that awaited them back in India and therefore stayed in South Africa to work. Other Indian populations relocated to South Africa, where majority came from the Gujarati region of India. The relocated Indians were termed “passenger” Indians as they relocated at their own expense during the 1880’s and 1890’s (Lemon 1990; Bhat 2010). Descendants of the “passenger” migrants now comprise about 30% of the Indian South African Population (Lemon 1990).

India has a magnitude of languages, religions and castes, which reflect in the populations now found in South Africa (Bhat and Narayan 2010). The differing origins among South African Indians have brought along different religions, cultures and languages within the Indian South African population group, namely Hindu, Tamil, and Muslim communities (Bhat and Narayan 2010). The South African Indian population is further divided into smaller groups known as Punjabi, Gujarati, Tamilian, and Sindhis (Bhat and Narayan 2010). The History, migration, and integration of the Indian population into South Africa has created a distinct population group that warrants investigation.

2.3. Anatomy and Ontogeny of the Zygoma

The zygoma forms part of the human craniofacial skeleton and is commonly referred to as the malar bone in mammals or the jugal bone in reptiles and birds (Dechow & Wang 2017; Gai *et al.* 2017; Márquez *et al.* 2017). The zygoma comprises three processes that articulate with other cranial bones to form part of the craniofacial complex, allows for the connection of the respiratory, masticatory and visual systems, and serves to connect the viscerocranium to the neurocranium (Heuzé *et al.* 2016; Márquez *et al.* 2017). The frontal process of the zygoma separates the temporal fossa from the orbit; the maxillary process forms the inferolateral surface of the orbit; and the temporal process joins the zygomatic process lateral to the temporal fossa (White & Folkens 2005b). The three processes join the zygoma to the temporal bone, the frontal bone, and the maxilla to form the zygomatic arch, the lateral margin of the orbit, and the inferior margin of the orbit, respectively (Gai *et al.* 2017).

The zygoma originates as three ossification centres that fuse during foetal development (White & Folkens 2005a). Growth of the zygoma occurs inferiorly and laterally by the deposition of bone on the lateral surface, inferior surface, and within the temporal fossa at the location of the posterior protuberance. Growth occurs as bone is resorbed on the anterior surface and deposited on the posterior surface (Enlow & Hans 1996; Oettlé *et al.* 2017). The resorption and deposition of bone causes the zygoma to enlarge posteriorly, to become displaced inferiorly when related to the frontomalar suture, and to become anteriorly displaced when associated with the zygomaticotemporal suture (Figure 2.1; Enlow & Hans 1996; Oettlé *et al.* 2017). Notable features of the zygoma include the zygomaticofacial foramen, the zygomaticotemporal foramen, the zygomatico-orbital foramina and the origin site of the masseter muscle that extends from the zygomaticomaxillary suture to the zygomaticotemporal suture (Figure 2.2; White & Folkens 2005a).



Figure 2.1. Post-natal growth of the Zygoma (superior view; Enlow & Bang 1965).

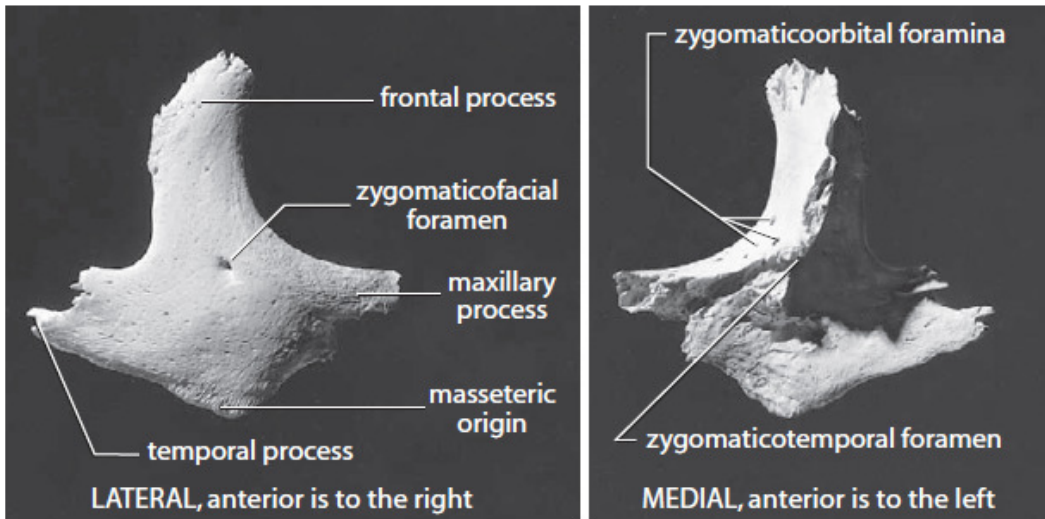


Figure 2.2. Right zygoma indicating features (White 2005b, p.116).

Additional sutures may be present on the zygoma, which results in the variation known as a bipartite zygoma or an *os japonicum* (Figures 2.3). The suture variations tend to extend dorsolaterally from the zygomaticomaxillary suture, thereby dividing the zygoma into more than one part (Wang & Dechow 2016). The *os japonicum* is seen more frequently in East Asians than any other geographical population, with Sub-Saharan Africans obtaining the second highest frequency (Hanihara *et al.* 1998).

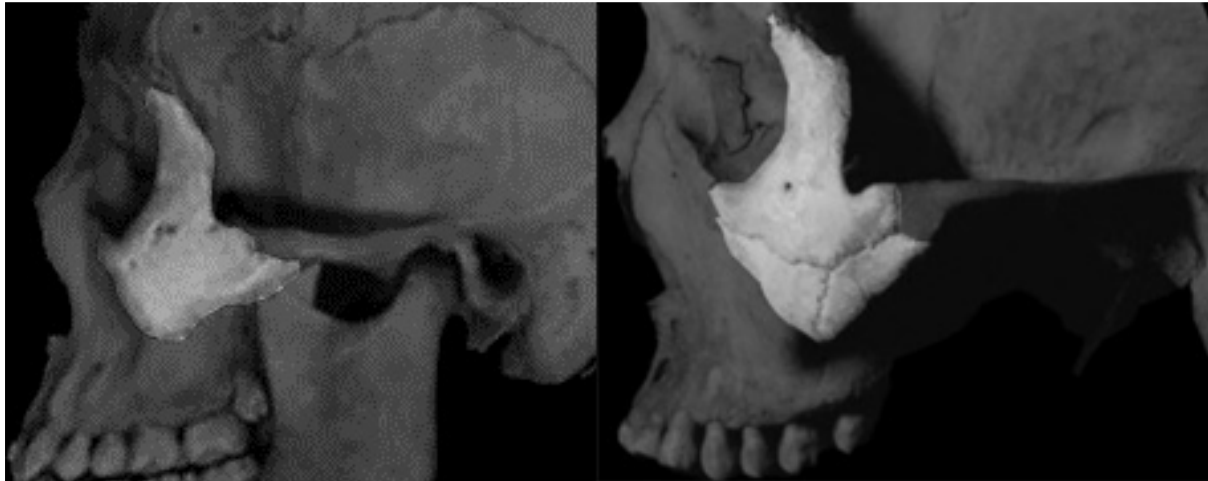


Figure 2.3. Image showing a normal zygoma, left, and an *os japonicum*, right (Hanihara *et al.* 1998; Caple & Stephan 2016).

2.4. Sexual Dimorphism of the Cranium

Sexual dimorphism refers to the shape and size differences between males and females. The inherent differences can be seen in the human skeleton and is studied by anthropologists to attain a biological profile. Sexual dimorphism is caused by the phenotypic expression of the underlying genes responsible for the determination of the sex of the individual. The X and Y chromosomes carry genes that determine whether an individual will express a male or female phenotype (Pierce 2014). Typically, when two X chromosomes are present, a female phenotype is expressed, whereas the presence of both an X and a Y chromosome produces a male phenotype (Pierce 2014). Once an individual reaches puberty the genes on the X and Y chromosomes generate the secondary sexual characteristics that are expressed physically in the soft tissue and the skeleton (Scheuer & Black 2004).

Sexual dimorphism differs amongst populations and is termed population-specific. (Saini *et al.* 2014). Therefore, sexual dimorphism needs to be assessed in different populations so that

population-specific standards can be created to aid in identification of unknown individuals (Saini *et al.* 2014). Different factors such as diet, climate, and genetics affect population variation, thus affecting sexual dimorphism. For example, white and black Americans showed varying degrees of sexual dimorphism of the face. Nasal and orbital height were the most discriminatory variables in white Americans, whereas nasion to prosthion height was more discriminatory for black Americans (Jantz & Moore-Jansen 1988). Differences between past and modern populations also indicate that secular changes affect the degree of sexual dimorphism. Saini *et al.* (2014) found differences between past and present populations of North Indians for the base of the cranium. Results of the study indicate that an improvement in nutrition and admixture amongst populations affected the degree of sexual dimorphism.

Age has been shown to influence the degree of sexual dimorphism (Kemkes & Göbel 2006). During adolescence, males have a longer and more intense maturation compared to females, allowing size and shape differences to be ascertained during analysis (Rogers 2005). Typically, the adolescent growth spurt occurs before the age of 13 years, where the growth of the craniofacial region slows for females and stops soon after but continues into adulthood for males (Rogers 2005). As the age of onset of maturation differs between males and females, differences can be noted in the cranium in areas that mature the latest (structures used during mastication). However, an area of particular interest is the midface, which undergoes maturation after the neurocranium but before the masticatory region, implying a smaller degree of sexual dimorphism in the midfacial region compared to the masticatory region (Humphrey 1998). Duration of growth differs from the onset of growth. Different systems of the human body start grow at different times (onset) and attain their adult size at different times (duration) (Humphrey 1998).

Morphoscopic and osteometric methods are common methods used to assess sexual dimorphism of the cranium. The Walker method (2008) is a morphoscopic technique used to assess one mandibular and four cranial traits associated with sexual dimorphism. The glabella, mental eminence, supraorbital margin, nuchal crest, and mastoid processes are assessed and scored using a scale from one to five, one being hyper-feminine, three being intermediate, and five being hyper-masculine (Walker 2008). Robust statistics are then used to estimate the sex of the individual based on the scores. While morphoscopic methods are commonly used to estimate sex, the approach does not come without disadvantages. Despite the inclusion of line drawings and trait definitions, there is still a degree of subjectivity associated with morphoscopic methods, and some user experience is required. To avoid some limitations

associated with morphoscopic techniques, osteometric or geometric morphometric methods can be used. Osteometrics and geometric morphometrics are considered more reliable and repeatable than morphological and morphoscopic methods and rely less on the observer's point of view (Decker *et al.* 2011; Garvin & Ruff 2012; Spradley 2016a).

2.5. Sexual Dimorphism of the Zygoma

While the methods mentioned have been used previously to assess the sexual dimorphism of the cranium, more in-depth research on the zygoma alone is needed to assess the sexual dimorphism present in the midface. There is evidence of inherent sexual dimorphism in the zygoma because of more intense and longer maturation rates in males compared to the maturation rates in females. The differing maturation rates have caused the zygoma to be larger and also more laterally displaced in males than in females (Rogers 2005). Rogers (2005) noted that the sexual dimorphism of the root of the zygoma is population-specific (i.e. ancestral differences) and is influenced by robusticity, which is seen in males and further explains why the root of the zygoma in males first extends towards the supra-mastoid crest and then continues past to the temporal line. The zygoma has also proven to be heavier in males compared to females (Caple & Stephan 2017).

Previous studies have assessed the use of various features of the cranium to estimate sex, including traits associated with the zygoma. Rogers (2005) investigated 17 cranial traits and found that the malar size and zygomatic extension achieved high accuracies for estimating sex (88%). A higher accuracy was achieved when all 17 traits were combined (89.1%) and indicated that using multiple traits performed better than when only a few traits were assessed (Rogers 2005). A morphoscopic study on German individuals assessed the zygomatic height, zygomatic process of the temporal bone and the surface structure of the zygoma to explore sexual dimorphism. While statistically significant differences were noted between the sexes for the three traits, the traits could not be used to reliably estimate sex (Monticelli & Graw 2008). Moreover, the researchers analysed the zygomatic process of the temporal bone that is not located on the zygoma. Further analysis on the temporal process of the zygoma may provide more information on the sexual dimorphism of the bone. While sexual dimorphism of the zygoma has been assessed using morphological and morphoscopic methods, the methods have not yet been validated on South Africans. Therefore, more robust analyses are needed to assess sexual dimorphism of the zygoma in this population.

Osteometric methods provide a more repeatable and reliable way of assessing sexual dimorphism. Multiple studies have been performed using linear measurements to assess the variation of the zygoma (Wilson-Taylor 2015; Muller 2018). Wilson-Taylor (2015) found that Southeast Asian and North American males were consistently larger than their female counterparts when the maximum width and height of the zygoma, and the maximum width of the frontal process were measured. The measurements could also be used to correctly classify individuals according to sex (Wilson-Taylor 2015). Similarly, Muller (2018) created measurements to assess the sexual dimorphism of the zygoma in black and white South Africans. Significant differences were noted for similar measurements to those used by Wilson-Taylor (2005), validating the methodology and indicating that sexual dimorphism is present at those points on the zygoma (Muller 2018). The South African results indicated a great classifying ability of the zygoma to estimate sex (89.2%). In addition to the measurements taken by Wilson-Taylor (2005), further measurements of the lateral margin of the orbit were included in the study by Muller (2018), as the zygoma forms a part of the lateral margin. Results showed no significant differences for the measurements of the lateral margin of the orbit indicating a small degree of sexual dimorphism. The results may be a consequence of the orbit maturing at an earlier age (Enlow 1990; Ferrario *et al.* 1993; Saini *et al.* 2011; Muller 2018). A further factor affecting the ability of the zygoma to estimate sex may be the number of measurements used. As Muller (2018) made use of more measurements than Wilson-Taylor (2005), more information on the sexual dimorphism of the zygoma was gathered, which may have resulted in the improved classification rates.

Sexual shape dimorphism of the zygoma is still a relatively new concept, and few studies have used a geometric morphometric approach to assess inherent shape differences and the associated classifying abilities. Results of a previous study showed that females had narrower zygomas as well as a greater elevation on the inferior border when compared to the zygomas of their male counterparts (Green & Curnoe 2009). A significant difference was observed in the zygomas of males and females, particularly in the surface shape, which has been shown to be more discriminatory when assessing sexual dimorphism. Results of geometric morphometric analyses of the zygoma predicted sex at rates of up to 70%, where males had lower correct classification rates than the females. Additionally, shape analysis has demonstrated that the zygomatic process is the least sexually dimorphic feature (Green & Curnoe 2009; Gonzalez *et al.* 2011; Schlager & Rüdell 2017; Small *et al.* 2018). Tawha *et al.* (2020) assessed the shape and size differences of the zygoma between males and females of

the South African population and found that the size of the zygoma attributed the most to sexual dimorphism. However, sample sizes were small, and unequally distributed. The Indian South African population was also not included in the sample demographics. Therefore, a further analysis of sexual dimorphism of the zygoma in the South African Indian population is needed to better understand the inherent variation within the population.

2.6. Ancestral Variation of the Zygoma

Ancestral variation of the morphology of the zygoma has been previously described in three broad geographic categories, namely Asian, European, and African, with each category encompassing multiple population groups (Oetlé *et al.* 2017). Individuals of European ancestry presented with zygomas that were less pronounced, with narrower and withdrawn zygomaticomaxillary, zygomaticotemporal and frontomalar sutures that curved more posteriorly (L'Abbé *et al.* 2011; Hefner 2009; Oetlé *et al.* 2017). Individuals of Asian ancestry presented with a large, inferiorly, laterally and posteriorly projecting zygomas that gave the face a flat appearance (Hamilton 2008; Oetlé *et al.* 2017). Asian population groups also showed more anteriorly projecting frontal processes of the zygomas and S-shaped zygomaticomaxillary sutures (Hanihara *et al.* 2000; Hefner 2009; Oetlé *et al.* 2017). Longer zygomatic processes of the maxillae were noted in Asian groups, causing the zygomatic arches to be less oblique (Novita 2006; Oetlé *et al.* 2017). African population groups presented with withdrawn zygomas and weaker projections of the zygomaticomaxillary tuberosities (L'Abbé *et al.* 2011; Baab *et al.* 2010; Oetlé *et al.* 2017). While the characteristics demonstrate differences amongst population groups, grouping ancestries together into major groups misses the smaller inherent differences. Further research on population groups specific to geographic region (i.e. black South Africans and black North Americans) could provide insight into the variation of the zygoma.

In 2011, L'Abbé and colleagues tested the macromorphoscopic traits proposed by Hefner (2009) for use in a South African sample. Results indicated differences between black, coloured, and white South Africans regarding the size of the malar tubercle and shape of the zygomaticomaxillary suture. The study showed that white South Africans lack a malar tubercle in the majority of the sample and that the zygomaticomaxillary suture shape usually had either an angled or a smooth shape (L'Abbé *et al.* 2011). Black South Africans in the sample most often presented with an incipient malar tubercle and a smooth zygomaticomaxillary suture shape. Similar to black South Africans, the majority of the coloured South Africans also presented with an incipient malar tubercle and a smooth zygomaticomaxillary suture shape.

The results of the L'Abbé *et al.* (2011) study were comparable to the findings by Hefner (2009) concerning the malar tubercle and zygomaticomaxillary suture shape observed in African and European populations. While Hefner (2009) noted that multiple traits should be scored to achieve an accurate ancestry estimate significant differences between the different ancestral groups on both continents were seen in the zygoma alone.

In South African biological anthropology, limited research on the zygoma is available and only morphological assessments have been used to examine the ancestral variation and the classifying ability of the bone. To overcome the lack of information on the ancestral variation of the zygoma in 2018, a study was performed to analyse the ancestral variation and classifying ability of the zygoma in a South African population using linear measurements (Muller 2018). Black and white South Africans were compared, and results showed that significant differences exist between white and black South Africans for most of the measurements used. The results also indicated that the linear measurements were able to correctly classify individuals according to ancestry with high accuracies (88.7%). However, while adequate results were obtained in the study, the limited population groups included in the sample necessitates additional research on populations such as coloured and Indian South Africans. This could provide a better understanding of the ancestral variation in modern South Africans.

Multiple studies have been performed using non-metric techniques to investigate the ancestral variation of the zygoma. However, few studies have relied on geometric morphometrics to assess the ancestral variation of the zygoma. Schlager and Rüdell (2017) employed geometric morphometrics to quantify the shape of the zygoma from CT scans of Chinese and German individuals. The results conclude that statistically significant shape differences exist between the two population groups in the zygoma (Schlager & Rüdell 2017). Additionally, geometric morphometrics has been used to quantify shape differences in the crania of modern black, coloured and white South Africans (Stull *et al.* 2014) The results indicate significant differences among the population groups; however, the number of landmarks on the zygoma are limited and thus does not capture the true amount of possible variation that may be present on the crania. The shape of the zygomaticomaxillary suture has also been studied amongst European, African, Native American, Asian, Aboriginal Australians and Arctic Circle populations using geometric morphometrics (Maddux *et al.* 2015). The shape of the suture was separated into three main types, namely 1) angled, where the suture extends inferolaterally so that the most inferior point is also the most lateral point when viewing the skull anteriorly; 2) curved, where the most lateral point is superior to the zygomaticomaxillary

anterior point; and 3) jagged or S-shaped, where there is more than one curve in the suture (Maddux *et al.* 2015). Angled sutures were noted for Native America and arctic populations, whereas African and Aboriginal Australians presented with a curved suture (Maddux 2015). However, when Asian and Europeans groups were assessed, equal distributions of the suture shapes were noted. The results indicate a possible link between the role of the zygomaticomaxillary suture and growth of the cranial facial region which, is in contradiction to the findings observed by Sholtz and Wärmländer (2012) who stated that a possible reason for the differences observed could be due to factors such as diet and activity patterns (Sholts & Wärmländer in press; Maddux 2015)..

Recently, the shape and size of the zygoma has been studied in a South African population (Tawha *et al.* 2020). Ancestral differences were not noted for the size of the zygoma; however, Bantu-speaking (black South Africans) individuals presented with narrow arches, smaller heights, and anteriorly projecting orbits (Tawha *et al.* 2020). Similarities were also noted between European (white South Africans) and Mixed population (coloured South Africans) groups, where the zygoma of both groups were elongated vertically (Tawha *et al.* 2020). While the findings of the study may provide further insight into the shape and size differences of the zygoma, population sample sizes were small. Compared to the linear measurements taken from similar groups in the South African population (Muller 2018), size differences were noted for both sex and ancestry. However, the differences between the studies could relate back to the methodologies used and sample size and distribution.

2.7. Projection of the Zygoma

Zygomatic projection has been used in forensic anthropology to distinguish between population groups (Cataldo-Ramirez *et al.* 2020). The projection of the zygoma, or the relative flatness of the midface, is described by the facial flatness index, which is calculated by dividing the bi-maxillary breadth by the zygomatic subtense (projection of the subspinale from bi-maxillary breath). A large value indicates a smaller projection of the zygoma, whereas a smaller value indicates a greater degree of projection of the zygoma (Raghavan *et al.* 2013; Oettlé *et al.* 2017). The zygomatic angle has also been used as an indicator of the projection of the zygoma. The zygomatic angle is formed by joining the right and left lines of the zygomatic anterior (the point where the masseter muscle attached to the zygomaticomaxillary suture) and the subspinale (the deepest point beneath the anterior nasal spine). The angle is then taken at the point where the lines meet at subspinale; results indicate the larger the angle, the flatter the maxillary area (Oettlé *et al.* 2017).

There have been attempts to assess the projection of the zygoma, each employing different methods (Rhine 1990; Bass 1995; Vitek 2012). Two methods have been described to score the projection of the zygoma: Vitek (2012) adapted the methodology used by Rhine (1990) so that the posterior angle and not the anterior angle was used (Rhine 1990; Vitek 2012). Rhine assessed the anterior projection of the zygoma by viewing the cranium in lateral view. He then made a line from the middle of the superior margin of the orbit down to the middle of the inferior margin of the orbit, thus creating an angle with the Frankfurt plane (Rhine 1990). However, because Rhine did not define the use of any device to measure the angle an, assumption can be made that the angle was “eyeballed” by the observer (Rhine 1990; Cataldo-Ramirez *et al.* 2020). Rhine’s method used three scores, namely vertical, retreating and projecting, and measured the anterior angle defined as the angle created where the Frankfurt plane and orbital line meet (Rhine 1990; Cataldo-Ramirez *et al.* 2020). As stated previously, Vitek (2012) then adapted the methodology used by Rhine (1990) by calculating the posterior angle created by the orbital margin and the Frankfurt plane (Figure 2.4; Vitek 2012). An angle less than 90° indicated a projecting zygoma, an angle of 90° indicated a vertical projection, while an angle over 90° indicated a retreating angle (Vitek 2012). Cataldo-Ramirez *et al.* (2020) employed the methodology used by Vitek (2012) to assess the projection of the zygoma (Cataldo-Ramirez *et al.* 2020). The second method used a pencil to indicate projection and was termed Bass’s (1995) method (Bass 1995). The pencil was placed horizontally across the nasal aperture while holding the cranium at the occipital region (Figure 2.5). Three scores were used to assess the projection of the zygoma using Bass’s (1995) methodology, namely projecting, retreating, and non-projecting (Bass 1995; Oettlé *et al.* 2017). However, both methodologies measured different variables indicating that zygomatic projection was difficult to define (Cataldo-Ramirez *et al.* 2020). Cataldo-Ramirez *et al.* (2020) also suggested that the methodology to assess zygomatic projection was highly subjective, proving that a more robust approach to assess the projection of the zygoma is needed.

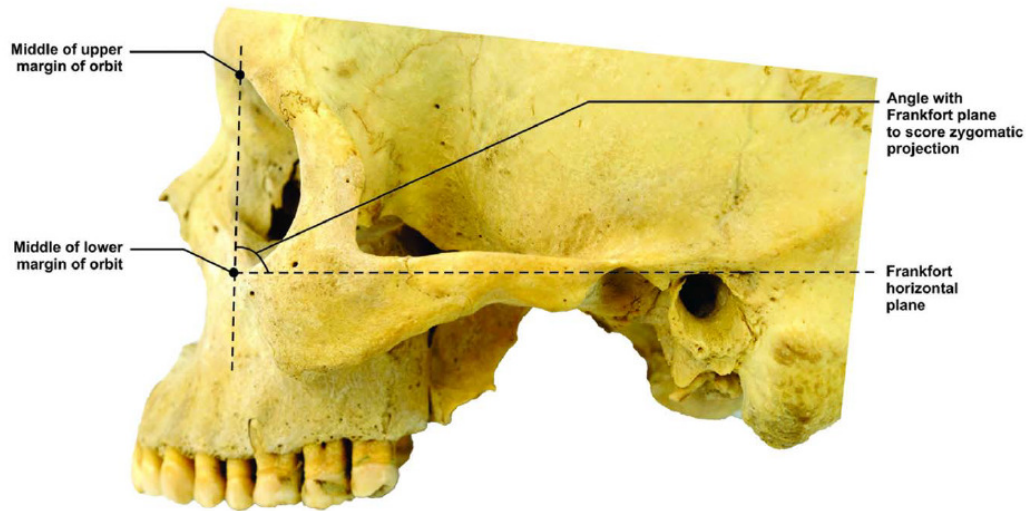


Figure 2.4. Vitek's technique used to score zygomatic projection (Oetlé et al. 2017).

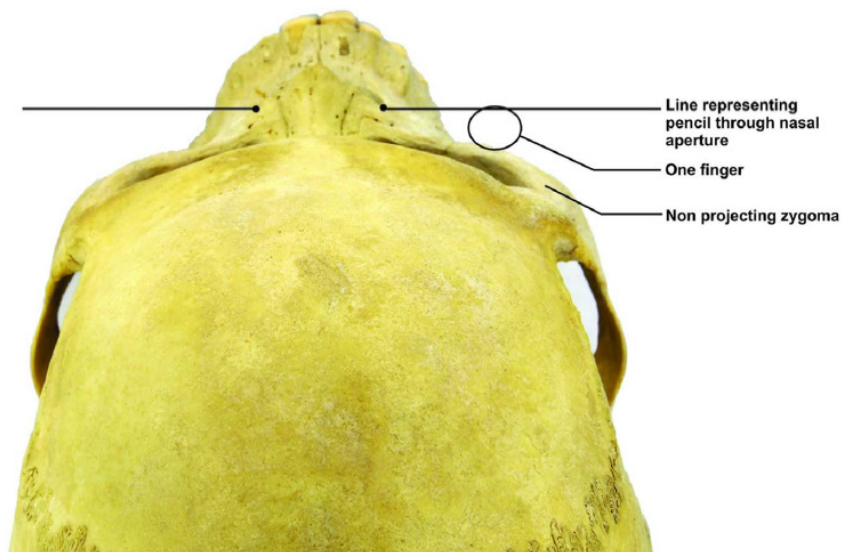


Figure 2.5. Bass's (1995) technique used to score zygomatic projection (Oetlé et al. 2017).

Projection of the zygoma has been described according to broad ancestral categories (Gill et al. 1988; Stavrianos et al. 2012; Cataldo-Ramirez et al. 2020). The zygomatic projection in African American and white North American populations has been noted to have a more receding and vertical projection, whereas a more prominent cheek projection has been associated with Asian or Native American populations (Gill et al. 1988; Stavrianos et al. 2012; Cataldo-Ramirez et al. 2020). L'Abbé et al. (2011) assessed the zygomatic projection in a

South African population using Bass's (1995) methodology. The results of the study indicated that black South Africans presented with a retreating zygoma (86%), white South Africans presented with a retreating zygoma (91%), and coloured South Africans presented with a retreating zygoma (73%) (L'Abbé *et al.* 2011). While Asian populations were found to present with a prominent projection of the zygoma in previous studies (Gill *et al.* 1988; Stavrianos *et al.* 2012; Cataldo-Ramirez *et al.* 2020), coloured South Africans did not. As the coloured population has received genetic contributions from Asian populations, a more projecting zygoma was expected; however, European as well as African populations have also contributed to the modern coloured South African, making the understanding of the projection of the zygoma amongst the coloured population complex. Furthermore, higher observer error rates were noted for the zygomatic projection, emphasising the subjectivity of the methodology and the lack of repeatability when assessing zygomatic projection (L'Abbé *et al.* 2011). Cataldo-Ramirez *et al.* (2020) attempted to quantify the projection of the zygoma by adapting the Vitek (2012) methodology to assess ancestral variation. The midpoints of the orbits were first landmarked on anterior facing 3D surface scans and then landmarked on laterally facing 3D surface scans. Posterior angles were then calculated (Cataldo-Ramirez *et al.* 2020). Ancestral differences were noted for both methodologies, but no sex differences were. However, landmarks placed on the anterior 3D surface scans were found to be measuring the orbital plane which has shown limited variation in human populations (Cataldo-Ramirez *et al.* 2020). The authors created two additional measurements, adapted from Bass's (1995) methodology to assess zygomatic projection. The first adaptation assessed the inferior zygomatic distances by placing landmarks on the most inferior point of the zygoma and on the most posterior point of the nasal aperture. Lines were then created to calculate the distance. The second adaptation assessed superior zygomatic distance by placing the superior zygomatic landmark on the most anterior projection of the zygoma lateral to the dental arcade and the posterior nasal landmarks on the most posterior point of the nasal aperture. The distances were then calculated between the two landmarks (Cataldo-Ramirez *et al.* 2020). Both ancestry and sex differences were noted for the projection of the zygoma using the adapted methodologies (Cataldo-Ramirez *et al.* 2020). While the results obtained from previous studies indicate sexual dimorphism and ancestral variation, a quantitative approach has not been undertaken on a South African population and Indian South Africans have also not been studied. Therefore, to reduce subjectivity and include modern South Africans, further research on the projection of the zygoma using a novel technique is needed.

2.8. Geometric Morphometrics in Anthropology

Landmark data along with geometric morphometric techniques have become popular amongst anthropologists to assess shape variation independent of size (Spradley & Jantz 2016). However, a study has also use geometric morphometrics to assess form. Where shape and size are both studied to ascertain how much of the difference is attributable to size (Tawha *et al.* 2020). The shape of biological structures such as the zygoma result from a process that occurs ontogenically, genetically, or as an adaptation to the environment, to allow for functional processes to occur, such as mastication, which may intern affect the shape of the zygoma (Zelditch *et al.* 2004). Traditional morphometrics quantitatively analyse the shape of an object and compares the shape to other shapes commonly known, such as C-shaped, more or less circular or reniform (Zelditch *et al.* 2004). However, traditional morphometrics have limitations that include difficulties in understanding and interpreting the outputs of the analyses, which are essentially just a list of numbers (Zelditch 2004a). Geometric morphometrics, on the other hand, enables the researcher to visualise the data on a Cartesian coordinate system based on the anatomical landmarks for the specific structure being studied (Slice 2007). The data is then further processed through a generalised Procrustes analysis (GPA) that transforms, rotates and scales the landmark coordinates into a single coordinate system where size is removed (Spradley and Jantz 2016). Once the GPA is performed a further reduction analysis called principal components analysis (PCA) is performed where normal multivariate statistics can be employed while maintaining the geometric properties of the specimen (Spradley and Jantz 2016).

Since anthropologists have developed an interest in the shape of bone to assess variation, the field of geometric morphometrics has improved (Slice 2007). Multiple studies have been performed by anthropologists using geometric morphometrics to better understand variation (Franklin *et al.* 2006, 2007; Galland & Friess 2016). The studies performed focused mainly on the cranium as more accurate results have been obtained for sex and ancestry estimations compared to those obtained from postcrania (Small 2016). Other skeletal elements have also been studied for their shape variation, such as the mandible (Franklin *et al.* 2007), sacrum (Rusk & Ousley 2016), pelvis (Steyn *et al.* 2004), dentition (Yong *et al.* 2018), and long bones (Mopin *et al.* 2018).

Geometric morphometrics faces similar limitations as traditional morphometric techniques such as missing landmarks or limited number of landmarks unable to capture the full amount of shape variation (Adams *et al.* 2004; Small 2016). Therefore, semi-landmarks, which slide

along a curve, allow for curve data to be compared (Small 2016). Two methods can be used to obtain semi-landmark coordinates. The first method slides the semi-landmarks along the curve in a parallel direction, to minimise the bending energy, allowing the landmarks to align themselves to the reference shape. The second method makes use of sliding the semi-landmarks by decreasing the Procrustes distances between the semi-landmarks allowing the landmarks to align themselves to the reference shape (Perez *et al.* 2006; Small 2016). Perez *et al.*, (2006) noted that the Procrustes method was more accurate and that the difference between the two methods increased with the number of semi-landmarks used, indicating that the number of semi-landmarks used to describe shape should be limited as much as possible while still capturing the full amount of shape variation (Perez *et al.* 2006; Small 2016).

Geometric morphometrics allows for subtle differences in shape to be analysed whereas metric and non-metric techniques typically cannot capture as much variation by maintaining the three-dimensional form of the object instead of collapsing the object into linear measurements (Adams 2004; Franklin *et al.* 2006; Pretorius *et al.* 2006; Bigoni *et al.* 2010; Gonzalez *et al.* 2011). There is also a decreased amount of subjectivity; however, subjectivity is still present when placing set landmarks manually (Bigoni *et al.* 2010). Major disadvantages of geometric morphometrics includes the time-consuming data collection procedure, expensive equipment, and experience needed to collect the data correctly (Adams 2004; Franklin *et al.* 2006; Pretorius *et al.* 2006).

2.9. Computed Tomography in Anthropology

Imaging technologies such as computed tomography (CT) scans have become an important aspect of biological anthropology in areas such as forensic case work, research and teaching (Garvin & Stock 2016). Computed tomography, previously termed computed axial tomography, involves taking multiple radiographs at many angles that can create a tomographic image stack viewable as a 3D object (Leon 2015; Garvin & Stock 2016).

The value of CT images for anthropologists has become greatly recognised as hidden structures (such as the nasal cavities or sinuses) can easily be analysed (Allard 2006). CT scans have also become important when skeletal collections are not available, or where religious or cultural backgrounds require cremation. Living individuals are also assessed when using CT scans, allowing a modern sample of the population to be evaluated. However, the cost of obtaining CT scans of living individuals as well as the expertise and computer software needed to manipulate the 3D images makes using CT scans more difficult than using skeletal remains

in anthropology (Garvin & Stock 2016). Furthermore, CT scans emit radiation that can prove harmful to living individuals and should be limited to decrease the exposure (Franklin *et al.* 2016)

The use of CT scans to circumvent the lack of skeletal collections allows further research on populations not previously studied. However, imaging conditions can differ between CT scans. Colman *et al.* (2017) explored the effect that differing imaging conditions such as the type of scanner, slice thickness, exposure level, and the standard protocols used to scan patients had on the precision of the scans by comparing pelvic scans of the same individual scanned under differing conditions. The results showed that even when imaging conditions were different, the differences remained within the acceptable 2mm error range for linear measurements (Colman *et al.* 2017). Colman further analysed if dry bone and imaging could be used interchangeably. The study showed that a substantial difference between dry bone and imaged bone occurred during the segmentation and landmarking procedures which may inevitably prevent the direct use of CT scans for anthropological studies (Colman *et al.* 2019).

While the use of imaging technologies is still new to the discipline of anthropology, the technology is allowing a better understanding of structures once too small or hidden to study. Using CT scans also allows research on populations that have yet to be studied, providing a better understanding of current populations.

CHAPTER 3: MATERIALS AND METHODS

3.1. Sample

A total of 400 three-dimensionally (3D) reconstructed models from head CT scans of black, coloured, white, and Indian South Africans were used with an equal sex and ancestry distribution (Table 3.1). The CT scans were obtained from the Groote Schuur Hospital in the Western Cape, the Steve Biko Academic Hospital in Gauteng, and the Inkosi Albert Luthuli Central Hospital in KwaZulu-Natal and reconstructed into 3D models under a previous PhD study (771/2018) by Ms GC Krüger (supervisor).

Table 3.1. Distribution and source of sample.

<i>Source</i>	<i>Ancestry-Sex group</i>	<i>N</i>	<i>Abbreviation</i>
<i>STEVE BIKO ACADEMIC HOSPITAL</i>	Black Males	50	BM
	Black Females	50	BF
	White Males	50	WM
	White Females	50	WF
<i>GROOTE SCHUUR HOSPITAL</i>	Coloured Males	50	CM
	Coloured Females	50	CF
<i>INKOSI ALBERT LUTHULI CENTRAL HOSPITAL</i>	Indian Males	50	IM
	Indian Females	50	IF

The CT scans were collected at a slice thickness of 0.3 - 0.5mm. To ensure the scans could be accurately reconstructed in 3D, the scans were resampled to 0.5mm in all three dimensions to create isotropic 3D models using the Thermo Scientific™ AVIZO™ software 9 (license: AVIZO.59228; Thermo Scientific™ AVIZO™ software 9 Users Guide 2018). Isotropic 3D models refer to data that has been reconstructed so that the dimensions are similar in each axis (Dalrymple *et al.* 2007). This allows the image resolution to be maintained so that the reconstruction is an accurate representation of the object being studied. A slice thickness ranging from 0.5mm to 0.8mm is required to obtain isotropic images (Dalrymple *et al.* 2007). The CT scans were then saved as Digital Imaging and Communications in Medicine files (DICOM) for further analysis (Cotter *et al.* 2015; Weber 2015).

The original CT scans were anonymised to remove any identifying patient information and only the demographic information necessary for the study (age, sex and ancestry) was recorded. Only scans of individuals older than 18 years were collected. Any skull reconstructions with pathological changes, trauma, supernumerary sutures (os japonicum), obliterated sutures or imaging artefacts that prevented the placement of landmarks were excluded from the study.

3.2. Procedure

3.2.1. Model Processing, Landmark Placement and Data Preparation

The CT scans were opened in the Thermo Scientific™ AVIZO™ software 9 (license: AVIZO.59228) and orientated in the Frankfort horizontal plane (Thermo Scientific™ AVIZO™ software 9 Users Guide 2018). The Frankfort horizontal plane is defined by three points, namely the left and right porions (superior aspect of the external acoustic meatus), and the left orbit; the skull is rotated so that the porion is in line with the bottom of the left orbital margin corresponding to the left *orbitale* landmark (White & Folkens 2005). Once placed in the correct orientation, the scans were uploaded into the program called Treatment and Increased Vision for Medical Imaging (TIVMI) where the 3D skull models were segmented from the surrounding tissue (Dutailly 2009). Segmentation requires knowledge of the threshold value indicative of bone to distinguish between the bone and surrounding tissues. As threshold values are on a continuous scale there are difficulties in determining the correct threshold value to segment the bone from the surrounding tissue (Coleman & Colbert 2007). A method termed the half-maximum height protocol (HMH) determines the threshold values by calculating the mean of the minimum and maximum values along a boundary defining two different structures (Coleman & Colbert 2007). Fajardo et al. (2002) modified the HMH protocol as they found that cortical and trabecular bone have different threshold values (Fajardo *et al.* 2002). The method was further modified by Coleman and Colbert (2007), whereby the threshold value between two structures was calculated across ten slices of the model. The mean of those ten slices was then calculated and the resulting threshold value used for the entire scan to obtain a proper segmentation (Coleman & Colbert 2007). The 3D models were then segmented using the modified version of the HMH protocol in TIVMI and saved as a mesh for later use in AVIZO 9 (Dutailly 2009; Guyomarc'h *et al.* 2012). Once the 3D models were segmented, the meshes were uploaded into AVIZO 9 and smoothed for better viewing. The next step involved the manual placement of landmarks on the segmented skulls. Eleven landmarks previously

described in the literature were used for the analysis (Table A1; Figure 3.1). Each landmark was used to depict the most prominent points on the outline of the zygoma. The landmarks were placed onto each specimen in AVIZO 9, where the order of landmarks was kept consistent across all specimens. In a normal forensic investigation the left side is measured and where the left side cannot be measured, measurements from the right side are taken (Langley *et al.* 2016). However, the landmarks in the current study were placed on the right zygoma and in cases where the right zygoma could not be used, the landmarks were placed on the left zygoma. Even though the landmarks were not placed on the left side, all landmarks were kept to the right side as much as possible to avoid the issue of asymmetry which, warrants further investigation.

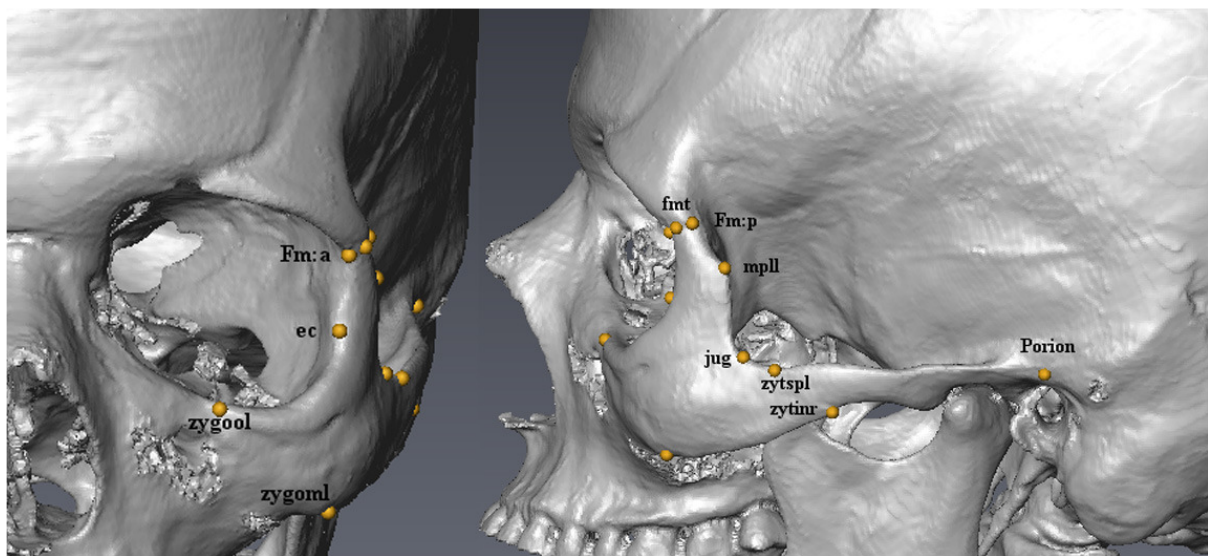


Figure 3.1. Anterior (left) and lateral (right) views of the skull demonstrating the landmarks used.

Slice (2007) stated that the curve of an object can provide more important biological information than standard landmarks and suggested that placing landmarks along a curve at a specified distance could provide important shape information (Slice 2007). Therefore, to further assess the shape of the zygoma, semi-landmarks were used in addition to individual landmarks to define the curvature of the zygoma.

The semi-landmarks were created using the Surface Path Set function found in AVIZO 9. The path was marked along the margin of the right zygoma and in cases where this was not possible, along the margin of the left zygoma. The *Arothron* package in R Studio was then used to convert the surface path set into 80 semi-landmarks spanning each zygoma (Profico *et al.* 2020). However, because the zygoma has multiple curves that make up the entire shape, a

specified number of semi-landmarks per curve of the zygoma was created to ensure homology (Small 2016).

The *Arothron* package R Studio was then used to group the 11 set landmarks per individual into a morphologika file format that is compatible with MorphoJ and the *geomorph* package found in R for further analysis (Adams *et al.* 2021). Furthermore, the pathset files containing the semi-landmarks were converted into a morphologika file in the same way, specifying 80 semi-landmarks per individual. MorphoJ is a program that provides a broad range of morphometric analyses within a user-friendly platform (Klingenberg 2011). The landmark and semi-landmark morphologika files were imported into R Studio where the package *geomorph* was used to perform multiple statistical tests to analyse the data (R Core Team 2018).

The data collected was assessed for outliers using the *plotOutliers* function in the *geomorph* package in R. To retain most of the biological variation in the dataset only major outliers were removed. Generalised Procrustes analysis (GPA) was then performed on the data using the *gpagen* function in the *geomorph* package in R (R Core Team 2018). GPA superimposes landmarks by rotating, scaling and translating them to fit a shared foundation, which allows the separation of size and shape (Nicholson & Harvati 2006). In the current study, GPA was used to position and orientate the specimens, while also removing differences in centroid size (Zelditch 2004b). The shape differences were then assessed using further statistical tests.

3.3. Statistics

3.3.1. Intra- and Inter-observer Repeatability

To test for inter-observer repeatability, both the principal investigator and a second investigator placed the eleven landmarks on ten randomly selected 3D CT scanned cranial models? from the sample. To test for the intra-observer repeatability, the principal investigator placed the landmarks on the same ten skulls after about two weeks had passed, to determine whether the landmark placement was repeatable. Intra- and inter-observer repeatability was assessed through dispersion analysis. Dispersion analysis calculates the distance between the repeated landmarks and the mean of the landmark (Guyomarc'h *et al.* 2014). Based on craniometric literature, a deviation from the mean of less than 2mm was deemed acceptable (Ridel *et al.* 2018).

3.3.2. Significance Test

Procrustes ANOVA using the GPA coordinates was used to test for significant differences between the sexes and among populations. The *procD.lm* function in the *geomorph* package in R was used to run the analyses (R Core Team 2018). Through this function, permutation testing was also conducted. Permutation tests recalculate the *p*-value of the significance test by randomly reordering the data. The process assesses the probability of getting a *p*-value equal to or greater than the original *p*-value observed under the null hypothesis, in the current case, whether there are significant differences within and among the different groups (Anderson 2001). A pairwise test was then performed as a post-hoc using the *pairwise* function in the *geomorph* package in R to test where significant differences occurred amongst the population groups (R Core Team 2018).

3.3.3. Principal Components Analysis

The following methods were used to assess both the landmark and semi-landmark coordinates. Principal component analyses (PCA) were performed as a dimensionality reduction technique to allow for easier interpretation of the data while minimising the loss of information (Jolliffe 2002). PCA simplifies descriptions of the points from the data and turns the variables into linear combinations of the original variables making them easier to interpret (Zelditch 2004c). A PCA output shows the principal component (PC) score (linear combination of the original coordinates) arranged from highest variance to lowest variance (Jolliffe 2002; Krüger *et al.* 2017). The PCA was also used to visualise the distribution of the data between the sexes and among the different population groups with the use of PCA plots. The loadings obtained from the PCA were also used to assess which landmarks contributed the most variation. Loadings are used to obtain the PC score by multiplying the loading by the standardised raw coordinates (Krüger *et al.* 2015). The *prcomp* function in the *stats* package in R was used to run the PCA (R Core Team 2018). To view the overall PCA diagrams the *fviz_pca_ind* function in the *factoextra* package was used (Kassambara & Mundt 2020).

Wireframe graphs were used to visualise the mean shape differences of the zygoma (between the sexes and among the population groups) using the landmark and semi-landmark coordinates. Wireframe graphs are created by linking the landmarks to each other with lines so that the shape of the object is graphically represented (Klingenberg 2013). Two groups were then compared at a time, using the GPA coordinates, to assess the differences between them. The wireframe graphs were created using the *plotRefToTarget* function in the *geomorph* package in R.

3.3.4. Linear Discriminant Analysis

Linear discriminant analysis (LDA) was used to evaluate the discriminatory strength of the landmarks and semi-landmarks to distinguish between the sexes and amongst the population groups. LDA involves the creation of a factor that is calculated for each landmark and when the factors are added together, maximise the mean differences between groups (Ousley & Jantz 2012). The score for each individual is then compared to the centroids for each group. The centroid closest to the individual is the group to which the individual most likely belongs. LDA has three requirements in order to obtain the best possible classification. First is the sample size, where the total number of measurements used in the investigation should be the minimum number of individuals in the smallest sample minus one (Jantz & Ousley 2017). Second is normality, where the sample is required to have a normal distribution. However, if the sample size is large enough (i.e. greater than thirty to forty specimens) a lack of normality no longer adversely affects the outcome of the analysis (Ghasemi & Zahediasl 2012). Lastly, homogeneity of variance, which is the assumption that there is an equal amount of variance between the groups being compared. When there is homogeneity of variance the groups can be compared and accurate results achieved (Ousley & Jantz 2012)

The LDA was performed using the PC scores obtained during analysis and run using the *LDA* function in the *FlipMultivariates* package in R. In order to decide which PC scores would be included in the equations, a scree plot was created showing the eigenvalues of the various PC scores obtained. Only PC scores with an eigenvalue above one were used in the equations. In the event that all scores had an eigenvalue below one, all PC scores that contributed to the total variance were included for the set landmarks, while PC scores that contributed 95% of the total variance were used for the semi-landmarks. A cumulative variance plot was then created to assess how much of the total variance the selected PC scores contributed to the equations. The scree plot along with the cumulative variance plot were created using the *screeplot* and *cumsum* function in the *stats* package, respectively.

A backward stepwise selection was used to remove any unnecessary variables from the discriminant functions. Backward stepwise selection involves starting with all the variables in the function and removing one variable at a time until the number of variables designated by the investigator is obtained or there has been an improvement in the classification accuracy by at least 5%. The variables that are removed from the function describe the least variation in the sample (Weihs *et al.* 2005). Backward stepwise selection was performed using the *stepclass* function found in the *klaR* package in R (R Core Team 2018). The results were then cross-

validated using leave-one-out cross-validation (LOOCV). LOOCV involves the use of all the data available thereby evaluating the classifying ability of the generated model (Wong 2015). LOOCV removes one individual at a time and uses the remaining individuals to generate the model. The model then attempts to classify the individual. The process is repeated for each individual resulting in a cross-validated accuracy thereby testing the reliability of the model (Liebenberg 2015). LOOCV also allows for an unbiased approach to cross-validating data (Cawley & Talbot 2008). LOOCV was run using the *caret* package in R (R Core Team 2018).

3.3.5. Analysis of the Projection of the Zygoma

3.3.5.1. Descriptive Statistics

To assess the variation of the length of the zygomatic arch in relation to *porion*, interlandmark distances were created between *po* and *zygool*, between *po* and *zygoml*, and between *zygool* and *zygoml* (Figure 3.2). Each interlandmark distance was then renamed as Superior Zygomatic Length (PorZygool)- a measure of the maximum length of the superior margin of the zygoma, Inferior Zygomatic Length (PorZygoml)- a measure of the maximum length of the inferior margin of the zygoma, and Zygomaticomaxillary Length (ZML)- the maximum distance between the *zygool* and *zygoml* landmarks, respectively. Once the interlandmark distances were calculated, the number of individuals, means and standard deviations were noted to assess the distribution of the interlandmark distances between the sexes as well as amongst the population groups. The mean is often described as the average of the data and describes the centre of the data, whereas the standard deviation describes the spread of the variation in the sample. The higher the standard deviation the greater the spread and the further from the mean the sample is (Ross 2004).

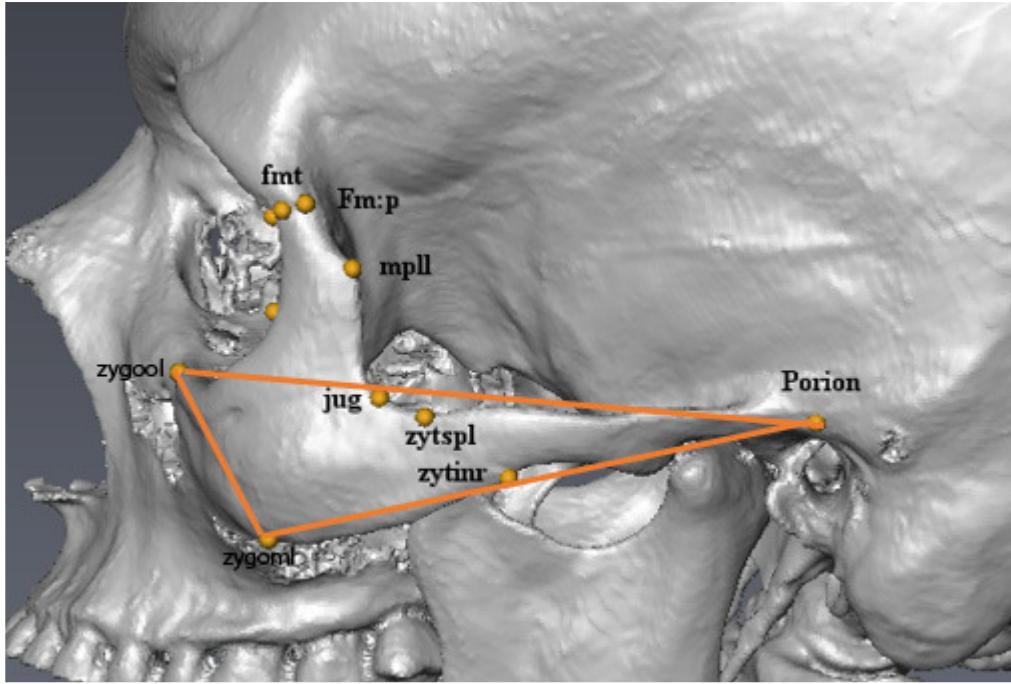


Figure 3.2. Lateral View of the skull showing the interlandmark distances taken to assess the projection of the zygoma.

3.3.5.2. Angles of Projection

A further analysis on the projection of the zygoma involved the calculation of the angles between the interlandmark distances (Figure 3.3). Three angles were calculated using the rule of cosines and the mean lengths of the three interlandmark distances. Angle 1: the angle at the intersection of ZML and PorZygoml indicating the anterior projection of the zygoma relative to the superior of the zygomatic arch; Angle 2: the angle at the intersection of ZML and PorZygoool indicating the anterior projection of the zygoma relative to the inferior of the zygomatic arch and Angle 3: the angle at the intersection of PorZygoool and PorZygoml indicating the projection relative to the anterior aspect of the zygomatic arch. The rule of Cosines states that if a triangle with lengths a, b, and c, along with angles A, B, and C is present then the rule can be applied as follows (Murray-Lasso 2002):

$$a^2 = b^2 + c^2 - 2bc \cos A$$

The rule was applied to the triangle created by the interlandmark distances and the angles were calculated for both the sexes and population groups. The angles were calculated for males and females separately as well as each population group separately. The resultant equation used to calculate the angles was as follows (Figure 3.3):

$$PorZygoool^2 = PorZygoml^2 + ZML^2 - 2(PorZygoml)(ZML) \cos Angle1$$

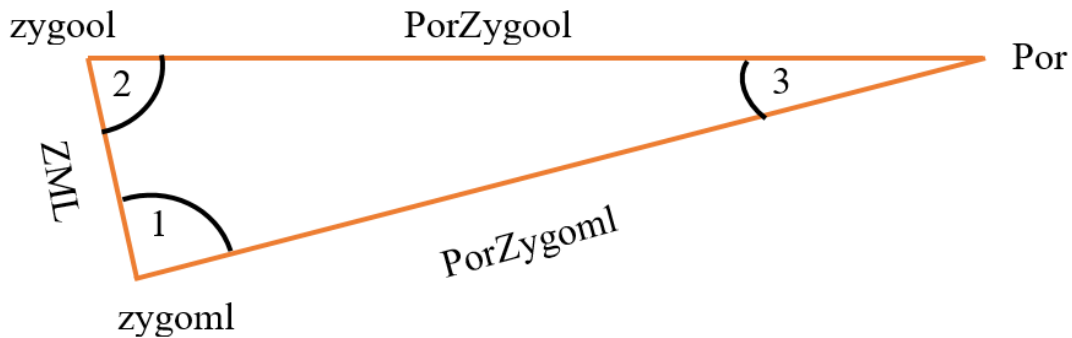


Figure 3.3. Figure showing the angles between the interlandmark distances.

3.3.5.3. Significance Tests

ANOVA was used to test for significant differences between the sexes as well as between the males and females of each ancestry group (i.e. between black South African males and black South Africans females) for the interlandmark distances and angles. ANOVA was also used to test for differences among the population groups as well as among the population groups when separated into males and females. The function *aov* in the *stats* package in R was used to run the analysis (R Core Team 2018). A Tukey's Honestly Significant Differences (HSD) *post hoc* test was performed to assess where the significant differences among the population groups occurred using the *Tukey HSD* function in the *stats* package in R (R Core Team 2018).

3.3.5.4. Linear Discriminant Analysis

An LDA was run to evaluate the discriminatory strength of the three interlandmark distances and the three angles to determine how well the projection of the zygoma would be able to distinguish between the sexes as well as amongst the population groups. PCA was used to assess the discriminatory ability of the three angles to avoid the multicollinearity assumption. Backward stepwise selection and LOOCV were then performed on the models to select the most discriminatory variables for model creation and to validate their classifying ability, respectively. The same packages used to perform the LDA for the shape differences were used to assess the projection of the zygoma.

CHAPTER 4: RESULTS

4.1. Intra- and Inter-observer Error

Mean values less than 2mm were obtained for both the intra- and inter-observer errors for the landmark and semi-landmark coordinates, indicating repeatability and reproducibility. A larger mean and standard deviation were obtained for the inter-observer error for both landmarks and semi-landmarks than for the intra-observer error (Tables 4.1 and 4.2).

Table 4.1. Mean dispersion error (mm) of manual landmark placements.

<i>Intra-observer</i>		<i>Inter-observer</i>	
<i>Mean</i>	<i>SD</i>	<i>Mean</i>	<i>SD</i>
0.597	0.430	0.762	0.453

Table 4.2. Mean dispersion error (mm) of semi-landmark placements.

<i>Intra-observer</i>		<i>Inter-observer</i>	
<i>Mean</i>	<i>SD</i>	<i>Mean</i>	<i>SD</i>
0.633	0.453	0.764	0.502

When the placement of individual landmarks was analysed, all landmarks showed high repeatability (Table 4.3). The landmark with the largest intra-observer error mean was *zytspl* (0.869 mm) and the landmark with the smallest intra-observer error mean was *jug* (0.330 mm). The landmark with the largest standard deviation for intra-observer error was *zygool* (0.885 mm) and the landmark with the smallest standard deviation for intra-observer error was *mpll* (0.142 mm).

The landmark with the largest inter-observer error mean was *zygool* (1.300 mm), and the smallest mean was obtained for *zytinr* (0.430 mm). The landmark with the largest standard deviation was *zygoml* (0.795 mm) whereas the smallest standard deviation was obtained for *zytinr* (0.220 mm).

Table 4.3. Mean dispersion error (mm) of individual manual landmark placements.

Landmarks	Intra-observer		Inter-observer	
	Mean	SD	Mean	SD
<i>fm:p</i>	0.588	0.395	0.607	0.339
<i>fm:a</i>	0.535	0.401	0.579	0.492
<i>Mpll</i>	0.349	0.142	0.540	0.396
<i>Ec</i>	0.792	0.509	0.816	0.387
<i>Jug</i>	0.330	0.181	0.471	0.221
<i>Zytinr</i>	0.428	0.271	0.430	0.220
<i>Zytspl</i>	0.869	0.686	0.674	0.508
<i>Zygool</i>	0.833	0.885	1.300	0.675
<i>Zygoml</i>	0.594	0.462	1.114	0.795
<i>Fmt</i>	0.529	0.234	0.708	0.415
<i>Po</i>	0.716	0.570	1.143	0.536

4.2. Sexual Dimorphism

4.2.1. Significance Tests (ANOVA)

Procrustes ANOVA was run on the generalised Procrustes coordinates of the landmark coordinates to test for significant differences between males and females. The results of the Procrustes ANOVA when all population groups were combined revealed significant differences between males and females for both set landmarks and semi-landmarks (Table 4.4).

Table 4.4. Results of the Procrustes ANOVA test (1000 permutations) of the landmarks and semi-landmarks showing significant differences of the sex and ancestry of the zygoma. Bold *p*-values indicate significant differences.

Landmarks		
	<i>Sex Differences</i>	<i>Ancestry Differences</i>
<i>p-value</i>	0.001	0.001
Semi-landmarks		
	<i>Sex Differences</i>	<i>Ancestry Differences</i>
<i>p-value</i>	0.001	0.001

However, as differences were noted in the general degree of sexual dimorphism among the various population groups, further Procrustes ANOVA tests were used to assess the sexual dimorphism of the black, coloured, white, and Indian South Africans, separately. The results

show that all population groups demonstrated significant differences between the sexes, except for coloured South Africans (p -value = 0.107; Table 4.5).

Table 4.5. Results of the Procrustes ANOVA test (1000 permutations) demonstrating whether a significant degree of sexual dimorphism is present from the landmarks and semi-landmarks amongst the population groups for the zygoma. Bold p -values indicate significant differences.

Landmarks				
	<i>Black South Africans</i>	<i>Coloured South Africans</i>	<i>White South Africans</i>	<i>Indian South Africans</i>
<i>p-value</i>	0.003	0.107	0.007	0.032
Semi-Landmarks				
	<i>Black South Africans</i>	<i>Coloured South Africans</i>	<i>White South Africans</i>	<i>Indian South Africans</i>
<i>p-value</i>	0.001	0.002	0.001	0.010

4.2.2. PCA and Wireframes

When all population groups were combined, the PCA for the landmarks revealed that PC1 explained a large proportion (19.5%) of the total variation, whereas PC2 contributed 11.4%. While, PC1 explained 20.73% of the total variation of the semi-landmark coordinates, PC2 explained 13.2% of the total variation of the semi-landmark coordinates. The corresponding PCA plots of PC1 and PC2 illustrates extensive overlap between males and females. Males showed more within-group variation than females for the landmark coordinates, whereas the semi-landmark coordinates showed similar within-group variation between males and females (Figures 4.1 and 4.2). The loadings of the landmark coordinates revealed that *zygool* and *po* contributed the most to PC1, whereas *zygoml* and *po* contributed the most to PC2 (Table A2).

The wireframes of the average zygoma shapes of the males and females (when all population groups were combined) showed that females have a shorter zygomaticomaxillary suture (*zygool* to *zygoml*) where, *zygool* extended more inferiorly. The zygomaticotemporal suture (*zytspl* to *zytinr*), and the inferior border of the zygoma also showed differences between males and females. The lateral margin of the orbit extended more inferiorly, and the frontal process extended more superiorly in females compared to males (Figures 4.1 and 4.2).

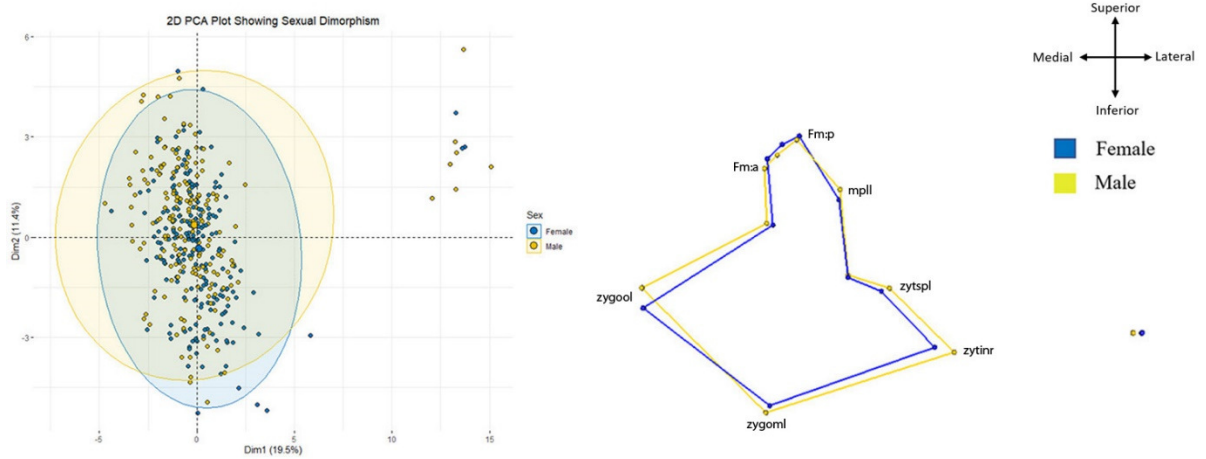


Figure 4.1. PCA plot and wireframe graph (anterior view) depicting the mean shape between males and females (combined ancestry) for set landmarks.

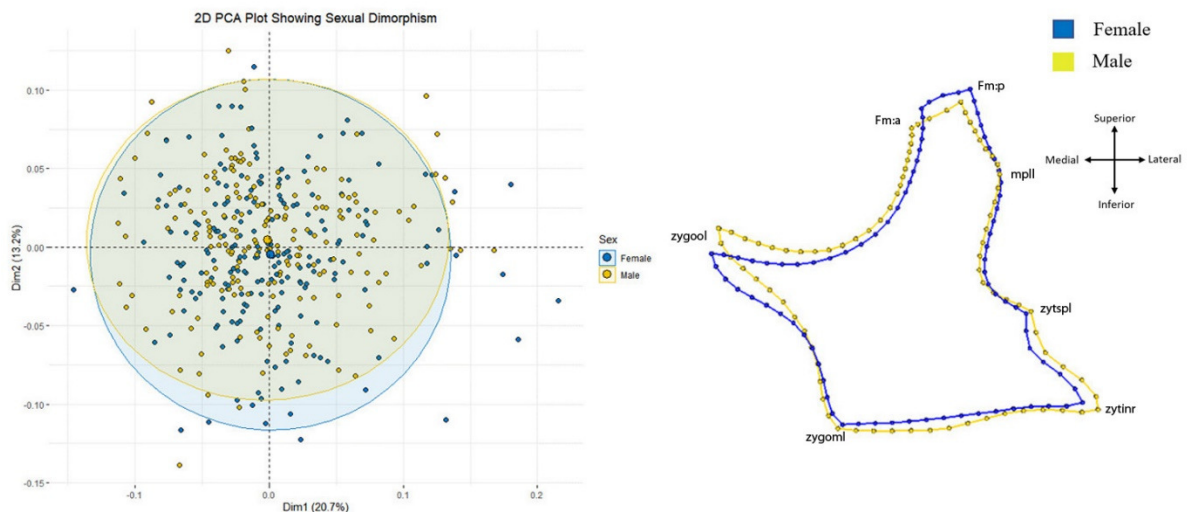


Figure 4.2. PCA plot and wireframe graph (anterior view) depicting the mean shape between males and females (combined ancestry) for semi-landmarks.

Further PCA's were run to assess the sexual dimorphism of each ancestry group. When black South Africans were assessed, PC1 explained a large proportion of the total variation (28.55%) for the landmark coordinates, whereas PC2 explained a slightly smaller proportion (13.3%) of the landmark coordinates. While PC1 explained 19.05% of the total variation for semi-landmark coordinates, PC2 explained 15% of the total variation for the semi-landmark coordinates. Similar to when all population groups were combined, the corresponding PCA plots showed extensive overlap between males and females, where males displayed a larger within-group variation for the landmark coordinates and both males and females had similar levels of within-group variation for the semi-landmark coordinates (Figure 4.3 and 4.4). The

loadings for the set landmark coordinates revealed that *zygoml* and *po* contributed the most variation to PC1, while *zygool* and *po* contributed the most variation to PC2 (Table A3).

The wireframes comparing the average shapes of black South African males and females showed that the most prominent differences occurred at the zygomaticomaxillary suture. The wireframes also indicated that the orbits in females extended more inferiorly and the frontal processes more superiorly than in males. Males also demonstrated a more laterally placed zygomaticotemporal suture compared to females (Figures 4.3 and 4.4).

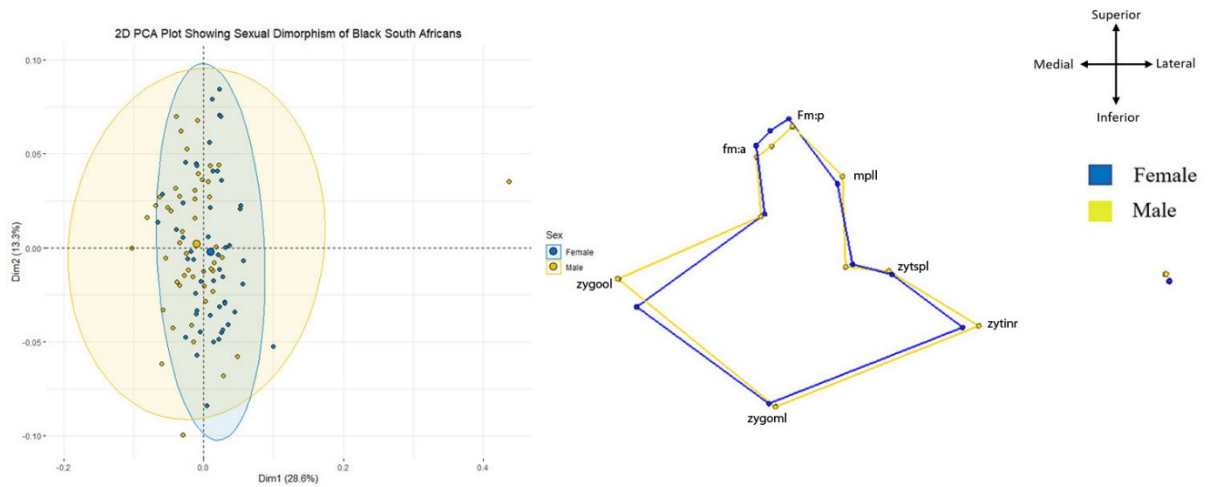


Figure 4.3. PCA plot and wireframe graph depicting the mean shape between black male and female South Africans for set landmarks.

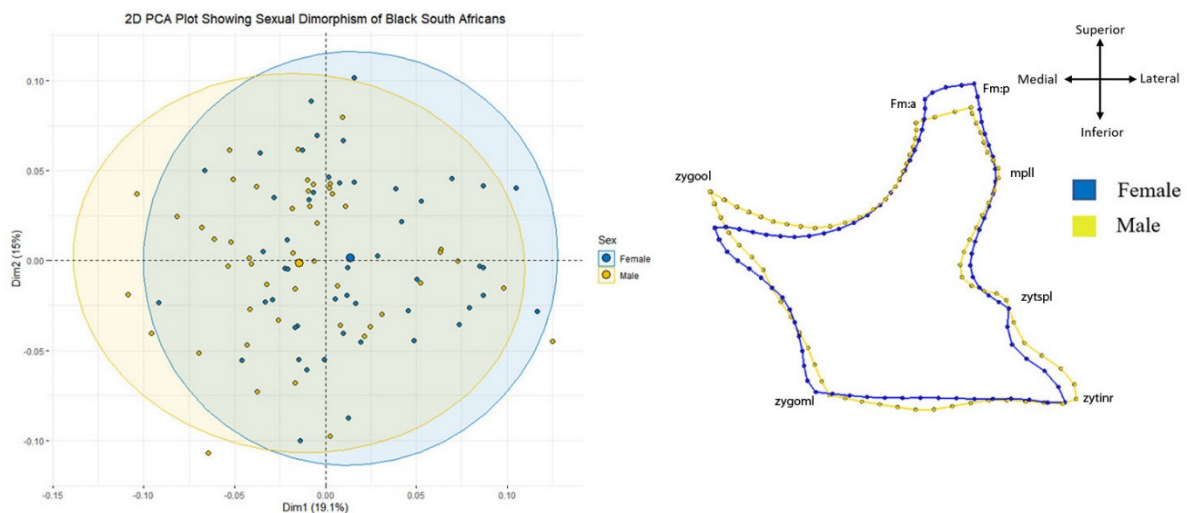


Figure 4.4. PCA plot and wireframe graph depicting the mean shape between black male and female South Africans for semi-landmarks.

The PCA to assess differences between coloured South African males and females showed that PC1 explained 44.32% of the total variation for the landmark coordinates, while PC2 explained only 10.2% of the total variation for the landmark coordinates. PCA for the semi-landmark coordinates showed that PC1 explained 24.7% of the total variation, while PC2 explained 11% of the total variation. The corresponding PCA plots demonstrated less overlap between the males and females compared to the black South African sample; however, coloured South African males displayed a slightly larger within-group variation than the females for both landmark and semi-landmark coordinates (Figures 4.5 and 4.6). The assessment of the loadings for the landmark coordinates revealed that *zygool*, *zygoml*, and *po* contributed the most to PC1, while *zytinr*, *zygool*, and *po* had the larger contributions to PC2 (Table A4).

Wireframe graphs for the coloured South Africans showed that there were shape differences between males and females at the zygomaticomaxillary and zygomaticotemporal sutures. The orbits again extended more inferiorly, and the frontal process extended more superiorly in females than in males (Figures 4.5 and 4.6).

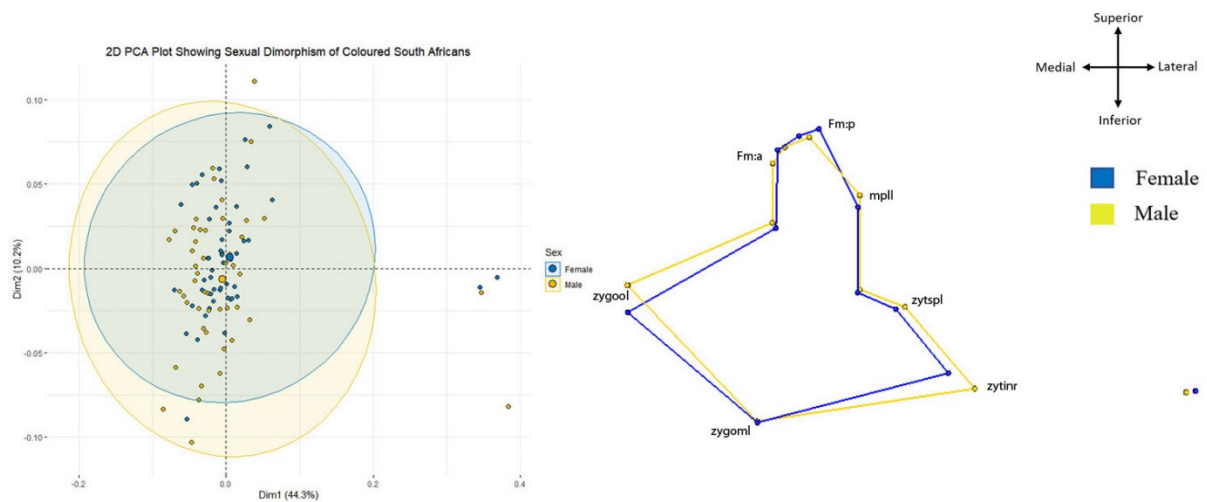


Figure 4.5. PCA plot and wireframe graphs (anterior view) depicting the mean shape between coloured male and female South Africans for set landmarks.

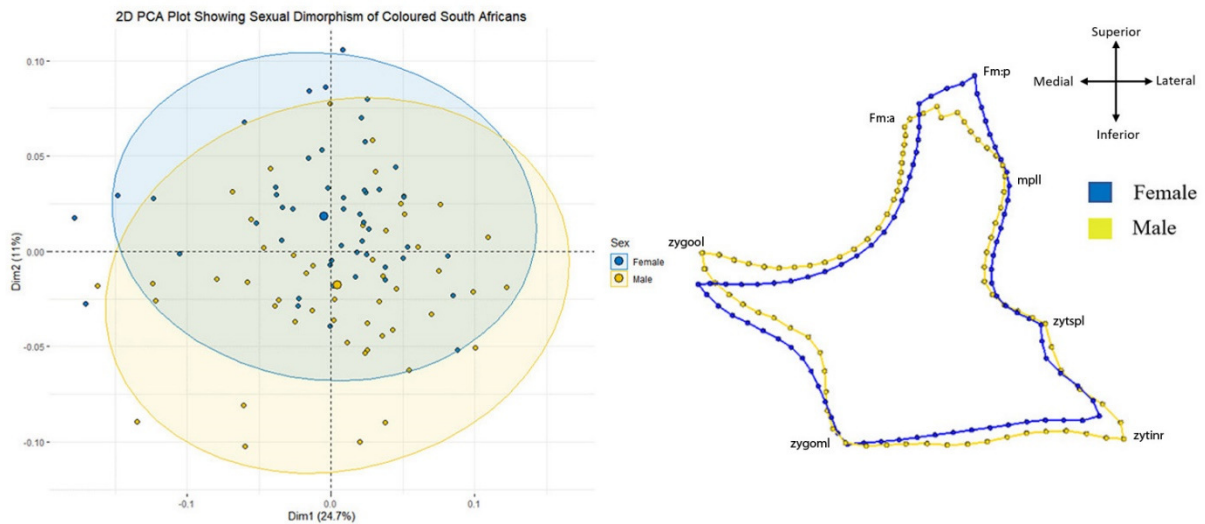


Figure 4.6. PCA plot and wireframe graphs (anterior view) depicting the mean shape between coloured male and female South Africans for semi-landmarks.

The PCA's of white South African males and females resulted in a PC1 that explained 39% of the total variation for landmark coordinates, while PC2 explained 11.9% of the total variation for the landmark coordinates. For the semi-landmark coordinates, PC1 explained 19.9% of the total variation, while PC2 explained 12.5% of the total variation. The corresponding PCA plots illustrated considerable overlap between the males and females, where the males had larger within-group variation than their female counterparts (Figures 4.7 and 4.8). The assessment of the PC loadings revealed that *zygoool* and *po* contributed the most to PC1, while *zygoml* and *po* contributed the most to PC2 for the landmark coordinates (Table A5).

The wireframes illustrating the average zygoma shapes for white South African males and females demonstrated similar shape profiles for both sexes; however, slight differences were present at the frontomalar suture where females exhibited a slightly more posterosuperior position when compared to their male counterparts. Furthermore, the orbits extended more inferiorly in females compared to males, whereas the zygomaticotemporal suture extended more posteriorly in males compared to females (Figures 4.7 and 4.8).

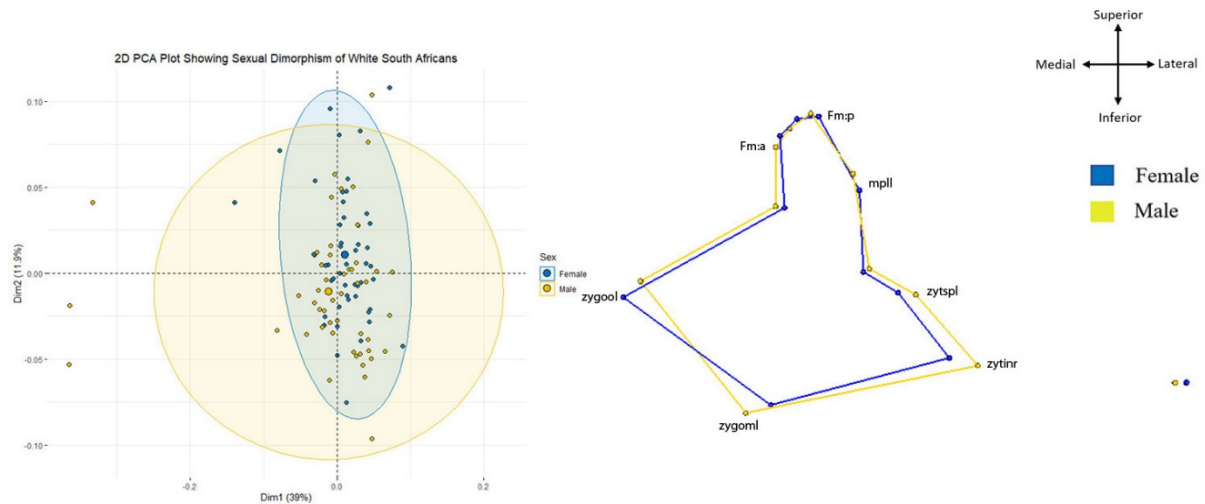


Figure 4.7. PCA plot and wireframe graphs (anterior view) depicting the mean shape between white male and female South Africans for set landmarks.

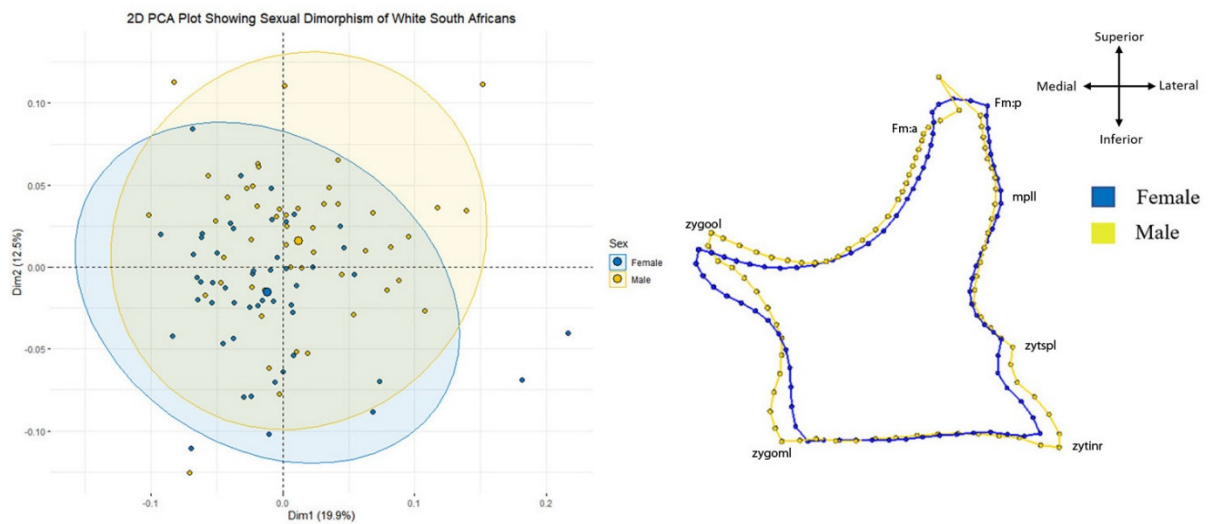


Figure 4.8. PCA plot and wireframe graphs (anterior view) depicting the mean shape between white male and female South Africans for semi-landmarks.

PCA for Indian South African males and females showed that for the landmark coordinates, PC1 explained 33% of the total variation, while PC2 explained 13.7% of the total variation. For the semi-landmark coordinates, PC1 explained 21.9% of the total variation, while PC2 explained 15.2% of the total variation. The corresponding PCA plots illustrated major overlap between the males and females. Unlike the other three population groups, the Indian South African females were the group with the larger within-group variation when compared to their male counterparts (Figures 4.9 and 4.10). For the landmark coordinates, *zygoool* and *po* contributed the most variation to PC1, while *zygoool*, *zygoml*, and *po* contribute the most variation to PC2 (Table A6).

Wireframes illustrating the differences between the mean shapes of the Indian South Africans showed that the females appeared consistently smaller than the males. The orbits also extended more inferiorly, and the frontal process extended more superiorly in females compared to males. The inferior margin of the zygoma extended more inferiorly and the zygomaticotemporal suture extended more posteriorly in males compared to females (Figures 4.9 and 4.10).

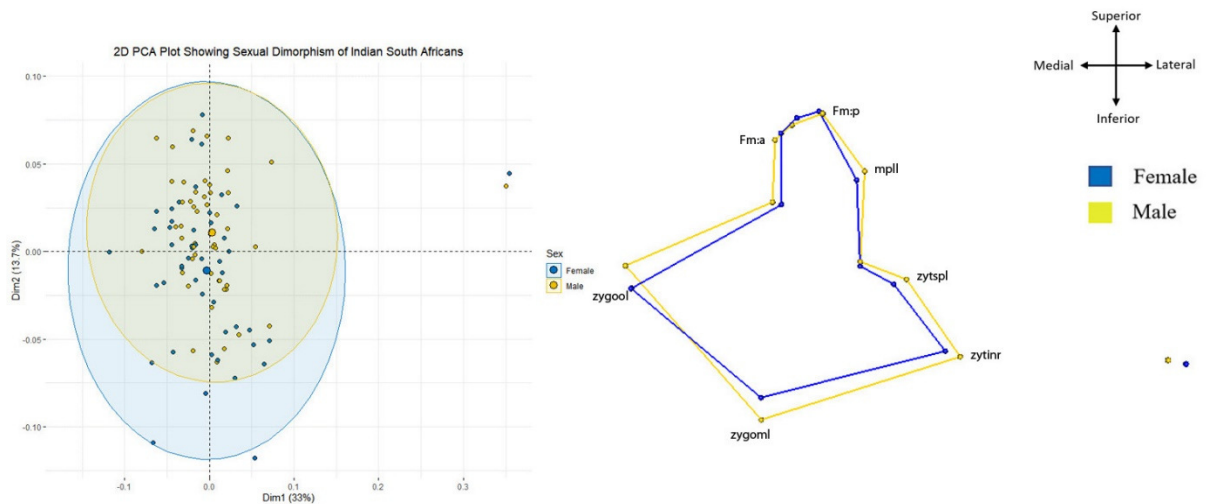


Figure 4.9. PCA plot and wireframe graphs (anterior view) depicting the mean shape between Indian male and female South Africans for set landmarks.

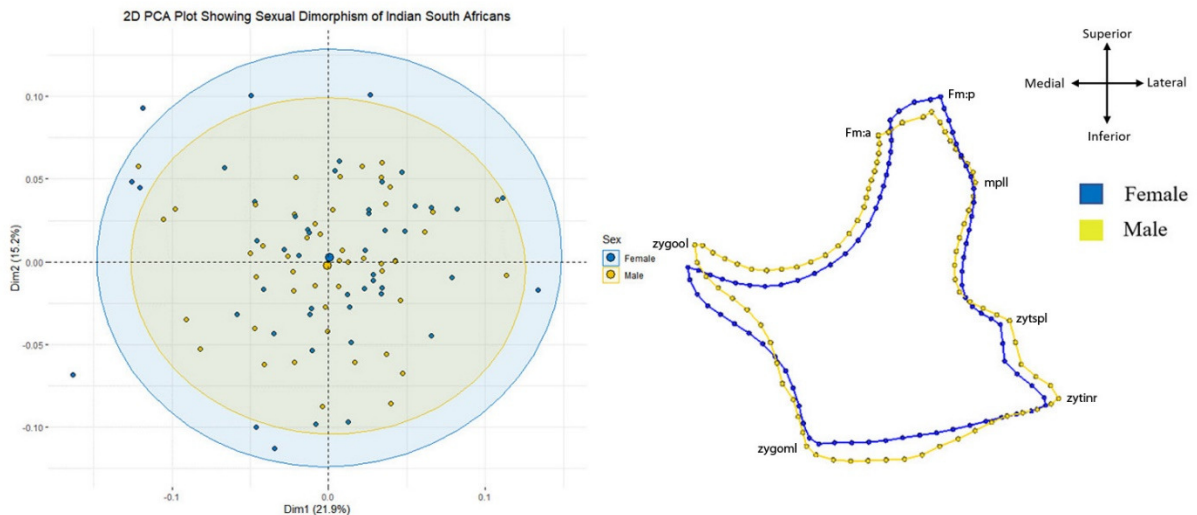


Figure 4.10. PCA plot and wireframe graphs (anterior view) depicting the mean shape between Indian male and female South Africans for semi-landmarks.

4.2.3. Linear Discriminant Analysis (LDA)

A discriminant analysis was run on the landmark coordinates to assess the discriminatory strength of the landmarks when used to estimate sex. All population groups were combined, and only sexual dimorphism was assessed. All 26 PC scores (100% of the variation) were used to run an initial analysis and the resulting LDA produced an average accuracy of 74.87%. However, as not all variables necessarily add valuable information and may even create statistical noise, backward stepwise selection was employed to remove superfluous variables and resulted in an overall classification accuracy of 77.66% when estimating sex. Leave-One-Out Cross-Validation (LOOCV) was then used and yielded a classification accuracy of 73.4% (Table 4.6). The analysis demonstrated a female sex bias, where the females classified better than the males. An exploration of the classification matrix demonstrated that among the females, coloured females classified the best, while black males classified the best among the males. Coloured South African males and black South African females had the lowest correct classification rates.

Results of the LDA for the semi-landmark coordinates, showed an overall correct classification rate of 78.9%. A backward stepwise selection resulted in an overall correct classification rate of 79.4% when estimating sex. LOOCV was then performed and yielded a correct classification rate of 76.9%. Overall females performed slightly better than males, where coloured females classified the best among the females and black males classified the best among the males (Table 4.7).

Table 4.6. LDA classification matrix when estimating sex from landmarks. Bold indicates highest accuracy obtained.

	<i>M</i>	<i>F</i>	<i>% Correct</i>	<i>Average Accuracy</i>	<i>Overall Accuracy</i>	<i>LOOCV Accuracy</i>
<i>BM</i>	38	10	79%	76%	77.66%	73.4%
<i>CM</i>	36	14	72%			
<i>WM</i>	38	11	78%			
<i>IM</i>	37	12	76%			
<i>BF</i>	13	37	74%	79%		
<i>CF</i>	8	41	84%			
<i>WF</i>	11	39	78%			
<i>IF</i>	9	40	82%			

Table 4.7. LDA classification matrix when estimating sex from semi-landmarks. Bold indicates highest accuracy obtained.

	<i>M</i>	<i>F</i>	% Correct	Average Accuracy	Overall Accuracy	LOOCV Accuracy
<i>BM</i>	36	12	75%	78%	79.4%	76.9%
<i>CM</i>	34	16	68%			
<i>WM</i>	44	5	89%			
<i>IM</i>	39	10	80%			
<i>BF</i>	11	39	80%	82%		
<i>CF</i>	10	39	80%			
<i>WF</i>	8	42	84%			
<i>IF</i>	9	40	82%			

4.3. Ancestral Variation

4.3.1. Significance Tests (ANOVA)

A Procrustes ANOVA was used to test for significant differences amongst the population groups using the landmark and semi-landmark coordinates. The results of the Procrustes ANOVA with pooled sexes showed significant differences among black, coloured, white, and Indian South Africans (Table 4.4).

A Procrustes ANOVA was also used to assess the ancestral variation when males and females were assessed separately for the landmark and semi-landmark coordinates. The results of the Procrustes ANOVA for males and females showed significant differences amongst the population groups for both sexes (Tables 4.8).

Table 4.8. Results of the Procrustes ANOVA test for landmarks and semi-landmarks showing significant differences between female and male of the zygoma. Bold *p*-values indicate significant differences.

Landmarks		
	<i>Males</i>	<i>Females</i>
<i>p-value</i>	0.002	0.001
Semi-Landmarks		
	<i>Males</i>	<i>Females</i>
<i>p-Value</i>	0.001	0.001

A pairwise comparison was then performed as a post-hoc test to assess where the significant differences occurred amongst the populations (Table 4.9). Overall white and Indian South Africans demonstrated more similarities compared to other population groups except for males using landmarks where coloured and Indian South Africans demonstrated more similarities.

Table 4.9. Results of the pairwise post-hoc test to assess where population differences occurred. Bold indicates largest values.

Sex (Pooled)						
Landmarks						
	B and C	B and W	B and I	C and W	W and I	C and I
<i>p</i>-value	0.001	0.001	0.001	0.007	0.083	0.011
Semi-Landmarks						
<i>p</i>-value	0.001	0.001	0.001	0.001	0.086	0.002
Males						
Landmarks						
<i>p</i>-value	0.009	0.001	0.003	0.185	0.0248	0.190
Semi-Landmarks						
<i>p</i>-value	0.017	0.001	0.001	0.047	0.165	0.040
Females						
Landmarks						
<i>p</i>-value	0.001	0.001	0.002	0.001	0.085	0.011
Semi-Landmarks						
<i>p</i>-value	0.004	0.001	0.001	0.001	0.156	0.010

4.3.2. PCA and Wireframes

Similar to the exploration of sexual dimorphism, ancestral variation was assessed using PCA plots and wireframes. In the first PCA, all population groups (with the sexes pooled) were assessed for both landmark and semi-landmark coordinates. For the landmark coordinates, PC1 explained 35.7% of the total variation, while PC2 explained 11.1% of the total variation. For the semi-landmark coordinates, PC1 explained 20.73% of the total variation, while PC2 explained 13.2% of the total variation. The corresponding PCA plots showed that there was considerable overlap between all population groups. Coloured South Africans showed the most within-group variation, whereas black South Africans showed the least within-group variation for the manual landmark coordinates. However, white and Indian South Africans showed the most within-group variation for the semi-landmark coordinates (Figure 4.11). When the PC score loadings were assessed, *zygool* and *po* were shown to contribute the most variation to

PC1, while *zygoml* and *po* were shown to contribute the most variation to PC2 for the landmark coordinates (Table A7).

Wireframes showed that shape differences are present among the population groups (Figure 4.12). Black and white South Africans demonstrated differences between the length of the zygomaticomaxillary suture and the zygomaticotemporal suture. The inferior border of the zygoma as well as the inferior margin of orbit also differed between these populations. Black and coloured South Africans showed differences at the inferior margin of the orbit where the inferior margin of the orbit extended more inferiorly in coloured South Africans than black South Africans. The zygomaticotemporal suture also extended more laterally in black South Africans than coloured South Africans. When the black South Africans were compared to Indian South Africans, differences were noted at the zygomaticomaxillary and zygomaticotemporal sutures. The zygomaticotemporal suture appeared to be shorter in Indian South Africans, while the suture extended more posteriorly in black South Africans. Coloured and white South Africans were also compared and revealed major similarities except for the length of the zygomaticomaxillary suture and the inferior margin of the orbit. White and Indian South Africans revealed remarkable similarities, only differing slightly differences at the posterior margin of the frontal process. Coloured and Indian South Africans revealed similar wireframes, except where the coloured South Africans indicated a more superiorly projecting frontal process and a slightly more posteriorly projecting zygomaticotemporal suture.

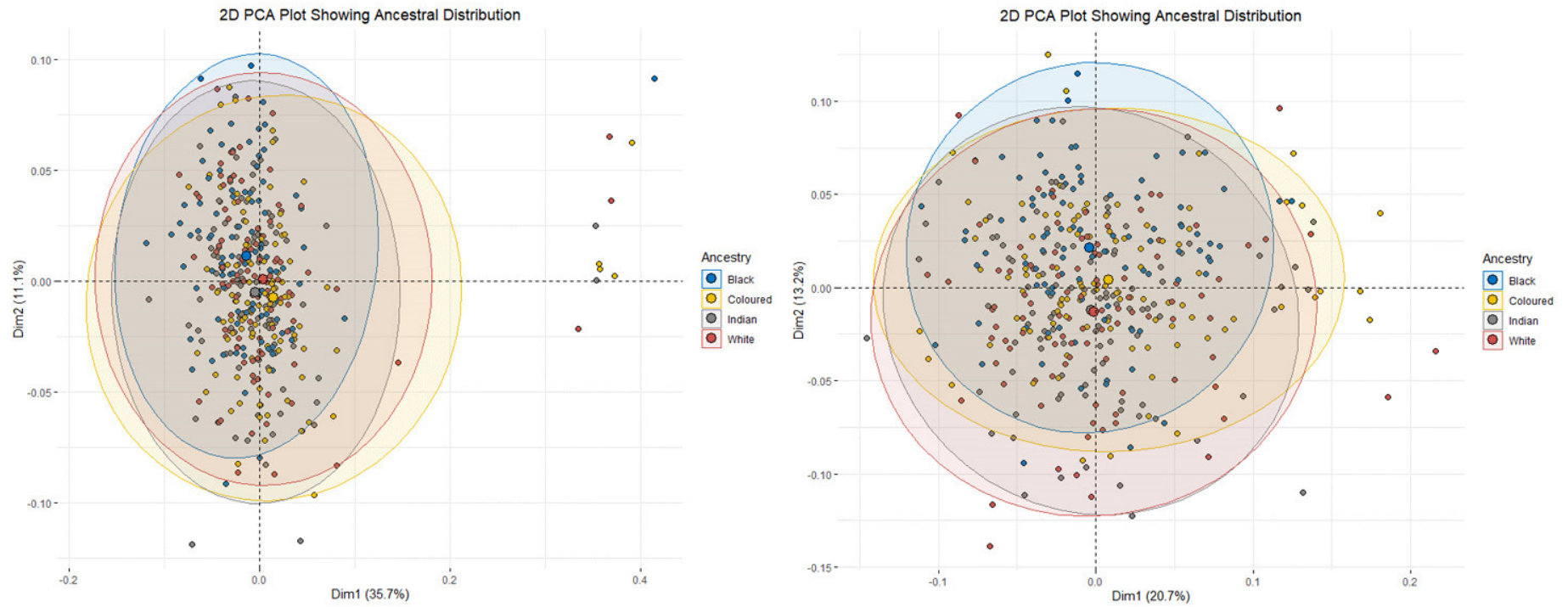


Figure 4.11. PCA plot showing ancestral variation (sexes pooled; set landmarks left, semi-landmarks right).

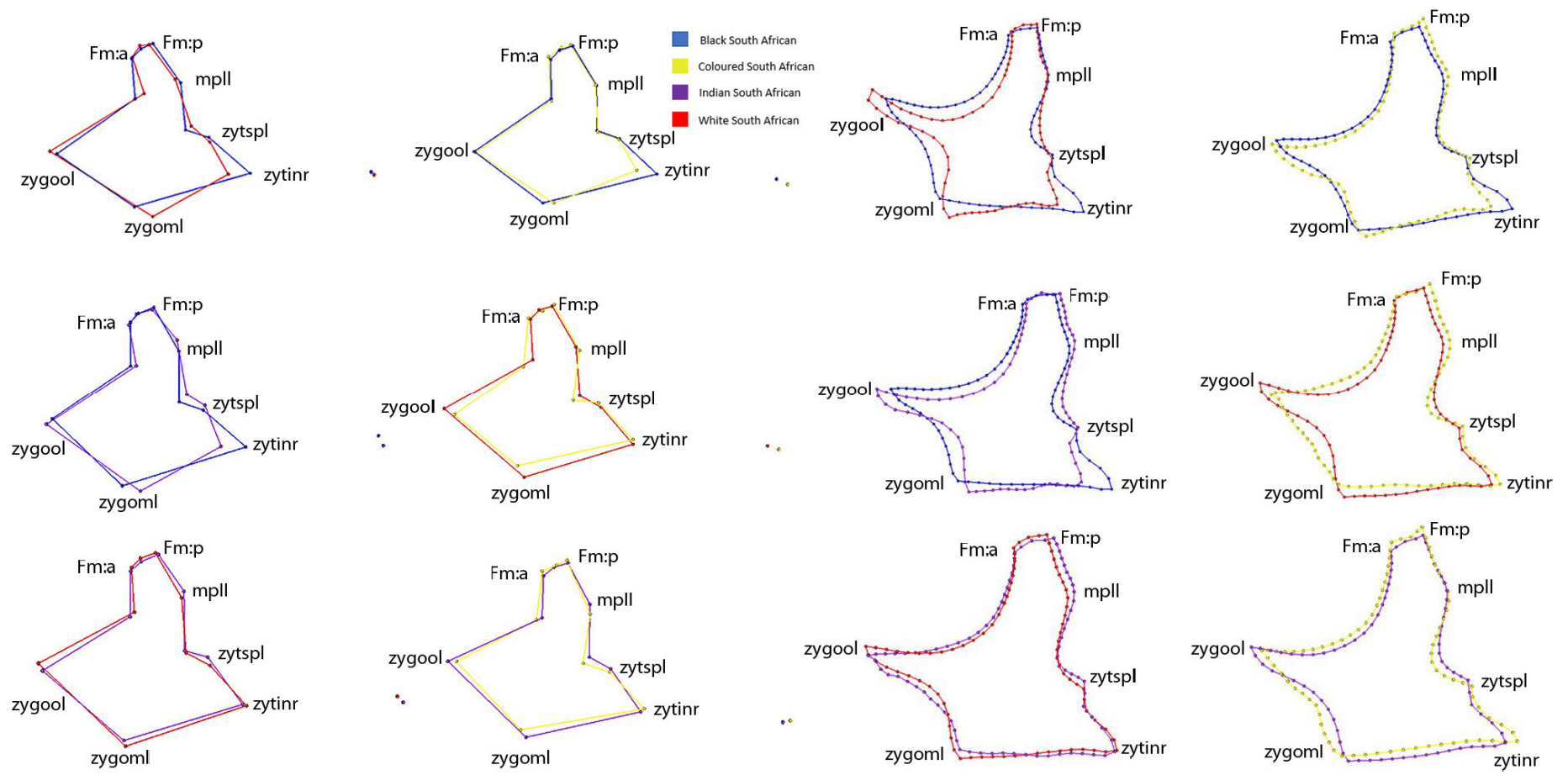


Figure 4.12. Wireframe graphs showing ancestral shape differences of the zygoma (sex combined; set landmarks left, semi-landmarks right).

An additional PCA was conducted to assess the shape variation of the zygoma when the sample is separated according to both sex and ancestry. The results for the PCA of male South Africans using the landmark coordinates, revealed that PC1 explained 42.90% of the total variation, while PC2 explained 9.3% of the total variation. For the semi-landmark coordinates, PC1 explained 20.26% of the total variation, while PC2 explained 12% of the total variation. The PCA plots illustrated extensive overlap amongst all of the population groups, with coloured and white South African males demonstrating the largest within-group variance, and black South African males the smallest within-group variance (Figure 4.13). *Zygool* and *po* were found to contribute the most to PC1, while *zytspl*, *zygool*, and *po* contributed the most to PC2 for the landmark coordinates (Table A8).

The wireframes created for the males revealed that black and white South Africans showed demonstrable differences at the shape of the zygomaticomaxillary suture and the zygomaticotemporal suture as well as at the inferior margin of the zygoma, which extended more inferiorly, and the frontal process, which extended more superiorly for white South Africans. The maximum height (*fmt to zygoml*) also appeared larger in black South Africans compared to white South Africans (Figure 4.7). Black and coloured South Africans differed at the zygomaticotemporal suture, which extended more laterally in black South Africans than coloured South Africans, and the frontal process, which extended more superiorly for coloured South Africans. The shape of the zygomaticomaxillary suture also differed between coloured and black South Africans. Marked differences in the shapes of the zygomaticomaxillary and zygomaticotemporal sutures were noted between black and Indian South Africans. A more inferiorly projecting inferior border of the zygoma was also noted in Indian South Africans compared to black South Africans. Coloured and white South Africans also showed substantial similarities in shape but differed at the zygomaticomaxillary and zygomaticotemporal sutures. The curve of the orbit was also noted to be different, with white South Africans presenting with a deeper curvature. White and Indian South Africans were compared and were nearly identical except for slight differences in the shape of the zygomaticomaxillary and zygomaticotemporal sutures were observed. The posterior margin of the frontal process was also larger in Indian South Africans. Coloured and Indian South Africans showed similarities in shape of the zygoma with only slight differences at the zygomaticomaxillary suture, zygomaticotemporal suture and frontal process.

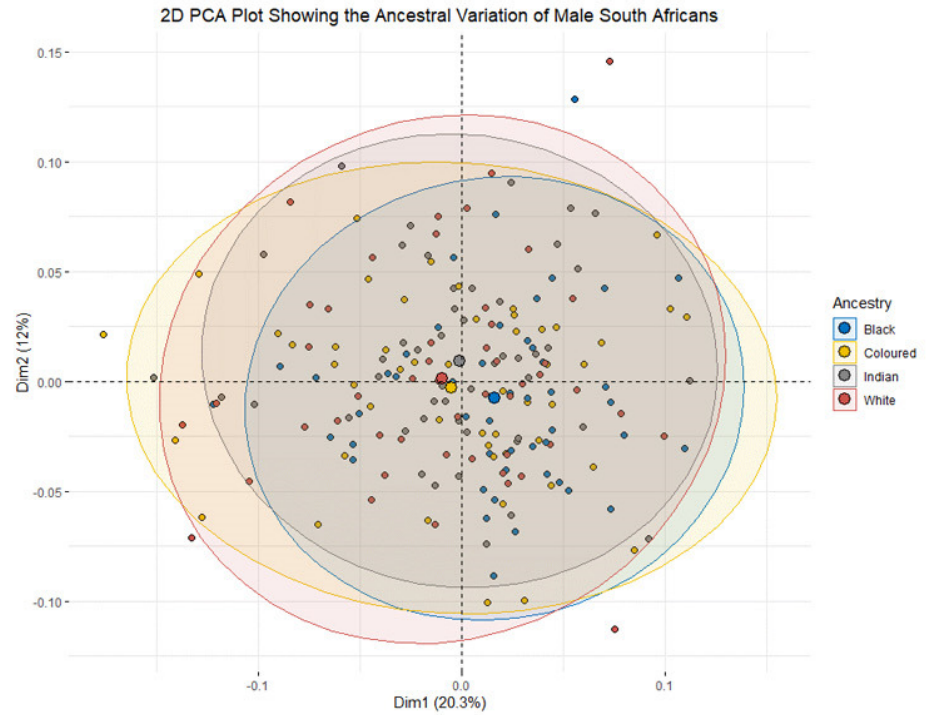
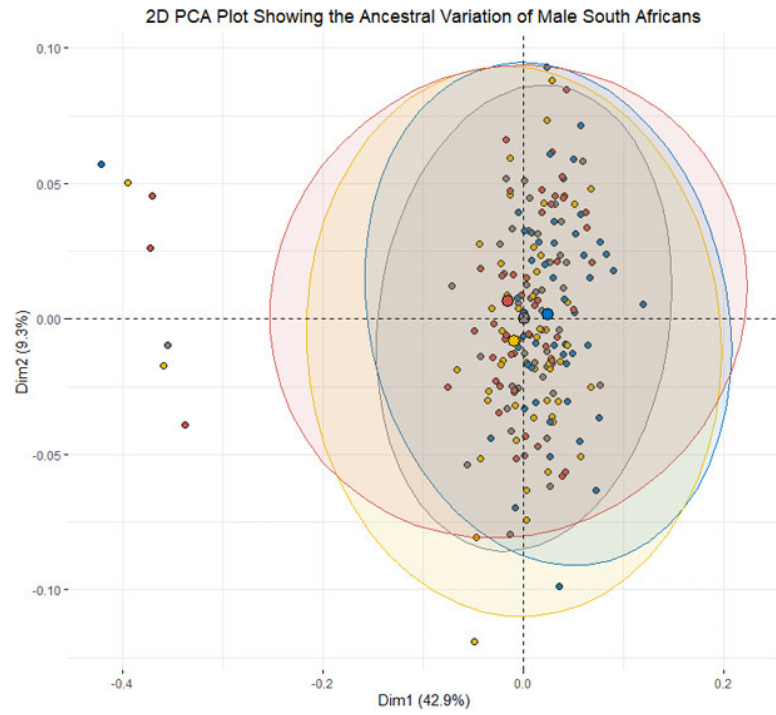


Figure 4.13. PCA plot showing ancestral variation (males; set landmarks left, semi-landmarks right).

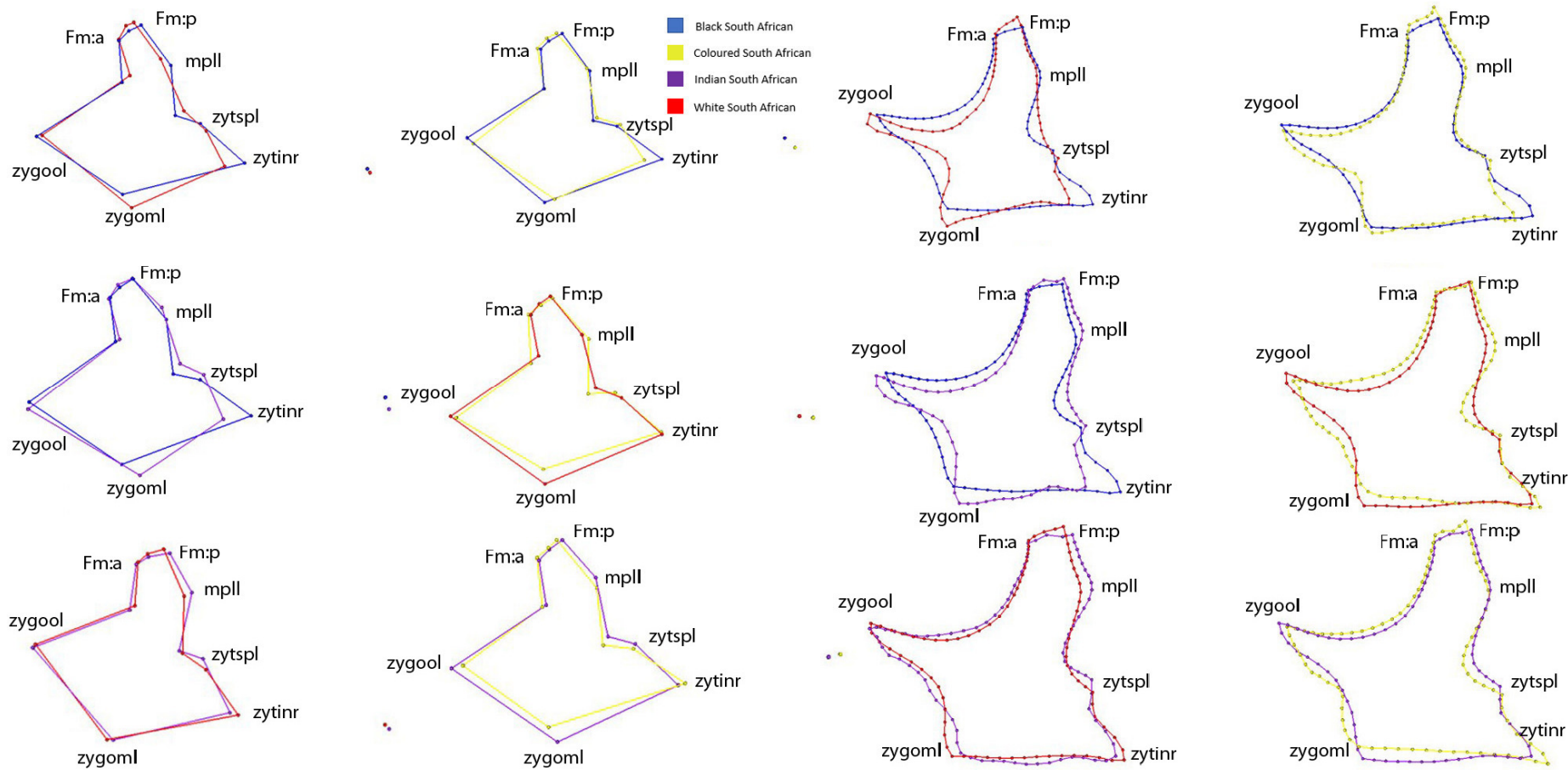


Figure 4.14. Wireframe graphs showing ancestral shape differences of the zygoma (males; set landmarks left, semi-landmarks right).

Results of the PCA exploring female South Africans revealed that PC1 explained 28.40% of the total variation, while PC2 explained 13% of the total variation for the landmark coordinates. For the semi-landmark coordinates, PC1 explained 22.37% of the total variation, while PC2 explained 15.4% of the total variation. The PCA plots revealed extensive overlap amongst all of the population groups. Similar to the males, coloured South Africans presented with the largest within-group variance, while black South African females had the smallest within-group variance for the landmark coordinates (Figure 4.14). In contrast, white and Indian South African females showed the largest within-group variation for the semi-landmark coordinates. *zygool* and *po* contributed the most variation to PC1, while *zytinr* and *zygoml* contributed the most variation to PC2 for male South Africans (Table A9).

The wireframes for female South Africans showed substantial differences between the shape of the zygomaticomaxillary suture and zygomaticotemporal suture between black and white South Africans (Figure 4.16). The orbit extended more inferiorly and had a deeper, more pronounced curvature in white South Africans compared to black South Africans. Black and coloured South Africans differed at the zygomaticotemporal suture, which extended more posteriorly in black South Africans than coloured South Africans. The orbit extended more inferiorly, and the posterior margin of the frontal process appeared larger in coloured South Africans compared to black South Africans. Marked differences in the shapes of the zygomaticomaxillary and zygomaticotemporal sutures were noted, and the orbit also extended more inferiorly and had a deeper curvature for Indian South Africans. Coloured and white South Africans also showed differences at the zygomaticomaxillary and zygomaticotemporal sutures, as well as the inferior margin of the orbit where white South Africans had a more pronounced curvature that extends more inferiorly. A difference was also noted at the inferior margin of the zygoma where white South Africans were larger than coloured South Africans. White and Indian South Africans showed slight differences in the shape of the orbit, where the orbit extended more inferiorly in Indian South Africans. Differences were also noted at the inferior margin of the zygoma, where white South Africans were larger than Indian South Africans. Coloured and Indian South Africans showed similarities in shape of the zygoma with only slight few differences in the shape of the zygomaticomaxillary and zygomaticotemporal sutures.

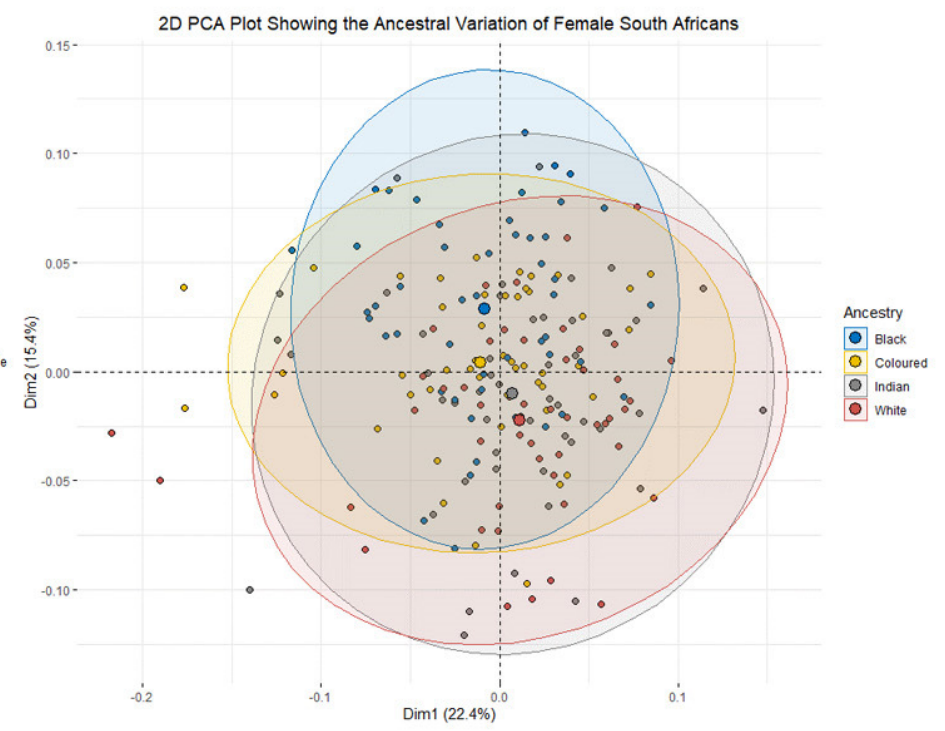
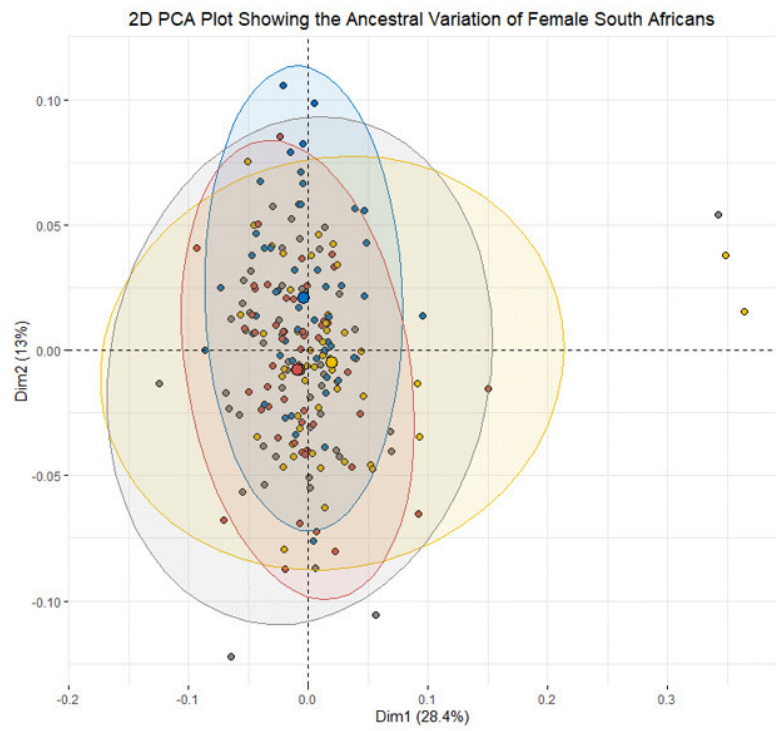


Figure 4.15. PCA plot showing ancestral variation (females; set landmarks left, semi-landmarks right).

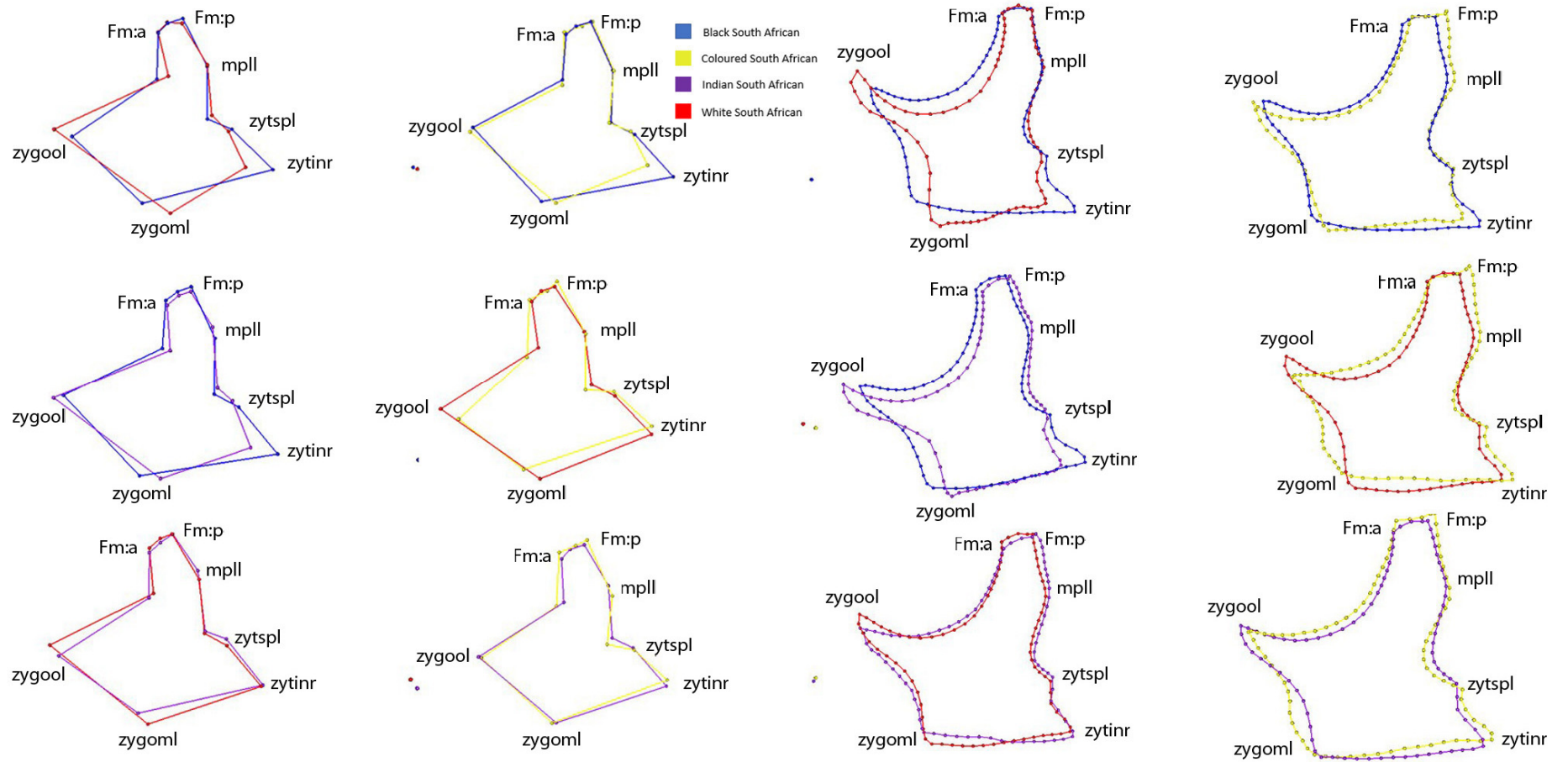


Figure 4.16. Wireframe graphs showing ancestral shape differences of the zygoma (females; set landmarks left, semi-landmarks right).

4.3.3. Linear Discriminant Analysis (LDA)

A discriminant analysis was conducted to assess the discriminatory strength of the landmarks and semi-landmarks when used to estimate ancestry (with the sexes pooled). Both males and females were combined, and only ancestral variation was assessed. All 26 PC scores were used and accounted for 100% of the variation. The results of the initial LDA showed a 65.48% accuracy. A backward stepwise selection was then used to remove any superfluous variables and the result showed an overall correct classification rate of 64.5%. LOOCV, was performed and yielded a correct classification rate of 53.8% (Table 4.10). Overall, black South Africans classified better than the other population groups (80.5%), with black female South Africans obtaining the highest correct classification rate (84%). The Indian South Africans had the overall lowest correct classification rate (49%), with the Indian females obtaining the lowest rate (47%).

The discriminant function using the semi-landmark coordinates to assess the ancestral variation yielded a 63% accuracy. After backward stepwise selection was used, an overall correct classification rate of 64% when estimating ancestry was obtained. A correct classification rate of 55.07% was achieved when LOOCV was performed. Overall, black South Africans again obtained the highest correct classification rate (74.5%). When looking at the individual correct classification rates black male and female South Africans had the highest classification rates, while coloured South Africans obtained the lowest accuracy (Table 4.11).

Table 4.10. Classification matrix for estimating ancestry using set landmarks. Bold indicates highest accuracy obtained.

	<i>B</i>	<i>C</i>	<i>W</i>	<i>I</i>	<i>%</i> <i>Correct</i>	<i>Overall</i> <i>Accuracy</i>	<i>LOOCV</i> <i>Accuracy</i>
<i>BM</i>	37	6	1	4	77%	64.5%	53.8%
<i>CM</i>	10	27	3	10	54%		
<i>WM</i>	3	5	37	4	76%		
<i>IM</i>	1	10	13	25	51%		
<i>BF</i>	42	3	0	5	84%		
<i>CF</i>	9	30	3	7	61%		
<i>WF</i>	1	5	33	11	66%		
<i>IF</i>	5	11	10	23	47%		

Table 4.11 Classification matrix for estimating ancestry using semi-landmarks. Bold indicates highest accuracy obtained

	<i>B</i>	<i>C</i>	<i>W</i>	<i>I</i>	<i>%</i> <i>Correct</i>	<i>Overall</i> <i>Accuracy</i>	<i>LOOCV</i> <i>Accuracy</i>
<i>BM</i>	35	7	2	4	73%	64%	55.07%
<i>CM</i>	14	21	8	7	42%		
<i>WM</i>	4	3	33	9	67%		
<i>IM</i>	3	6	11	29	59%		
<i>BF</i>	38	5	2	5	76%		
<i>CF</i>	8	31	4	6	63%		
<i>WF</i>	3	6	36	5	72%		
<i>IF</i>	6	9	5	29	59%		

4.4. Projection of the Zygoma

4.4.1. Interlandmark Distances

4.4.1.1 Descriptive Statistics

The number of individuals per group, the mean, and standard deviation were calculated for each population group and sex (Table 4.12). The descriptive statistics allowed for a broad inspection of the ancestral variation and sexual dimorphism of the three interlandmark distances.

Overall, the means and standard deviations were higher for the males when compared to females. White South Africans displayed the largest means and standard deviations when compared to other population groups, while Indian South Africans displayed the smallest means and standard deviations.

Table 4.12. A summary of the descriptive statistics for the three interlandmark distances comparing both ancestry and sex. *n* = number of individuals; *SD* = Standard deviation.

	Black South African						Coloured South African					
	BM			BF			CM			CF		
	<i>n</i>	Mean	<i>SD</i>	<i>N</i>	Mean	<i>SD</i>	<i>n</i>	Mean	<i>SD</i>	<i>n</i>	Mean	<i>SD</i>
PorZygoml	48	68.752	3.883	50	68.609	3.901	50	68.914	3.697	49	68.886	3.719
ZML	48	29.022	4.622	50	28.737	4.588	50	29.578	4.903	49	29.730	4.926
PorZygool	48	83.415	4.326	50	83.237	4.375	50	85.312	4.220	49	85.419	4.231
	White South African						Indian South African					
	WM			WF			IM			IF		
	<i>N</i>	Mean	<i>SD</i>	<i>N</i>	Mean	<i>SD</i>	<i>n</i>	Mean	<i>SD</i>	<i>n</i>	Mean	<i>SD</i>
PorZygoml	49	69.226	4.673	50	66.412	5.058	49	66.770	4.135	49	65.601	4.141
ZML	49	31.620	4.226	50	30.724	4.046	49	30.839	3.745	49	29.509	4.155
PorZygool	49	86.257	4.206	50	83.591	4.523	49	83.694	3.826	49	81.846	4.302
	Ancestry (sexes pooled)						Sex (pooled populations)					
							Males			Females		
	<i>N</i>	Mean	<i>SD</i>	<i>N</i>	Mean	<i>SD</i>	<i>n</i>	Mean	<i>SD</i>	<i>n</i>	Mean	<i>SD</i>
PorZygoml	394	67.152	4.361	394	67.152	4.361	196	68.879	4.207	198	65.444	3.812
ZML	394	29.516	4.383	394	29.516	4.383	196	30.826	4.293	198	28.218	4.084
PorZygool	394	83.182	4.484	394	83.182	4.484	196	85.283	4.062	198	81.102	3.879

4.4.1.2. Significance Tests (ANOVA)

An ANOVA was run to assess the sexual dimorphism of the interlandmark distances when the population groups were combined. The results indicated significant differences between males and females for all three interlandmark distances (Table 4.13). Ancestral variation of the interlandmark distances was also assessed when males and females were combined. The results showed significant differences for all three interlandmark distances (Table 4.13).

An ANOVA was then run to assess sexual dimorphism of each ancestry group individually. Results revealed significant differences between males and females for all ancestry groups across all three interlandmark distances, except for white South Africans at *ZML* (p -value = 0.202; Table 4.14).

Result of the assessment of the ancestral variation between male and female interlandmark distances separately showed significant differences for all interlandmark distances amongst the population groups for females except for *PorZygool* (p -value = 0.0945) and significant differences for all interlandmark distances amongst population groups for males except for *ZML* (p -value = 0.151; Table 4.15).

Table 4.13. p-values for the ANOVA test showing significant differences of the interlandmark distances in combined sex and ancestry of the zygoma. Bold indicates significant differences.

Interlandmark Distance	<i>Sex Differences</i>	<i>Ancestry Differences</i>
<i>PorZygool</i>	<2e-16	0.004
<i>PorZygoml</i>	<2e-16	6.22e-06
<i>ZML</i>	7.74e-12	0.000

Table 4.14. ANOVA results showing significant differences of the interlandmark distances between the population groups to test for sexual dimorphism of the zygoma. Bold indicates significant differences.

Interlandmark Distance	<i>Black South Africans</i>	<i>Coloured South Africans</i>	<i>White South Africans</i>	<i>Indian South Africans</i>
<i>PorZygool</i>	1.84e-07	1.52e-07	7.57e-07	9e-06
<i>PorZygoml</i>	1.16e-05	1.55e-06	1.03e-06	0.005
<i>ZML</i>	2.52e-06	0.002	0.202	0.001

Table 4.15. *p*-values for the ANOVA test showing significant differences of the interlandmark distances between females and males of the zygoma. Bold indicates significant differences.

Interlandmark Distance	Males	Females
<i>PorZygool</i>	0.012	0.0945
<i>PorZygoml</i>	0.000	0.001
<i>ZML</i>	0.151	7.34e-06

4.4.1.3. Tukey's Post Hoc Analysis

A Tukey's HSD *post hoc* test was conducted to determine among which population groups significant differences occurred with ANOVA (with the sexes combined) for the three interlandmark distances. The results showed significant differences for *PorZygoml* between black and white South Africans, between coloured and Indian South Africans, and between black and Indian South Africans (Figure A1; Table 4.16). Significant differences were observed for *ZML* between black and white South Africans, white and Indian South Africans, and white and coloured South Africans (Figure A2). Significant differences were also noted for *PorZygool* between white and Indian South Africans (Figure A3).

When assessing the males for each population group, the Tukey's HSD results revealed significant differences for *PorZygoml* between coloured and Indian South Africans, between black and Indian South Africans, and between white and Indian South Africans (Figure A4; Table 4.16). No differences were noted amongst the groups for *ZML* (Figure A5). Lastly, for *PorZygool* significant differences were noted between white and Indian South Africans (Figure A6).

Finally, when assessing the females for each population group, the Tukey's HSD results revealed significant differences for *PorZygoml* between black and white South Africans and black and Indian South Africans (Figure A7; Table 4.16). For *ZML* significant differences were noted between white and black South Africans, between Indian and white South Africans, and between white and coloured South Africans (Figure A8). For *Porzygool* no groups showed any significant differences (Figure A9).

Table 4.16. Breakdown of group overlap for interlandmark distances based on ANOVA and Tukey's HSD. B = Black; C = Coloured; W = White; I = Indian.

Sex (pooled)						
No overlap	B and C	B and W	B and I	C and W	W and I	C and I
		PorZygoml ZML	PorZygoml	ZML	ZML PorZygoool	PorZygoml
Males						
ZML			PorZygoml		PorZygoml PorZygoool	PorZygoml
Females						
PorZygoool		PorZygoml ZML	PorZygoml	ZML	ZML	

4.4.1.4. Linear Discriminant Analysis (LDA)

4.4.1.4.1. Sexual Dimorphism

A discriminant function was created to assess the ability of the interlandmark distances to classify sex when population groups were combined. The function resulted in an overall correct classification rate of 72.08%. A male sex bias was noted (73%). Black South African males (85%) and Indian South African females (78%) achieved the highest correct classification rates. After backward stepwise selection was performed, the combination of *PorZygoool*, *PorZygoml* and *ZML* resulted in a correct classification rate of 72.08%. LOOCV was then performed using the stepwise selected variables and correct classification rate of 71% was obtained (Table 4.17).

Table 4.17. Classification matrix for estimating sex from interlandmark distances. Bold indicates highest accuracy obtained.

	M	F	% Correct	Average Accuracy	Overall Accuracy	LOOCV Accuracy
<i>BM</i>	41	7	85%	73%	72.08%	71%
<i>CM</i>	36	13	73%			
<i>WM</i>	38	11	78%			
<i>IM</i>	27	22	55%			
<i>BF</i>	13	37	74%	72%		
<i>CF</i>	13	36	73%			
<i>WF</i>	18	32	64%			
<i>IF</i>	11	38	78%			

4.4.1.4.2. Ancestral Variation

A discriminant function was created to assess the ability of the interlandmark distances to classify ancestry when the sexes were combined. The initial function resulted in a correct

classification rate of 42.25%. Overall, black South Africans had the highest correct classification rate (50%), while Indian South Africans had the lowest correct classification rate (37%), with Indian males having the lowest correct classification rate of all subgroups (27%; Table 4.18). Coloured females demonstrated the highest classification accuracy of the female subgroups (49%). Backward stepwise selection selected all three variables for the function and resulted in a correct classification rate of 40.1%. LOOCV was then performed using the variables from the stepwise selection and achieved a correct classification rate of 38.32%.

Table 4.18. Classification matrix for estimating ancestry from interlandmark distances. Bold Indicates highest accuracy obtained.

	<i>B</i>	<i>C</i>	<i>W</i>	<i>I</i>	<i>% Correct</i>	<i>Overall Accuracy</i>	<i>LOOCV Accuracy</i>
<i>BM</i>	31	5	10	2	64%	40.1%	38.32%
<i>CM</i>	12	20	16	2	40%		
<i>WM</i>	16	12	18	3	37%		
<i>IM</i>	10	13	13	13	27%		
<i>BF</i>	16	18	4	12	36%		
<i>CF</i>	8	22	4	15	49%		
<i>WF</i>	4	12	15	19	38%		
<i>IF</i>	8	13	5	23	47%		

4.4.2. Angle of Projection

4.4.2.1. Mean Angles

Angles created between the measurements were used to further assess the anterior projection of the zygoma (Figure 3.3). The largest mean value noted for *Angle1* was for coloured South African females, whereas the smallest mean value noted for *Angle1* was for black South African males. The largest mean value observed for *Angle2* was for black South African males, whereas the smallest mean value was observed for white South African females. The largest mean value for *Angle3* was for white and Indian South African males, whereas the smallest value was for coloured South Africans (Table 4.19). Male South Africans obtained the largest mean values for *Angle2* and *Angle3*; however, female South Africans obtained the largest mean value for *Angle1* (Table 4.20).

Table 4.19. Angles of projection for ancestry when sexes were pooled and separated (°). Bold indicates largest mean.

<i>Sex (pooled)</i>				
<i>Angle</i>	<i>B</i>	<i>C</i>	<i>W</i>	<i>I</i>
Angle1	110.5	114.0	112.8	113.0
Angle2	50.5	47.5	47.4	47.4
Angle3	18.9	18.5	19.8	19.6
Males				
Angle1	110.4	113.9	112.1	112.8
Angle2	50.6	47.6	48.0	47.3
Angle3	19.0	18.5	19.9	19.9
Females				
Angle1	110.7	114.0	113.6	113.2
Angle2	50.4	47.4	46.7	47.5
Angle3	18.8	18.5	19.7	19.4

Table 4.20 Angles of projection for the sexes when populations were pooled (°).

<i>Angle</i>	<i>M</i>	<i>F</i>
Angle1	112,3	112,9
Angle2	48,4	48,0
Angle3	19,3	19,1

4.4.2.2. Significance Tests (ANOVA)

An ANOVA was run to assess the sexual dimorphism of the angles when the population groups were combined. The results indicated significant differences between males and females for all three angles (Table 4.21). An ANOVA was also run to assess the ancestral variation of the angles when both males and females were combined. The results of the ANOVA showed significant differences for all three angles (Table 4.21).

An ANOVA was then run to assess sexual dimorphism of each ancestry group, individually. The results of the ANOVA tests revealed significant differences between males and females of black and coloured South Africans for *Angle1* and *Angle3* and significant differences for white South Africans for *Angle2* (Table 4.22).

To assess the ancestral variation between males and females separately, an ANOVA was run. The results of the ANOVA showed significant differences for all angles amongst the population groups for both males and females (Table 4.23).

Table 4.21. *p*-values for the ANOVA test showing significant differences of the angles in sex and ancestry. Bold indicates significant differences.

Angles of Projection	Sex Differences	Ancestry Differences
Angle1	0.000	2.33e-07
Angle2	0.024	3.06e-08
Angle3	0.000	1.34e-05

Table 4.22. ANOVA results showing significant differences of the angles of projection between the different population groups to test for sexual dimorphism. Bold indicates significant differences.

Angles of Projection	Black South Africans	Coloured South Africans	White South Africans	Indian South Africans
Angle1	0.000	0.0398	0.073	0.392
Angle2	0.0945	0.266	0.0422	0.974
Angle3	6.44e-05	0.0368	0.798	0.073

Table 4.23. *p*-values for the ANOVA test showing significant differences of the angles of projection between females and males. Bold indicates significant differences.

Angles of Projection	Males	Females
Angle1	8.34e-06	0.008
Angle2	0.000	0.000
Angle3	0.0116	1.4e-05

4.4.2.3. Tukey's Post Hoc Analysis

A Tukey's HSD *post hoc* test was conducted to determine among which population groups significant differences occurred with ANOVA when the sexes were combined for the three angles. The results showed significant differences for *Angle1* between black and white South Africans, between black and coloured South Africans, and between black and Indian South Africans (Figure A10; Table 4.24). Significant differences were observed for *Angle2* between black and white South Africans, black and coloured South Africans, and black and Indian South

Africans (Figure A11). Significant differences were also noted for *Angle3* between black and coloured South Africans, coloured and white South Africans, and coloured and Indian South Africans (Figure A12).

A Tukey’s HSD was run on the population groups of male South Africans, the results revealed significant differences for *Angle1* between black and white South Africans, between black and coloured South Africans, and between black and Indian South Africans (Figure A13; Table 4.24). Significant differences were observed for *Angle2* between black and white South Africans, black and coloured South Africans, and between black and Indian South Africans (Figure A14). Lastly, for *Angle3* significant differences were noted between black and coloured South Africans (Figure A15).

Finally, a Tukey’s HSD was run on the population groups of female South Africans, the results revealed significant differences for *Angle1* between black and coloured South Africans (Figure A16; Table 4.24). For *Angle2* significant differences were noted between black and white South Africans, black and coloured South Africans, and between black and Indian South Africans (Figure A17). For *Angle3* significant differences were noted between black and white South Africans and coloured and white South Africans (Figure A18).

Table 4.24. Breakdown of group overlap for angles of projection based on ANOVA and Tukey’s HSD. B = Black; C = Coloured; W = White; I = Indian.

Sex (pooled)						
<i>No overlap</i>	B and C	B and W	B and I	C and W	W and I	C and I
	Angle1 Angle2 Angle3	Angle1 Angle2	Angle1 Angle2	Angle3		Angle3
Males						
	Angle1 Angle2 Angle3	Angle1 Angle2	Angle1 Angle2			
Females						
	Angle1 Angle2	Angle2 Angle3	Angle2	Angle3		

4.4.2.4. Linear Discriminant Analysis (LDA)

4.4.2.4.1. Sexual Dimorphism

A discriminant function was created using PC scores to assess the ability of the angles to classify sex when population groups were combined. The function resulted in an overall correct

classification rate of 58%. Females achieved a higher correct classification rate compared to males (59%). Black South African males (77%) and coloured South African females (75.5%) achieved the highest correct classification rates. After backward stepwise selection was performed, two PC scores were used and resulted in a correct classification rate of 58%. LOOCV was then performed using the stepwise selected variables and correct classification rate of 57% was obtained (Table 4.25).

Table 4.25. Classification matrix for estimating sex from angles of projection. Bold indicates highest accuracy obtained.

	<i>M</i>	<i>F</i>	<i>% Correct</i>	<i>Average Accuracy</i>	<i>Overall Accuracy</i>	<i>LOOCV Accuracy</i>
<i>BM</i>	37	11	77%	58%	58%	57%
<i>CM</i>	19	31	38%			
<i>WM</i>	31	18	63%			
<i>IM</i>	26	23	53%			
<i>BF</i>	20	30	60%	59%		
<i>CF</i>	12	37	75.5%			
<i>WF</i>	27	23	46%			
<i>IF</i>	22	27	55%			

4.4.2.4.2. Ancestral Variation

A discriminant function was created using PC scores to assess the ability of the angles to classify ancestry when the sexes were combined. The initial function resulted in a correct classification rate of 38%. Overall, black South Africans had the highest correct classification rate (50%), while Indian South Africans had the lowest correct classification rate (7%), with Indian males having the lowest correct classification rate of all subgroups (4.1%; Table 4.26). Coloured females demonstrated the highest classification accuracy of the female subgroups (57%). Backward stepwise selection selected two PC scores for the function and resulted in a correct classification rate of 37.5%. LOOCV was then performed using the variables from the stepwise selection and achieved a correct classification rate of 37%.

Table 4.26. Classification matrix for estimating ancestry from the angles of projection. Bold indicates highest accuracy obtained.

	<i>B</i>	<i>C</i>	<i>W</i>	<i>I</i>	<i>% Correct</i>	<i>Overall Accuracy</i>	<i>LOOCV Accuracy</i>
<i>BM</i>	29	5	12	2	60%	37.5%	37%
<i>CM</i>	15	19	15	1	38%		
<i>WM</i>	16	12	21	0	43%		
<i>IM</i>	10	15	22	2	4.1%		
<i>BF</i>	20	20	9	1	40%		
<i>CF</i>	12	28	7	2	57%		
<i>WF</i>	9	14	24	3	48%		
<i>IF</i>	9	22	13	5	10%		

CHAPTER 5: DISCUSSION

Sexual dimorphism and ancestral variation of the zygoma have been explored among South Africans in the past but have not included Indian South Africans and further research on the zygoma including all four major socially constructed population groups in South Africa was needed. Therefore, the current research aimed to assess the zygoma through both manual set landmarks and semi-landmarks between black, coloured, white and Indian South Africans so that when fragmentary remains are found, a presumptive identification is still possible so that a semblance of closure can be brought to families. The current study was the first to assess the facial variation of Indian South Africans, thereby providing insight into the variation of the population when compared to other populations in South Africa. Furthermore, the current study aimed to assess whether the zygoma could classify individuals according to sex and ancestry to help estimate the biological profile (sex, age, stature, and ancestry) during analysis of unknown remains.

5.1. Shape Variation of the Zygoma

Size differences of the zygoma have been observed between sexes and amongst populations in South Africa (Muller 2018; Tawha *et al.* 2020). Results revealed that the most variation for both sex and ancestry is attributable to the zygomaticomaxillary suture. The zygomaticomaxillary suture is situated between the zygomatic bone and maxilla on either side of the nasal bones and creates an irregular course as it passes between the two bones (Sholts & Wärmländer 2012). L'Abbé *et al.* (2011) showed that significant differences were present between black, white and coloured South Africans for the zygomaticomaxillary suture shape. While the study conducted by L'Abbé *et al.* (2011) analysed the shape of the zygomaticomaxillary suture shape, the current study did not. L'Abbé *et al.* (2011) studied three suture shapes (Angled, Smooth and S-shaped) in black, coloured and white South Africans. Black, coloured and white South Africans presented with a smooth zygomaticomaxillary suture. However, white South Africans had an equal distribution of smooth and angled zygomaticomaxillary sutures. An angled zygomaticomaxillary suture has a lateral projection near the midline and a smooth zygomaticomaxillary shape has a lateral projection near the inferior border (L'Abbé *et al.* 2011). Therefore, inferences can be made that the location of the landmarks on either end of the suture may differ depending on the shape of the zygomaticomaxillary suture.

Additionally, the current study demonstrated differences at the zygomaticomaxillary suture (longer in males compared to females and amongst populations), zygomaticotemporal (more lateral projection in males compared to females and amongst populations), and frontomalar sutures (more superiorly placed in females compared to males). Differences were also noted along the lateral margin of the orbit with a more inferior placement in females which is consistent with previous research (Tawha *et al.* 2020). Overall, females appeared smaller than males. However, the study did not compare centroid sizes indicating that some of the differences observed could be due to size differences between males and females. The differences observed between sexes may have also been caused by the extended maturation period in males compared to females (Rogers 2005). Evidence suggests that the extended growth of the zygoma in males causes a larger zygoma and more laterally displaced zygomatic arch in males compared to females further explaining the more laterally projecting zygomaticotemporal suture in males (Rogers 2005). Furthermore, the lateral placement of the zygomatic arch could be in part due to the size of the temporalis muscle. The temporalis muscle has an origin at the floor of the temporal fossa as well as the deep surface of the temporal fascia. The muscle then inserts on the coronoid process' medial surface and the anterior surface of the mandible (Moore *et al.* 2014). The growth of the nasal bones and the maxilla also affect the growth and development of the zygoma as the three bones work together as a complex which may explain the variation observed at the orbit (Enlow 1982).

The orbit undergoes maturation at an earlier stage than other bones of the craniofacial region indicating a smaller degree of sexual dimorphism (Barbeito-Andre *et al.* 2016). Although the orbit forms part of the craniofacial complex, the sexual dimorphism observed at the orbit in the current study is unlikely to have been caused by the sexual dimorphism of the orbit itself, impart due to the earlier maturation rate decreasing the sexual dimorphism observed. However, the variation of the orbit and the zygomaticomaxillary suture may be due to the location of the landmarks. Females displayed a smaller/shorter zygomaticomaxillary suture length, which may explain the sexual dimorphism observed at the orbit. The result in part could be due to the scaling of the data during Procrustes superimposition. The size and shape of the orbit may be the same in males and females but because of the scaling, a smaller zygoma in females may make the orbit appear larger in females. As stated previously, the shape of the zygomaticomaxillary suture may have also played a role in the variation observed between males and females (L'Abbé *et al.* 2011). Previous research has also demonstrated differences for the length of the zygomaticomaxillary suture between black and white South

African males and females where males presented with a longer zygomaticomaxillary suture length (Muller 2018).

Growth of the zygoma occurs by the deposition of bone on the posterior surface of the zygoma and resorption on the anterior surface (Enlow & Hans 1996; Oettlé *et al.* 2017). The zygoma then becomes displaced inferiorly due to sutural growth, relative to the frontomalar suture providing an explanation as to why the frontomalar suture is more superior in females (Enlow 1996; Oettlé *et al.* 2017). As males undergo a longer maturation period, a more inferior displacement of the zygoma occurs when compared to females. Differences have been noted between males and females across studies and indicate that sexual dimorphism of the zygoma is most likely due to the different maturation rates of males and females (Rogers 2005; Schlager & Rüdell 2017; Muller 2018; Tawha *et al.* 2020).

Significant differences were noted between sexes for all groups except coloured South Africans ($p = 0.107$). The nasal aperture of black, coloured and white South Africans indicate that white South Africans have a higher degree of sexual dimorphism whereas coloured South Africans had a lower degree of sexual dimorphism, consistent with the results obtained in the current study (McDowell 2012). However, research on the postcrania of black, white and coloured South Africans indicate that coloured South Africans have a higher degree of sexual dimorphism and white South Africans have a lower degree of sexual dimorphism with black South Africans intermediate (Krüger *et al.* 2017), inconsistent with the current results. The contradictory results of the crania versus the postcrania of the population groups may be because coloured South Africans have contributions from indigenous Khoi and San populations, Asian populations, Bantu-speaking Africans and Europeans (de Wit *et al.* 2010). Furthermore, the crania of white females misclassify as males more frequently than the postcrania demonstrating the differing levels of sexual dimorphism of the populations (L'Abbé *et al.* 2013b).

While variation observed between sexes can be attributed to differing maturation rates, ancestral variation is more complex as the population history of South Africa is intricate. The intentional and forced migration of different populations to South Africa as well as the decreased amount of admixture during the *Apartheid* era may have increased the amount of observed variation attributable to ancestry (McDowell 2012). Admixture between white South Africans and the other population groups was forbidden under the Prohibition of Mixed Marriages Act of 1949 and Immorality Act of 1950, limiting the amount of gene flow between

white South Africans and other socially identified groups. While the Prohibition of Mixed Marriages Act of 1949 and Immorality Act of 1950 were put to an end in 1991, restrictions continued due to social constraints (Jacobson *et al.* 2004; Liebenberg 2015).

Black South Africans demonstrated the greatest differences when compared to the other population groups. In contrast, coloured, white and Indian South Africans demonstrated similarities and only slight differences when compared. The results are inconsistent with previous research on the cranium amongst black, coloured, and white South Africans. Stull *et al.* (2014) indicated that black and coloured South African crania were most similar in shape, whereas white and coloured South Africans were more similar in size (Stull *et al.*, 2014). Evidence suggests that the inclusion of zygomatic variables to the standard craniometric variables may better discern between population groups compared to the zygomatic variables on their own. The differences observed between black South Africans and the other population groups may be due to the original geographical locations of the populations. Coloured, white and Indian South Africans have parent groups from Europe and Asia, whereas black South Africans are the only group to have origins entirely attributable to the African continent. Although coloured South Africans have a major contribution from indigenous Khoi and San populations, which are also African groups, there are still major differences among the groups. Differences were also noted at the zygomaticomaxillary, zygomaticotemporal and, frontomalar sutures as well as the orbits amongst the populations studied. The differences noted at the zygomaticotemporal and frontomalar sutures are comparable to past research on black and white South Africans. Muller (2018) found variation in the length of the sutures between black and white South Africans. Black South Africans presented with longer suture lengths compared to white South Africans consistent with the current research (Muller 2018). Furthermore, Tawha *et al.*, (2020) found that individuals of mixed ancestry (coloured South Africans) and European ancestry (white South Africans) presented with similar shape profiles of the zygoma consistent with the current study. Previous craniometric and geometric morphometric studies, however, noted that separation into population groups based on nasal aperture grouped black and coloured South Africans together and white South Africans on their own (McDowell 2012). Considering that the nasal aperture forms part of the craniofacial complex, one would expect similar results. The differences in results could be due to the use of one variable (size or shape) at a time, in the current study, which limit the amount of information provided. Further research combining shape and size of the zygoma simultaneously may provide further insight into ancestral variation.

Projection of the zygoma was thought to be a contributing factor to both sexual dimorphism and ancestral variation (Oettlé *et al.* 2017). Individuals in colder environments tend to have a larger projection of the zygoma compared to warmer environments, indicating that environment plays a role in the projection of the zygoma (Oettlé *et al.* 2017). Previous research has used multiple methods, such as Bass's (1995) and Vitek's (2012) methods, to assess the projection of the zygoma; however, interlandmark distances have yet to be used. The current study made use of three interlandmark distances to assess the anterior projection of the zygoma. Results demonstrated differences between sexes and amongst populations. However, *ZML* was not significant for white South Africans, indicating that the interlandmark distance is not highly sexually dimorphic between males and females of white South Africans, which is inconsistent with the linear distance observed with caliper measurements (Muller 2018). Muller (2018) obtained the maximum linear distance from *zygool* to *zygoml* to create the zygomaticomaxillary length (*ZML*), whereas, in the current study, landmarks were digitally placed and the interlandmark distance calculated from there which, could have created the inconsistent result obtained between the studies. The lack of difference between males and females of white South Africans for *ZML* does not have a direct indication of the projection of the zygoma as the interlandmark distance is measuring the maximum length of the zygoma from *zygool* to *zygoml*, in the population. The interlandmark distance does, however, have an impact on the size of the zygoma in the population.

When further analysing the projection of the zygoma, the interlandmark distances *Porzygool* and *ZML* were also not significantly different for males and females, respectively. The results were inconsistent with the findings by L'Abbé *et al.* (2011) for the projection of the zygoma, where significant differences were noted amongst black, coloured, and white South Africans. However, the trait was also found to not be repeatable when studied by L'Abbé *et al.* (2011). The current study relied on landmarks to calculate interlandmark distances in relation to *po*, whereas the previous study relied on Bass's method to analyse the projection of the zygoma (L'Abbé *et al.* 2011). Bass's method uses a pencil placed horizontally across the nasal aperture and scores the projection of the zygoma (Bass 1995; Oettlé *et al.* 2017). The anterior projection of the zygoma was assessed in both the study by L'Abbé *et al.* (2011) and the current study; Further research using interlandmark distances in relation to the nasal aperture may provide useful information on the projection of the zygoma. Furthermore, sexual dimorphism was not analysed in the study conducted by L'Abbé *et al.* (2011). Other landmarks contributing to the projection of the zygoma, such as those surrounding the nasal region or

other landmarks from the zygoma, were not used in the current study. Therefore, while the current study was not able to find perceptible differences in the projection, further analyses incorporating more landmarks from the midfacial region may be able to note variation.

Projection of the zygoma was further explored using angles calculated between the interlandmark distances. Coloured South Africans demonstrated the largest mean value for *Angle1* demonstrating that *zygool* projects more anteriorly in coloured South Africans and that coloured South Africans present with a flatter facial projection consistent with a retreating zygoma (L'Abbé *et al.* 2011). The effect of climate has been known to affect the projection of the face (Oettlé *et al.* 2017). Secular trends could have also had an effect on the zygoma's projection. Migration from the homeland to another country causes an adaptation to the new environment causing changes in both the genotype and phenotype of the population group and is called secular change (Relethford 2004; Spradley 2006). The projection of the cheek has been linked to environmental conditions. A greater cheek projection has been observed in colder environments along with masticatory stress (Oettlé *et al.*, 2017). Therefore, adaptation to a new environment could have caused the variation observed for zygomatic projection. Results obtained in the current study for the projection of the zygoma were not comparable to past research due to the differences in methodology. Environmental conditions may have played a role. However, adaptation to the environment occurs over time. Evidence shows that short term evolutionary changes occur as an adaptation to the environment but do not accumulate over time. Research demonstrates that evolutionary adaptations can take up to one million years to accumulate and be a lasting change (Uyeda *et al.* 2011). Furthermore, the facial skeleton demonstrates adaptations to the environment but the adaptations cannot conceal population history and structure (Relethford 2004; Harvati & Weaver 2006). Therefore, the possibility of geographical adaptation accounting for variation observed for the projection of the zygoma is unlikely. A more likely explanation is that population admixture amongst population groups may have caused the variation observed.

5.2. Forensic Application of the Zygoma

Sexual dimorphism and ancestral variation of the zygoma has an application in a forensic context. The ability of the shape of the zygoma to correctly classify individuals according to sex and ancestry may assist in the identification of unknown persons. In the current study, the zygoma was able to predict sex with fairly high accuracies of 73.4% for set landmarks and 76.9% for semi-landmarks, considering only a single bone was explored and that extensive overlap is present between males and females of each population group. Indian and coloured

South Africans presented with the most overlap between males and females compared to black and white South Africans. The population-specific nature of sexual dimorphism of the zygoma has been demonstrated in the current study which, could be due to the population histories of the specific populations but could also be an indication of reduced sexual dimorphism in the populations. Craniofacial morphology has been found to retain population history and the environmental adaptations generally cannot remove the underlying population variation (Relethford 2004). Environmental conditions such as diet, have also demonstrated an effect on sexual dimorphism. Furthermore, genetic contributions from the Khoi and San and Bantu-speaking individuals to the modern white South African population could have contributed to the sexual dimorphism observed in the population group (Steyn & İşcan 1998; Greeff 2007).

Age also may have had an effect on the sexual dimorphism observed in the current study (Kemkes & Göbel 2006). The age of the sample ranged from 18 to 89 years old and demonstrated a mean of 48 years old. Of the total sample, females had an average age of 47 years old and males had an average of 48 years old. Furthermore, more than half of the sample consisted of individuals above 40 years of age. The age distribution of the sample may have affected the results obtained in the current study as research has indicated that older females, particularly in the white South African population, display more robust cranial features similar to that of males (Krüger 2014). Additionally, the effect of edentulism could have also influenced results. Small (2016) demonstrated that no significant effect on the zygoma was found due to edentulism even though the masseter muscle is affected. However, the study was only conducted on white South Africans (Small 2016). Therefore, further research on the effect of age and edentulism on the shape of the zygoma will provide a better understanding of the variation observed among South Africans.

The classification accuracies obtained in the current study indicate that the semi-landmarks were able to better classify the shape of the zygoma according to sex. Classification accuracies for the projection of the zygoma as well as the angles of projection according to sex resulted in <75% which is better than chance but indicates that the variables on their own may not correctly classify individuals according to sex (Liebenberg *et al.* 2015).

The overall shape variation among the population groups demonstrated a complex relationship. A large amount of overlap between the coloured, white and Indian population groups was present. Black South Africans presented with less within-group variation compared to the other population groups indicating less heterogeneity within the group, whereas coloured

South Africans presented with more within-group variation indicating the most heterogeneity within the group which is consistent with the multiple-origins of this socially defined group. Furthermore, the population history of South Africa further explains the similarities observed amongst the coloured, white and Indian South Africans. The broad geographical contributions to the coloured South African population, as well as the European contribution to the Indian South African population could explain the amount of overlap amongst the groups (Reich *et al.* 2009; de Wit *et al.* 2010). Differences observed amongst the populations could also be due to the large migration of different populations to South Africa as well as the decreased amount of admixture during the *Apartheid* era (McDowell 2012).

While ancestral differences were observed for the shape of the zygoma, the models created to classify individuals according to ancestry resulted in 53.8% for set landmarks and 55.07% for semi-landmarks, which according to Liebenberg *et al.* (2015) cannot be considered practical and an accuracy of 75% is deemed practical for estimating ancestry. The model accuracies were also noted to decrease after employing stepwise variable selection. The decrease indicates that while stepwise selection removed noisy variables, in the multivariate sense, the variables removed provided additional information about the populations. Essentially, by removing the noisy variables the functions became less accurate. The low correct classification accuracies indicate that the zygoma should preferably be used in conjunction with other cranial variables when classifying individuals according to ancestry. Additionally, the accuracy obtained for the projection of the zygoma was 38.32% which is extremely low and cannot correctly classify individuals according to ancestry. The misclassification of population groups when zygomatic projection was analysed also indicates the large amount of overlap between groups. The classification accuracies obtained indicate that ancestry should not be estimated for the projection of the zygoma. The zygoma also demonstrates little ability to estimate ancestry overall.

5.3. Future Recommendations

The current study analysed the shape variation of the zygoma and demonstrated differences between sexes and among groups. However, classifying individuals according to ancestry from the zygoma has proven to be a difficult task. Ancestry is a complex and fluid concept because variation exists within and amongst groups due to geographical locations or admixture (Edgar and Hunley 2009). Ancestry is also a social concept whereby individuals self-classify into distinct groups even post-*Apartheid* and is not considered a biological concept

(Posel 2001a; Liebenberg 2015). However, as forensic anthropologists, identification of unknown individuals is of utmost importance and the use of biological differences allows the assumption of the social construct. Therefore, appropriate methods and standards such as, metric and geometric morphometric methods, need to be developed to accurately assess the variation within the socially defined groups.

The PCA loadings indicated that *po*, *zygool* and *zygoml* contributed the most variation to the zygoma, the landmarks also obtained larger mean differences for intra- and inter-observer error. The large values indicate that observer error may account for some of the variation observed at the landmarks. Although the mean differences were in a repeatable range, a 1mm difference may provide error due to the small size of the zygoma. Ultimately, all landmarks and semi-landmarks used were deemed to be repeatable by making use of a dispersion method to analyse the repeatability. However, multiple methods are typically used to assess observer error in geometric morphometrics. One method employs Generalised Procrustes coordinates to assess the variation observed between landmarks but the method causes an effect termed the “Pinocchio Effect” (von Cramon-Taubadel *et al.* 2007). The “Pinocchio Effect” distributes the landmark error across the sample, decreasing the variation around inaccurate landmarks (floating) and increasing the variation around accurate landmarks (Type I; Bookstein 1991). Other methods used to assess observer error include Euclidean distances whereby the distance between a landmark and the mean are calculated. Procrustes ANOVA is also used to assess observer error, where one can assess how much of the variation is due to error or due to sexual dimorphism and ancestral variation. The methods described are similar to the method employed in the current study and signifying that a standard technique is needed to assess observer error.

Although the landmarks and semi-landmarks of the current study were found to be repeatable, a more accurate methodology can be used that removes observer subjectivity from the equation (Lindner 2017). The zygoma has proven to be a difficult bone to place landmarks and semi-landmarks on because of the irregular shape of the bone. Landmarks generally cluster together at certain points (Schlager & Rüdell 2017). Therefore, a semi-automatic surface registration method will allow for the surface as well as the curves of the zygoma to be assessed. The methodology uses statistical shape models to accurately place semi-landmarks and landmarks on the zygoma. A point distribution model is created using the landmark placements, which allows for the automatic placement of landmarks across specimens. The average placement for the landmarks is found to create the model template, which is then projected onto the test specimen (Cootes *et al.* 1995; Schlager & Rüdell 2017) . The statistical shape

models can also be applied to segmentations, surfaces as well as landmarks (Heimann & Meinzer 2009; Lindner 2017; Schlager & Rüdell 2017). Another methodology, outlined in Schlager & Rüdell (2017) automatically places the semi-landmarks by finding the mean shape of the sample and applying the shape as a template to the rest of the sample. While landmark placements in the current study were repeatable, further research using automatic landmark placement may increase the repeatability of the landmarks allowing for more accurate results (Cootes *et al.* 1995; Heimann & Meinzer 2009; Lindner 2017; Schlager & Rüdell 2017).

CHAPTER 6: CONCLUSION

Sexual dimorphism and ancestral variation of the zygoma across the four major population groups of South Africa were assessed. Through the use of geometric morphometrics the shape of the zygoma demonstrated differences among the population groups and between sexes, except for coloured South Africans, that demonstrated no differences between males and females. Furthermore, the zygoma demonstrated differences at all three sutures as well as the inferior margin of the orbit for both sex and ancestry. that extensive overlap between the population groups occurred mostly between coloured, white, and Indian South Africans. Black South Africans showed little within-group variation and little overlap with the other population groups. The projection of the zygoma demonstrated that males had a larger projection than females, whereas little difference was demonstrated amongst the population groups. The angles of projection demonstrated that males were larger for *Angle2* and *Angle3*, whereas females were larger for *Angle1*. Sex and ancestry differences were also noted for the angles of projection.

Classification accuracies using a linear discriminant function for sexual shape dimorphism (73.4% for set landmarks and 76.9% for semi-landmarks) and ancestral variation (53.8% for set landmarks and 55.07% for semi-landmarks) of the zygoma indicate that the shape of the zygoma may not be useful in classifying an unknown individual according to ancestry and should only be used in conjunction with other methods. However, the shape of the zygoma would be useful for estimating sex. Furthermore, classification accuracies for the projection of the zygoma (71% for sex and 38.32% for ancestry) and angles of projection (57% for sex and 37% for ancestry) also indicate projection should not be used for ancestry estimation purposes. While the zygoma has limited use in forensic contexts, applications outside of forensic anthropology such as, medical uses for zygomatic implants, can benefit from the knowledge gained during the study.

While the use of CT scans aided in the assessment of the shape of the zygoma, sutures were often difficult to visualise making data acquisition difficult. The use of other imaging methods (MicroCT, CBCT scans) may help overcome the limitation and provide a better resolution to visualise sutures in further research. The sample also consisted of individuals who self-identified as a particular population group which could have led to misleading results. Furthermore, the study highlighted the need for further evaluation of the Indian South African population group so that a better understanding of the variation within the population group

and between the population groups of South Africa so that a presumptive identification can be made during a forensic investigation. The analysis of the zygoma to further assess the effect of diet, climate and symmetry may aid in further understanding the shape of the zygoma for future applications in anthropology as well as in medical fields. The use of a semi-automatic surface registration method outlined in Schlager & Rüdell (2017), will also reduce subjectivity and increase repeatability of the methodology.

REFERENCES

- Adams, D.C., Rohlf, F.J. & Slice, D.E. 2004. Geometric morphometrics: Ten years of progress following the 'revolution'. *Italian Journal of Zoology*. 71(1): pp. 5–16.
- Adams, D., Collyer, M., Kaliontzopoulou, A. & Baken, E. 2021. "Geomorph: Software for geometric morphometric analyses. R package version 3.3.2. [online]. Available from: <https://cran.r-project.org/package=geomorph>.
- Adhikari, M. 2005. Contending approaches to coloured identity and the history of the coloured people of South Africa: Contending Approaches to Coloured Identity in South Africa and their History. *History Compass*. 3(1). pp. 1-16.
- Agarwal, S., Jain. S.K. 2014. Evaluation of cephalic index in females of western up region by simple regression analysis. *Journal of Evolution of Medical and Dental Sciences*. 03(03): pp. 718–725.
- Allard, T.T. 2006. The role of 3D printing in biological anthropology. MA Dissertation. University of Manitoba. p. 140.
- Anderson, M.J. 2001. Permutation tests for univariate or multivariate analysis of variance and regression. *Canadian Journal of Fisheries and Aquatic Science*. 58: pp. 626–639.
- Baab, KL., Friedline, SE., Wang, SL. & Hanson, T. 2010. Relationship of cranial robusticity to cranial form, geography and climate in *Homo sapiens*. *Journal of Physical Anthropology*. 141: pp. 97–115.
- Barbeito-Andre, J., Anzelmo, M., Ventrice, F., Pucciarelli, C.M. & Sardi, M.L. 2016. Morphological integration of the orbital region in a human ontogenetic sample. *The Anatomical Record*. 299: pp. 70–80.
- Bass, W.M. 1995. *Human osteology: a laboratory and field manual*. 4th ed. Columbia: MO: Missouri Archaeological Society.
- Barrier, I.L.O. 2007. Sex determination from the bones of the forearm in a modern South African sample. MSc Thesis. University of Pretoria. pp. 115.

- Beck, R.B. 2000. European invasion 1488-1795. In: Beck, R.B. The history of South Africa. Greenwood Publishing Group, Incorporated. pp.25–40.
- Bhat, C. & Narayan, K.L. 2010. Indian diaspora, globalization and transnational networks: The South African context. *Journal of Social Sciences*. 25(1–3): pp. 13–23.
- Bigoni, L., Velemínská, J. & Brůžek, J. 2010. Three-dimensional geometric morphometric analysis of cranio-facial sexual dimorphism in a Central European sample of known sex. *HOMO*. 61(1):pp. 16–32.
- Bookstein, F., L. 1991. Morphometric tools for landmark data: Geometry and biology. Cambridge,UK: Cambridge University Press.
- Brace, C. Loring. 1995. Region does not mean “Race”- reality versus convention in forensic anthropology. *Journal of Forensic Science*. 40(2): pp. 171–175.
- Burton, J.L. & Underwood, J. 2007. Clinical, educational, and epidemiological value of autopsy. *The Lancet*. 369(9571):1471–1480.
- Caple, J. & Stephan, C.N. 2016. A standardized nomenclature for craniofacial and facial anthropometry. *International Journal of Legal Medicine*. 130(3): pp. 863–879.
- Caple, J. & Stephan, C.N. 2017. Photo-realistic statistical skull morphotypes: new exemplars for ancestry and sex estimation in forensic anthropology. *Journal of Forensic Sciences*. 62(3): pp. 562–572.
- Caspari, R. 2003. From types to populations: A century of race, physical anthropology, and the American Anthropological Association. *American Anthropologist*. 105(1): pp. 65–76.
- Cataldo-Ramirez, C., Garvin, H.M. & Cabo, L. 2020. A quantitative assessment of zygomatic projection for ancestry estimation. *Journal of Forensic Sciences*. 65(2): pp. 580–590.
- Cawley, G.C. & Talbot, N.L.C. 2008. Efficient approximate leave-one-out cross-validation for kernel logistic regression. *Machine Learning*. 71(2–3): pp. 243–264.
- Choi, J.W., Jung, S.Y., Kim, H.J. & Lee, S.-H. 2015. Positional symmetry of porion and external auditory meatus in facial asymmetry. *Maxillofacial Plastic and Reconstructive Surgery*. 37(33): pp. 1-9.

- Coleman, M.N. & Colbert, M.W. 2007. Technical note: CT thresholding protocols for taking measurements on three-dimensional models. *American Journal of Physical Anthropology*. 133(1): pp. 723–725.
- Colman, K.L., Dobbe, J.G.G., Stull, K.E., Ruijter, J.M., Oostra, R.J., van Rijn, R.R., van der Merwe, A.E., de Boer, H.H., et al. 2017. The geometrical precision of virtual bone models derived from clinical computed tomography data for forensic anthropology. *International Journal of Legal Medicine*. 131(4): pp. 1155–1163.
- Colman, K.L., de Boer, H.H., Dobbe, J.G.G., Liberton, N.P.T.J., Stull, K.E., van Eijnatten, M., Streekstra, G.J., Oostra, R.-J., et al. 2019. Virtual forensic anthropology: The accuracy of osteometric analysis of 3D bone models derived from clinical computed tomography (CT) scans. *Forensic Science International*. 304: pp. 1-34.
- Cootes, T.F., Taylor, C.J., Cooper, D.H. & Graham, J. 1995. Active shape models- their training and application. *Computer Vision and Image Understanding*. 61(1): pp. 38–59.
- Cotter, M.M., Whymys, B.J., Kelly, M.P., Doherty, B.M., Gentry, L.R., Bersu, E.T. & Vorperian, H.K. 2015. Hyoid bone development: an assessment of optimal ct scanner parameters and three-dimensional volume rendering techniques: hyoid bone segmentation from CT. *The Anatomical Record*. 298(8): pp. 1408–1415.
- Crawfurd, J. 1868. On the classification of the races of man according to the form of the skull. *Transactions of the Ethnological Society of London*. 6: pp. 127–134.
- Daboul, A., Ivanovska, T., Bülow, R., Biffar, R. & Cardini, A. 2018. Procrustes-based geometric morphometrics on MRI images: An example of inter-operator bias in 3D landmarks and its impact on big datasets. *PLOS ONE*. 13(5): pp. 1-20.
- Dalrymple, N.C., Prasad, S.R., El-Merhi, F.M. & Chintapalli, K.N. 2007. Price of isotropy in multidetector CT. *RadioGraphics*. 27(1): pp. 49–62.
- Dechow, P.C. & Wang, Q. 2017. Evolution of the jugal/zygomatic bones: evolution of the zygoma. *The Anatomical Record*. 300(1): pp. 12–15.

- Decker, S.J., Davy-Jow, S.L., Ford, J.M. & Hilbelink, D.R. 2011. Virtual determination of sex: metric and nonmetric traits of the adult pelvis from 3D computed tomography models. *Journal of Forensic Science*. 56(5): pp. 1107–1114.
- Dereli, A.K., Zeybek, V., Sagtas, E., Senol, H., Ozgul, H.A. & Acar, K. 2018. Sex determination with morphological characteristics of the skull by using 3D modeling techniques in computerized tomography. *Forensic Science, Medicine and Pathology*. 14(4): pp. 450–459.
- de Wit, E., Delpont, W., Rugamika, C., Meinjies, A., Möller, M., van Helden, P.D., Seoighe, C. & Hoal, E.G. 2010. Genome-wide analysis of the structure of the South African Coloured Population in the Western Cape. *Human Genetics*. 128(2): pp. 145–153.
- Dutailly, B. 2009. TIVMI: Treatment and increased vision for medical imaging [computer program]. Bordeaux, France: CNRS. [Accessed: 07/7/2020]. Available from: <http://projets.pacea.u-bordeaux.fr/TIVMI/index.php?page=download>.
- Edgar, H.J.H. & Hunley, K.L. 2009. Race reconciled?: How biological anthropologists view human variation. *American Journal of Physical Anthropology*. 139(1): pp. 1–4.
- Enlow, D.H. 1982. *Handbook of facial growth*. 2nd ed. Toronto: W.B. Saunders Company.
- Enlow, D.H. 1990. *Facial growth*. 3rd ed. Philadelphia, PA, USA:Saunders: Elsevier. pp. 562.
- Enlow, D.H. & Bang, S. 1965. Growth and remodeling of the human maxilla. *American Journal of Orthodontics*. 51(6): pp. 446–464.
- Enlow, D.H. & Hans, M.G. 1996. The nasomaxillary complex. In: Enlow, D.H. *Essentials of Facial Growth*. W.B. Saunders Company. p.79–98.
- Fajardo, R.J., Ryan, T.M. & Kappelman, J. 2002. Assessing the accuracy of high-resolution x-ray computed tomography of primate trabecular bone by comparisons with histological sections. *American Journal of Physical Anthropology*. 118(1): pp. 1–10.
- Ferrario', V.F., Sforza', C., Pizzini, G., Vogel, G. & Mianii, A. 1993. Sexual dimorphism in the human face assessed by euclidean distance matrix analysis. *Journal of Anatomy*. 183: pp. 593–600.

- Franklin, D., Flavel, A., Kuliukas, A., Cardini, A., Marks, M.K., Oxnard, C. & O'Higgins, P. 2012. Estimation of sex from sternal measurements in a Western Australian population. *Forensic Science International*. 217(1–3): pp. 230.e1-230.e5.
- Franklin, D., Freedman, L., Milne, N. & Oxnard, C.E. 2006. A geometric morphometric study of sexual dimorphism in the crania of indigenous southern Africans. *South African Journal of Science*. pp. 229-238.
- Franklin, D., Freedman, L., Milne, N. & Oxnard, C.E. 2007a. Geometric morphometric study of population variation in indigenous southern African crania. *American Journal of Human Biology*. 19(1): pp. 20–33.
- Franklin, D., Oxnard, C.E., O'Higgins, P. & Dadour, I. 2007b. Sexual dimorphism in the subadult mandible: Quantification using geometric morphometrics. *Journal of Forensic Sciences*. 52(1):6–10.
- Franklin, D., Cardini, A., Flavel, A. & Marks, M.K. 2014. Morphometric analysis of pelvic sexual dimorphism in a contemporary Western Australian population. *International Journal of Legal Medicine*. 128(5): pp.861–872.
- Franklin, D., Swift, L. & Flavel, A. 2016. 'Virtual anthropology' and radiographic imaging in the forensic medical sciences. *Egyptian Journal of Forensic Sciences*. 6(2): pp. 31–43.
- Gai, Z., Yu, X. & Zhu, M. 2017. The evolution of the zygomatic bone from Agnatha to Tetrapoda: the evolution of the zygomatic bone. *The Anatomical Record*. 300(1): pp. 16–29.
- Frith, A. 2011a. Chatsworth: Main place 599161 from census 2011. [online]. Available from: <https://census2011.adrianfrith.com/place/599161>. [Accessed: 01/02/2021].
- Frith, A. 2011b. Laudium: Main place 799058 from census 2011. [online]. Available from: <https://census2011.adrianfrith.com/place/799058>. [Accessed: 01/02/2021].
- Frith, A. 2011c. Arena Park: Sub place 599161009 from census 2011. [online]. Available from: <https://census2011.adrianfrith.com/place/599161009>. [Accessed: 01/02/2021].

- Galland, M. & Friess, M. 2016. A three-dimensional geometric morphometrics view of the cranial shape variation and population history in the New World: Cranial Shape Variation in the New World. *American Journal of Human Biology*. 28(5):646–661.
- Garvin, H.M. & Ruff, C.B. 2012. Sexual dimorphism in skeletal browridge and chin morphologies determined using a new quantitative method. *American Journal of Physical Anthropology*. 147(4): pp. 661–670.
- Garvin, H.M. & Stock, M.K. 2016. The utility of advanced imaging in forensic anthropology. *Academic Forensic Pathology*. 6(3): pp. 499–516.
- Ghasemi, A. & Zahediasl, S. 2012. Normality tests for ttatistical analysis: A guide for non-statisticians. *International Journal of Endocrinology and Metabolism*. 10(2): pp. 486–489.
- Gill, G.W., Hughes, S.S., Bennett, S.M. & Miles Gilbert, B. 1988. Racial identification from the midfacial skeleton with special reference to American Indians and whites. *Journal of Forensic Sciences*. 33(1): pp. 92-99.
- Gonzalez, P.N., Bernal, V. & Perez, S.I. 2011. Analysis of sexual dimorphism of craniofacial traits using geometric morphometric techniques. *International Journal of Osteoarchaeology*. 21(1): pp. 82–91.
- Greeff, J.M. 2007. Deconstructing Jaco: genetic heritage of an Afrikaner. *Annals of Human Genetics*. 71(5): pp. 674–688.
- Green, H. & Curnoe, D. 2009. Sexual dimorphism in Southeast Asian crania: A geometric morphometric approach. *HOMO*. 60(6): pp. 517–534.
- Guyomarc’h, P., Santos, F., Dutailly, B., Desbarats, P., Bou, C. & Coqueugniot, H. 2012. Three-dimensional computer-assisted craniometrics: A comparison of the uncertainty in measurement induced by surface reconstruction performed by two computer programs. *Forensic Science International*. 219(1–3): pp. 221–227.
- Guyomarc’h, P., Dutailly, B., Charton, J., Santos, F., Desbarats, P. & Coqueugniot, H. 2014. Anthropological facial approximation in three dimensions (AFA3D): Computer-

- assisted stimulation of the facial morphology using geometric morphometrics. *Journal of Forensic Sciences*. 59(6): pp. 1502–1516.
- Hamilton, A. 2008. Taxonomic approaches to race. pp. 11–36.
- Hanihara, T. 2000. Frontal and facial flatness of major human populations. *American Journal of Physical Anthropology*. 111: pp. 105.
- Hanihara, T., Ishida, H. & Dodo, Y. 1998. Os zygomaticum bipartitum: frequency distribution in major human populations. *Journal of Anatomy*. 192(4): pp. 539–555.
- Harvati, K. & Weaver, T.D. 2006. Human cranial anatomy and the differential preservation of population history and climate signatures. *The Anatomical Record Part A: Discoveries in Molecular, Cellular, and Evolutionary Biology*. 288A(12): pp. 1225–1233.
- Hefner, J.T. 2009. Cranial nonmetric variation and estimating ancestry. *Journal of Forensic Sciences*. 54(5): pp. 985–995.
- Heimann, T. & Meinzer, H.-P. 2009. Statistical shape models for 3D medical image segmentation: A review. *Medical Image Analysis*. 13(4): pp. 543–563.
- Herbert, R.K. 1990. The sociohistory of clicks in Southern Bantu. *Anthropological linguistics*. 32(3/4): pp. 295–315.
- Heuzé, Y., Kawasaki, K., Schwarz, T., Schoenebeck, J.J. & Richtsmeier, J.T. 2016. Developmental and evolutionary significance of the zygomatic bone: significance of the zygomatic bone. *The Anatomical Record*. 299(12): pp. 1616–1630.
- Hiernaux, J. 1966. Human biological diversity in central africa. *Man*. 1(3): pp. 287.
- Howells, WW. 1996. Who's who in skulls: Ethnic identification of crania from measurements. MA: Papers of the Peabody Museum: Cambridge. 82: pp. 118.
- Humphrey, L.T. 1998. Growth patterns in the modern human skeleton. 105(2):57–72.
- İşcan, M.Y. & Steyn, M. 2013. Ancestry. In: 3rd ed. *The human skeleton in forensic medicine*. Charles C Thomas Publisher, Ltd. pp.195–226.

- Jacobson, C.K., Amoateng, A.Y. & Heaton, T.B. 2004. Inter-racial marriages in South Africa. *Journal of Comparative Family Studies*. 35(3): pp. 443–458.
- Jantz, R.L. & Ousley, S.D. 2017. Introduction to Fordisc 3 and human variation statistics. In: Langley, N.R., Tersigni-Tarrant, M.A. *Forensic Anthropology: A Comprehensive Introduction*. 2nd Edition. Boca Raton, FL: CRC Press. pp.255–270.
- Joliffe, I. 2002. Principal components as a small number of interpretable variables: some examples. In: 2nd ed. *Principal Components Analysis*. Springer. pp.63–76.
- Kassambara, A. & Mundt, F. 2020. factoextra: Extract and visualize the results of multivariate data analyses. [online]. Available from: <https://CRAN.R-project.org/package=factoextra>.
- Kemkes, A. & Göbel, T. 2006. Metric assessment of the “Mastoid Triangle” for sex determination: A validation study. *Journal of Forensic Sciences*. 51(5): pp. 985–989.
- Klales, A.R. & Kenyhercz, M.W. 2015. Morphological assessment of ancestry using cranial macromorphoscopies,. *Journal of Forensic Sciences*. 60(1): pp. 13–20.
- Klingenberg, C.P. 2011. MorphoJ: an integrated software package for geometric morphometrics: Computer program note. *Molecular Ecology Resources*. 11(2): pp. 353–357.
- Klingenberg, C.P. 2013. Visualizations in geometric morphometrics: how to read and how to make graphs showing shape changes. *Hystrix, the Italian Journal of Mammalogy*. 24(1). pp. 353-357.
- Krüger, G.C. 2014. Comparison of sexually dimorphic patterns in the postcrania of South Africans and North Americans. MSc Thesis. University of Pretoria. pp. 134.
- Krüger, G.C., L’Abbé, E.N., Stull, K.E. & Kenyhercz, M.W. 2015. Sexual dimorphism in cranial morphology among modern South Africans. *International Journal of Legal Medicine*. 129(4): pp. 869–875.
- Krüger, G.C., L’Abbé, E.N. & Stull, K.E. 2017. Sex estimation from the long bones of modern South Africans. *International Journal of Legal Medicine*. 131(1): pp. 275–285.

- Krüger, G.C., Sutherland, C., Liebenberg, L., Myburgh, J., Brits, D.M., Meyer, A., Boths, D., Oettlé, A.C., et al. 2018. Forensic anthropology and the biological profile in South Africa: Recent advances and developments. In: K. Latham, E. Bartelink and M. Finnegan. 1st Edition. New perspectives in forensic human skeletal identification. Academic Press. pp. 313-322.
- L'Abbé, E.N., Van Rooyen, C., Nawrocki, S.P. & Becker, P.J. 2011. An evaluation of non-metric cranial traits used to estimate ancestry in a South African sample. *Forensic Science International*. 209(1-3): pp. 195.e1-195.e7.
- L'Abbé, E.N., Kenyhercz, M., Stull, K.E., Keough, N. & Nawrocki, S. 2013a. Application of Fordisc 3.0 to explore differences among crania of North American and South African blacks and whites. *Journal of Forensic Sciences*. 58(6): pp. 1579-1583.
- L'Abbé, E.N., Kenyhercz, M.W., Stull, K.E. & Ousley, S.D. 2013b. Craniometric assessment of modern 20th Century black, white, and coloured South Africans. Proceedings of the 65th annual meeting of the American Academy of Forensic Sciences. Washington, DC. Proceedings of the 65th Annual Meeting of the American Academy of Forensic Sciences, Washington DC. pp. 444.
- Langley, N.R., Jantz, L.M., Ousley, S.D., Jantz, R.L. & Milner, G. 2016. Data collection procedures for Forensic skeletal material 2.0.
- Lemon, A. 1990. The political position of Indians in South Africa. In: *South Asians overseas: migration and ethnicity*. New York: Cambridge University Press. p.131-148.
- Leon, J.G.D. 2015. Three-dimensional image technology in forensic anthropology: Assessing the validity of biological Pprofiles derived from CT-3D images of the Skeleton. MSc Thesis. Boston University. pp. 1-102.
- Liebenberg, L. 2015. Postcraniometric analysis of ancestry among modern South Africans. MSc Thesis. University of Pretoria. pp. 1-106.
- Liebenberg, L., Stull, K.E., L'Abbé, E.N. & Botha, D. 2015. Evaluating the accuracy of cranial indices in ancestry estimation among South African groups. *Journal of Forensic Sciences*. 60(5): pp. 1277-1282.

- Lindner, C. 2017. Automated image interpretation using statistical shape models. In: Statistical shape and deformation analysis. Elsevier. pp.3–32.
- Livingstone, F.B. & Dobzhansky, T. 1962. On the non-existence of human races. *Current Anthropology*. 3(3): pp. 279–281.
- Maddux, S.D., Sporleder, A.N. & Burns, C.E. 2015a. Geographic variation in zygomaxillary suture morphology and its use in ancestry estimation. *Journal of Forensic Sciences*. 60(4): pp. 966–973.
- Márquez, S., Pagano, A.S., Schwartz, J.H., Curtis, A., Delman, B.N., Lawson, W. & Laitman, J.T. 2017. Toward understanding the mammalian zygoma: Insights from comparative anatomy, growth and development, and morphometric analysis: mammalian zygoma. *The Anatomical Record*. 300(1): pp. 76–151.
- McDowell, J. 2012. Nasal aperture shape and its application for estimating ancestry in modern South Africans. MSc Thesis. University of Pretoria. pp. 102.
- Mehta, M., Saini, V., Nath, S., Patel, M.N. & Menon, S.K. 2014. CT scan images to determine the origin from craniofacial indices for Gujarati population. *Journal of Forensic Radiology and Imaging*. 2(2): pp. 64–71.
- Mehta, M., Saini, V., Nath, S. & Menon, S.K. 2015. CT scan images for sex discrimination – a preliminary study on Gujarati population. *Journal of Forensic Radiology and Imaging*. 3(1): pp. 43–48.
- Monticelli, F. & Graw, M. 2008. Investigation on the reliability of determining sex from the human os zygomaticum. *Forensic Science, Medicine, and Pathology*. 4(3): pp. 181–186.
- Moore, K.L., Dalley, A.F. & Agur, A.M.R. 2014. Head. In: 7th ed. Moore: Clinically orientated anatomy. Baltimore: Lippincott Williams & Wilkins. p.820–980.
- Moore-Jansen, P.M., Ousley, S.D. & Jantz, R.L. 1994. Data collection procedures for forensic skeletal material. pp. 70–82.

- Moorjani, P., Thangaraj, K., Patterson, N., Lipson, M., Loh, P.-R., Govindaraj, P., Berger, B., Reich, D., et al. 2013. Genetic evidence for recent population mixture in India. *The American Journal of Human Genetics*. 93(3): pp. 422–438.
- Mopin, C., Chaumoître, K., Signoli, M. & Adalian, P. 2018. Developmental stability and environmental stress: A geometric morphometrics analysis of asymmetry in the human femur. *American Journal of Physical Anthropology*. 167(1): pp. 144–160.
- Muller, S. 2018. Metric assessment of ancestry and sex variation in the zygoma. pp. 1-48.
- Murray-Lasso. 2002. On the generalization of the law of cosines of triangles to three and more dimensions. *Ingeniería Investigación y Tecnología*. 3(4): pp. 169–183.
- Newman, J.L. 1995. *The peopling of Africa: A Geographic Interpretation*. London: Yale University Press.
- Nicholson, E. & Harvati, K. 2006. Quantitative analysis of human mandibular shape using three-dimensional geometric morphometrics. *American Journal of Physical Anthropology*. 131(3): pp. 368–383.
- Novita, M. 2006. Facial, upper facial, and orbital index in Batak, Klaten, and Flores students of Jember University. *Dental Journal*. 39: pp. 116–119.
- Oettlé, A.C., Demeter, F.P. & L'abbé, E.N. 2017. Ancestral variations in the shape and size of the zygoma: ancestral variations of The zygoma. *The Anatomical Record*. 300(1): pp. 196–208.
- Ousley, S.D. & Jantz, R.L. 2012. FORDISC 3 and statistical methods for estimating sex and ancestry. In: Dirmaat, D.C. *Companion to forensic anthropology*. Wiley-Blackwell. pp.311–329.
- Ousley, S.D. & Mckeown, A. 2001. Three-dimensional digitising of human skulls as an archival procedure. In: Williams, E. *Human remains conservation, Retrieval and Analysis*. Archaeopress. pp.173–186.
- Ousley, S., Jantz, R. & Freid, D. 2009. Understanding race and human variation: Why forensic anthropologists are good at identifying race. *American Journal of Physical Anthropology*. 139(1): pp. 68–76.

- Patterson, N., Peterson, D.C., Van Der Ross, R.E., Sudoyo, H., Glashoff, R.H., Marzuki, S., Reich, D. & Hayes, V.M. 2010. Genetic structure of a unique admixed population: Implications for medical research. *Human Molecular Genetics*. 19(3): pp. 411–419.
- Perez, S.I., Bernal, V. & Gonzalez, P.N. 2006. Differences between sliding semi-landmark methods in geometric morphometrics, with an application to human craniofacial and dental variation. *Journal of Anatomy*. 208(6): pp. 769–784.
- Peterson, D.C., Libiger, O., Tindall, E.A., Hardy, R.A., Hannick, L.I., Glashoff, R.H., Mukerji, M., Fernandez, P., et al. 2013. Complex patterns of genomic admixture within Southern Africa. *PLoS Genetics*. 9(3): pp. e1003309.
- Pierce, B.A. 2014. Sex determination and sex-linked characteristics. In: Freeman, W.H. *Genetics: A conceptual approach*. 5th Edition. United States of America: W.H. Freeman and Company: a Macmillan Higher Education Company. pp.77–102.
- Posel, D. 2001a. What's in a name? Racial categorisations under Apartheid and their afterlife. *Transformation*. 47: pp. 50–74.
- Posel, D. 2001b. Race as common sense: Racial classification in twentieth-century South Africa. *African Studies Review*. 44(2): pp. 87-113.
- Pretorius, E., Steyn, M. & Scholtz, Y. 2006. Investigation into the usability of geometric morphometric analysis in assessment of sexual dimorphism. *American Journal of Physical Anthropology*. 129(1): pp. 64–70.
- Profico, A., Buzi, C., Castiglione, S., Melchionna, M., Piras, P., Raia, P. & Veneziano, A. 2020. Arothron: Geometric morphometric methods and virtual anthropology tools. [online]. Available from: <https://CRAN.R-project.org/package=Arothron>.
- Quintana-Murci, L., Harmant, C., Quach, H., Balanovsky, O., Zaporozhchenko, V., Bormans, C., van Helden, P.D., Hoal, E.G., et al. 2010. Strong maternal Khoisan contribution to the South African coloured Population: A case of gender-biased admixture. *The American Journal of Human Genetics*. 86(4): pp. 611–620.
- R Core Team. 2018. R: A language and environment for statistical computing. R Foundation for Statistical Computing.

- Raghavan, P., Bulbeck, D., Pathmanathan, G. & Rathee, S.K. 2013. Indian craniometric variability and affinities. *International Journal of Evolutionary Biology*. 2013: pp. 1–25.
- Reich, D., Thangaraj, K., Patterson, N., Price, A.L. & Singh, L. 2009. Reconstructing Indian population history. *Nature*. 461(7263): pp. 489–494.
- Relethford, J.H. 2004. Boas and beyond: Migration and craniometric variation. *American Journal of Human Biology*. 16(4): pp. 379–386.
- Report of the High Level Committee on the Indian Diaspora: South Africa. 2001. Indian Council of World Affairs. pp. 71–88.
- Rhine, S. 1990. Nonmetric skull racing. In: *Skeletal attribution of race: methods for forensic anthropology*. Albuquerque: NM: Maxwell Museum of Anthropology. p.7–20.
- Ridel, A.F., Demeter, F., Liebenberg, J., L'Abbé, E.N., Vandermeulen, D. & Oetlé, A.C. 2018. Skeletal dimensions as predictors for the shape of the nose in a South African sample: A cone-beam computed tomography (CBCT) study. *Forensic Science International*. 289: pp. 18–26.
- Rogers, T.L. 2005. Determining the sex of human remains through cranial morphology. *Journal of Forensic Sciences*. 50(3): pp. 1–8.
- Ross, S.M. 2004. Descriptive statistics. In: Ross, S.M. *Introduction to probability and statistics for engineers and scientists*. 3rd Edition. Amsterdam: Academic Press.
- Rusk, K.M. & Ousley, S.D. 2016. An evaluation of sex- and ancestry-specific variation in sacral size and shape using geometric morphometrics: Sex-and ancestry-Specific sacral variation. *American Journal of Physical Anthropology*. 159(4): pp. 646–654.
- Saini, V., Srivastava, R., Rai, R.K., Shamal, S.N., Singh, T.B. & Tripathi, S.K. 2011. An osteometric study of Northern Indian populations for sexual dimorphism in craniofacial region: sexual dimorphism in craniofacial region. *Journal of Forensic Sciences*. 56(3): pp. 700–705.

- Saini, V., Srivastava, R., Shamal, S.N., Singh, T.B., Kumar, V., Kumar, P. & Tripathi, S.K. 2014. Temporal variations in basicranium dimorphism of North Indians. *International Journal of Legal Medicine*. 128(4): pp. 699–707.
- Scheuer, L. & Black, S. 2004. *The juvenile skeleton*. New York: Elsevier Academic Press.
- Schlager, S. & Rüdell, A. 2017. Sexual dimorphism and population affinity in the human zygomatic structure-comparing surface to outline data: Analyzing zygomatic shape. *The Anatomical Record*. 300(1): pp. 226–237.
- Sholts, S.B. & Wärmländer, S.K.T.S. 2012. Zygomaticomaxillary suture shape analyzed with digital morphometrics: Reassessing patterns of variation in American Indian and European populations. *Forensic Science International*. 217(1–3): pp. 234.e1-234.e6.
- Slice, D.E. 2007. Geometric morphometrics. *Annual Review of Anthropology*. 3: pp. 261–281.
- Small, C. 2016. Sexual dimorphism in white South African crania. PhD Dissertation. University of the Witwatersrand. pp. 207.
- Small, C., Schepartz, L., Hemingway, J. & Brits, D. 2018. Three-dimensionally derived interlandmark distances for sex estimation in intact and fragmentary crania. *Forensic Science International*. (February). pp. 1-29.
- Spradley, M.K. 2006. Biological anthropological aspects of the African diaspora; geographic origins, secular trends, and plastic versus genetic influences utilizing craniometric data. pp. 138.
- Spradley, M.K. 2016a. Metric methods for the biological profile in forensic anthropology: sex, ancestry, and stature. *Academic Forensic Pathology*. 6(3): pp. 391–399.
- Spradley, M. & Jantz, R.L. 2016b. Ancestry estimation in forensic anthropology: geometric morphometric versus standard and nonstandard interlandmark distances. *Journal of Forensic Sciences*. 61(4): pp. 892–897.
- Statistics South Africa. 2011. *Census*. South Africa. pp 1–88.
- Statistics South Africa. 2020. *Mid-year population estimates 2020*.

- Stavrianos, C., Papadopoul, C., Pantelidou, O., Emmanouil, J. & Petalotis, N. 2012. Facial anatomy and mapping across races. *Research Journal of Medical Sciences*. 6(4): pp. 159–162.
- Steyn, M. & İşcan, M.Y. 1998. Sexual dimorphism in the crania and mandibles of South African whites. *Forensic Science International*. 98(1–2): pp. 9–16.
- Steyn, M., Pretorius, E. & Hutten, L. 2004. Geometric morphometric analysis of the greater sciatic notch in South Africans. *HOMO*. 54(3): pp. 197–206.
- Stull, K.E., Kenyhercz, M.W. & L'Abbé, E.N. (2014). Ancestry estimation in South Africa using craniometrics and geometric morphometrics. *Forensic Science International*. 245: pp. 206.e1-206.e7.
- Tawha, T., Dinkele, E., Mole, C. & Gibbon, V.E. 2020. Assessing zygomatic shape and size for estimating sex and ancestry in a South African sample. *Science & Justice*. 60(3): pp. 284–292.
- Thermo Scientific™ AVIZO™ software 9 Users Guide. 2018.
- Thompson, L.M. 2001. The white invaders: The Cape colony. In: Thompson, L.M. *The history of South Africa: 3rd Edition*. New Haven and London: Yale University Press. pp.31–69.
- Triarhou, L.C. 2013. Anders Retzius (1796–1860). *Journal of Neurology*. 260(5): pp. 1445–1446.
- Uyeda, J.C., Hansen, T.F., Arnold, S.J. & Pienaar, J. 2011. The million-year wait for macroevolutionary bursts. *PNAS*. 108(38): pp. 15908–15913.
- Vitek, C.L. 2012. A critical analysis of the use of non-metric traits for ancestry estimation among two North American population samples. pp. 116.
- von Cramon-Taubadel, N., Frazier, B.C. & Lahr, M.M. 2007. The problem of assessing landmark error in geometric morphometrics: Theory, methods, and modifications. *American Journal of Physical Anthropology*. 134(1): pp. 24–35.

- Walker, P.L. 2008. Sexing skulls using discriminant function analysis of visually assessed traits. *American Journal of Physical Anthropology*. 136(1): pp. 39–50.
- Walker, P.L. & Cook, D.C. 1998. Brief communication: Gender and sex: Vive la difference. *Sex and Gender*. pp. 5.
- Wang, Q. & Dechow, P.C. 2016. Divided zygomatic bone in primates with implications of skull morphology and biomechanics: divided zygoma in primates. *The Anatomical Record*. 299(12): pp. 1801–1829.
- Weber, G.W. 2015. Virtual anthropology: Virtual anthropology. *American Journal of Physical Anthropology*. 156: pp. 22–42.
- Weihs, C., Ligges, U., Luebke, K. & Raabe, N. 2005. KLaR analyzing German business cycles. In: *Data analysis and decision support*. Berlin, Germany: Springer-Verlag. pp.335–343.
- Wheat, A.D. 2009. Assessing ancestry through nonmetric traits of the skull: A test of education and experience. MA Thesis. Texas State University. pp. 1–60..
- White, T.D. & Folkens, P.A. 2000. *Human osteology*. Second ed. London: Academic Press. pp. 58.
- White, T.D. & Folkens, P.A. 2005a. Skeletal biology of individuals and populations. In: *The human bone manual*. Elsevier. pp.359–418.
- White, T.D. & Folkens, P.A. 2005b. Skull. In: *The human bone manual*. Elsevier Academic Press. pp. 75 - 126.
- Wilson-Taylor, R.J. 2015. Sexual dimorphism of the zygomatic bone in a Southeast Asian Sample. In: Vol. 21. *Proceedings of the American Academy of Forensic Sciences 67th Annual Scientific Meeting*. pp.112.
- Wong, T.-T. 2015. Performance evaluation of classification algorithms by k-fold and leave-one-out cross validation. *Pattern Recognition*. 48(9): pp. 2839–2846.
- Yong, R., Ranjitkar, S., Lekkas, D., Halazonetis, D., Evans, A., Brook, A. & Townsend, G. 2018. Three-dimensional (3D) geometric morphometric analysis of human premolars

to assess sexual dimorphism and biological ancestry in Australian populations. *American Journal of Physical Anthropology*. 166(2): pp. 373–385.

Zelditch, M. ed. 2004a. *Geometric morphometrics for biologists: a primer*. Amsterdam; Boston: Elsevier Academic Press. pp. 1-20.

Zelditch, M. 2004b. Superimposition methods. In: *Geometric morphometrics for biologists: A primer*. Amsterdam; Boston: Elsevier Academic Press. pp.105–128.

Zelditch, M. 2004c. Ordination methods. In: *Geometric morphometrics for biologists: A primer*. Amsterdam; Boston: Elsevier Academic Press. pp.155–187.

APPENDIX

Appendix I

Table A1. Landmarks used for the analysis (Moore-Jansen et al. 1994; White & Folkens 2000; Ousley & Mckeown 2001; Choi et al. 2015)

<i>Landmark</i>	<i>Symbol</i>	<i>Description</i>
Frontomalaretemporale	<i>fmt</i>	The point found on the most lateral part of the frontomalar suture.
Ectoconchion	<i>ec</i>	The anterior-most point on the lateral margin of the orbit when a line is drawn parallel to the supra-orbital margin from dacryon.
Zygoorbitale	<i>zygool</i>	Where the zygomaticomaxillary suture intersects the orbital rim.
Zygomaxilare	<i>zygoml</i>	The inferior most point on the zygomaticomaxillary suture.
Zygotemporale inferior	<i>zytinr</i>	The inferior most point on the zygomaticotemporal suture.
Zygotemporale superior	<i>zytspl</i>	The superior most point on the zygomaticotemporal suture.
Frontomalare Anterior	<i>fm:a</i>	The anterior most point of the frontomalar suture. Note this point is not in the orbit but on the margin of the orbit.
Frontmalare Posterior	<i>fm:p</i>	The posterior most point on the frontomalar suture.
Marginal process lateral	<i>mpll</i>	The most posteriorly projecting point on the frontal process of the zygomatic bone.
Jugale	<i>jug</i>	The deepest point found at the notch between the temporal and frontal processes of the zygomatic bone.
Porion	<i>po</i>	The most superior point on the external acoustic meatus.

Table A2. Loadings associated with PC1 and PC2 for all landmarks to assess sexual dimorphism. Bold values indicate landmarks with the largest contribution.

Landmarks		PC1	PC2
<i>fm:p</i>	X	0.049	-0.049
	Y	-0.033	0.117
	Z	-0.046	0.016
<i>fm:a</i>	X	0.065	-0.046
	Y	-0.039	0.115
	Z	-0.029	-0.007
<i>mpll</i>	X	0.044	-0.098
	Y	0.002	-0.107
	Z	0.084	0.062
<i>ec</i>	X	0.048	0.013
	Y	-0.017	0.051
	Z	0.034	-0.020
<i>jug</i>	X	0.022	-0.227
	Y	0.003	-0.184
	Z	0.255	0.002
<i>zytinr</i>	X	0.007	-0.362
	Y	0.029	-0.140
	Z	0.280	0.083
<i>zytspl</i>	X	-0.020	-0.320
	Y	0.008	-0.195
	Z	0.276	-0.002
<i>zygool</i>	X	-0.082	0.375
	Y	0.014	0.028
	Z	-0.675	0.021
<i>zygoml</i>	X	0.020	0.401
	Y	0.071	0.238
	Z	0.218	0.023
<i>fnt</i>	X	0.042	-0.054
	Y	-0.041	0.121
	Z	0.045	0.028
<i>po</i>	X	-0.195	0.366
	Y	0.004	-0.043
	Z	-0.442	-0.206

Table A3. Loadings associated with PC1 and PC2 for all landmarks to assess sexual dimorphism of black South Africans. Bold values indicate landmarks with the largest contribution.

Landmarks		PC1	PC2
<i>fm:p</i>	X	0.041	0.001
	Y	-0.021	0.026
	Z	-0.016	-0.005
<i>fm:a</i>	X	0.051	-0.035
	Y	-0.054	0.116
	Z	-0.015	-0.022
<i>mpll</i>	X	-0.008	-0.104
	Y	0.022	-0.255
	Z	0.083	0.057
<i>ec</i>	X	0.033	-0.028
	Y	-0.015	0.101
	Z	0.014	-0.074
<i>jug</i>	X	0.025	-0.254
	Y	-0.030	-0.239
	Z	0.239	0.020
<i>zytinr</i>	X	-0.056	-0.227
	Y	-0.003	-0.048
	Z	0.234	0.066
<i>zytspl</i>	X	-0.003	-0.378
	Y	-0.001	-0.239
	Z	0.263	0.033
<i>zygool</i>	X	-0.009	0.327
	Y	0.062	0.162
	Z	-0.692	0.145
<i>zygoml</i>	X	0.060	0.266
	Y	0.093	0.196
	Z	0.278	0.019
<i>fnt</i>	X	0.020	0.005
	Y	-0.046	0.090
	Z	0.055	-0.026
<i>po</i>	X	-0.154	0.426
	Y	-0.008	0.090
	Z	-0.441	-0.212

Table A4. Loadings associated with PC1 and PC2 for all landmarks to assess sexual dimorphism of coloured South Africans. Bold values indicate landmarks with the largest contribution.

Landmarks		PC1	PC2
<i>fm:p</i>	X	0.024	0.037
	Y	-0.035	-0.180
	Z	-0.061	0.015
<i>fm:a</i>	X	0.059	0.011
	Y	-0.039	-0.038
	Z	-0.044	0.052
<i>mpll</i>	X	0.045	0.055
	Y	-0.032	0.102
	Z	0.078	-0.057
<i>ec</i>	X	0.046	-0.014
	Y	-0.003	-0.020
	Z	0.035	0.084
<i>jug</i>	X	0.001	0.240
	Y	0.003	0.162
	Z	0.274	-0.049
<i>zytinr</i>	X	0.025	0.347
	Y	0.048	0.097
	Z	0.328	-0.168
<i>zytspl</i>	X	-0.010	0.312
	Y	-0.0001	0.203
	Z	0.302	-0.086
<i>zygool</i>	X	-0.095	-0.511
	Y	0.009	-0.103
	Z	-0.644	-0.139
<i>zygoml</i>	X	0.034	-0.115
	Y	0.105	-0.090
	Z	0.148	0.091
<i>fnt</i>	X	0.040	0.015
	Y	-0.042	-0.064
	Z	0.038	-0.015
<i>po</i>	X	-0.168	-0.379
	Y	-0.012	-0.068
	Z	-0.455	0.272

Table A5. Loadings associated with PC1 and PC2 for all landmarks to assess sexual dimorphism of white South Africans. Bold values indicate landmarks with the largest contribution.

Landmarks		PC1	PC2
<i>fm:p</i>	X	-0.056	0.084
	Y	0.020	-0.137
	Z	0.032	-0.016
<i>fm:a</i>	X	-0.057	0.074
	Y	0.025	-0.130
	Z	0.010	-0.010
<i>mpll</i>	X	-0.066	0.070
	Y	-0.032	0.041
	Z	-0.093	-0.047
<i>ec</i>	X	-0.054	-0.012
	Y	0.032	-0.021
	Z	-0.039	-0.043
<i>jug</i>	X	-0.035	0.253
	Y	-0.034	0.156
	Z	-0.229	0.035
<i>zytinr</i>	X	0.020	0.228
	Y	-0.028	0.134
	Z	-0.255	-0.021
<i>zytspl</i>	X	0.043	0.271
	Y	-0.018	0.138
	Z	-0.260	0.060
<i>zygool</i>	X	0.075	-0.204
	Y	0.035	0.021
	Z	0.691	0.033
<i>zygoml</i>	X	-0.036	-0.660
	Y	-0.043	-0.264
	Z	-0.232	-0.028
<i>fnt</i>	X	-0.045	0.107
	Y	0.023	-0.156
	Z	-0.060	-0.040
<i>po</i>	X	0.210	-0.211
	Y	0.020	0.217
	Z	0.435	0.077

Table A6. Loadings associated with PC1 and PC2 for all landmarks to assess sexual dimorphism of Indian South Africans. Bold values indicate landmarks with the largest contribution.

Landmarks		PC1	PC2
<i>fm:p</i>	X	0.091	-0.135
	Y	-0.057	0.099
	Z	-0.064	0.014
<i>fm:a</i>	X	0.083	-0.079
	Y	-0.040	0.145
	Z	-0.025	-0.049
<i>mpll</i>	X	0.052	-0.144
	Y	-0.001	-0.162
	Z	0.067	0.133
<i>ec</i>	X	0.063	0.008
	Y	-0.023	0.084
	Z	0.051	-0.036
<i>jug</i>	X	0.035	-0.140
	Y	0.011	-0.214
	Z	0.234	0.075
<i>zytinr</i>	X	-0.040	-0.192
	Y	0.001	-0.163
	Z	0.273	0.0527
<i>zytspl</i>	X	-0.032	-0.201
	Y	0.008	-0.240
	Z	0.231	0.057
<i>zygool</i>	X	-0.141	0.494
	Y	0.033	0.024
	Z	-0.673	-0.004
<i>zygoml</i>	X	0.008	0.212
	Y	0.052	0.379
	Z	0.275	0.007
<i>fnt</i>	X	0.066	-0.138
	Y	-0.042	0.121
	Z	0.046	-0.010
<i>po</i>	X	-0.186	0.316
	Y	0.079	-0.072
	Z	-0.416	-0.239

Table A7. Loadings associated with PC1 and PC2 for all landmarks to assess ancestral variation. Bold values indicate landmarks with the largest contribution.

Landmarks		PC1	PC2
<i>fm:p</i>	X	0.049	-0.049
	Y	-0.033	0.117
	Z	-0.046	0.016
<i>fm:a</i>	X	0.065	-0.046
	Y	-0.039	0.115
	Z	-0.029	-0.007
<i>mpll</i>	X	0.044	-0.098
	Y	0.002	-0.107
	Z	0.084	0.062
<i>ec</i>	X	0.048	0.013
	Y	-0.017	0.051
	Z	0.034	-0.020
<i>jug</i>	X	0.022	-0.227
	Y	0.003	-0.184
	Z	0.255	0.002
<i>zytinr</i>	X	0.007	-0.362
	Y	0.029	-0.140
	Z	0.029	0.083
<i>zytspl</i>	X	-0.020	-0.320
	Y	0.008	-0.195
	Z	0.276	-0.002
<i>zygool</i>	X	-0.082	0.375
	Y	0.014	0.028
	Z	-0.675	0.021
<i>zygoml</i>	X	0.020	0.401
	Y	0.071	0.238
	Z	0.218	0.023
<i>fnt</i>	X	0.042	-0.054
	Y	-0.041	0.121
	Z	0.045	0.028
<i>po</i>	X	-0.195	0.366
	Y	0.004	-0.043
	Z	-0.442	-0.206

Table A8. Loadings associated with PC1 and PC2 for all landmarks to assess ancestral variation of male South Africans. Bold values indicate landmarks with the largest contribution.

Landmarks		PC1	PC2
<i>fm:p</i>	X	-0.044	-0.020
	Y	0.028	0.103
	Z	0.044	-0.004
<i>fm:a</i>	X	-0.057	-0.029
	Y	0.038	0.108
	Z	0.026	-0.027
<i>mpll</i>	X	-0.037	-0.101
	Y	0.002	-0.107
	Z	-0.083	0.073
<i>ec</i>	X	-0.038	0.009
	Y	0.022	0.023
	Z	-0.034	-0.067
<i>jug</i>	X	-0.023	-0.288
	Y	0.004	-0.237
	Z	-0.256	0.034
<i>zytinr</i>	X	0.020	-0.216
	Y	-0.031	-0.068
	Z	-0.288	0.081
<i>zytspl</i>	X	0.015	-0.406
	Y	-0.011	-0.228
	Z	-0.287	0.053
<i>zygool</i>	X	0.036	0.399
	Y	-0.031	0.109
	Z	0.666	0.104
<i>zygoml</i>	X	-0.007	0.316
	Y	-0.061	0.191
	Z	-0.205	-0.022
<i>fnt</i>	X	-0.037	-0.045
	Y	0.040	0.108
	Z	-0.051	-0.002
<i>po</i>	X	0.175	0.380
	Y	-0.001	-0.002
	Z	0.466	-0.223

Table A9. Loadings associated with PC1 and PC2 for all landmarks to assess ancestral variation of female South Africans. Bold values indicate landmarks with the largest contribution.

Landmarks		PC1	PC2
<i>fm:p</i>	X	0.061	-0.039
	Y	-0.046	0.109
	Z	-0.044	0.006
<i>fm:a</i>	X	0.081	-0.034
	Y	-0.041	0.083
	Z	-0.029	0.020
<i>mpll</i>	X	0.062	-0.060
	Y	0.012	-0.050
	Z	0.085	0.028
<i>ec</i>	X	0.068	0.009
	Y	-0.009	0.076
	Z	0.039	-0.001
<i>jug</i>	X	0.028	-0.202
	Y	0.023	-0.146
	Z	0.243	-0.021
<i>zytinr</i>	X	0.063	-0.434
	Y	0.025	-0.216
	Z	0.251	0.099
<i>zytspl</i>	X	-0.027	-0.291
	Y	0.004	-0.168
	Z	0.244	-0.040
<i>zygool</i>	X	-0.189	0.257
	Y	-0.023	0.024
	Z	-0.681	-0.059
<i>zygoml</i>	X	0.040	0.516
	Y	0.082	0.227
	Z	0.239	0.092
<i>fnt</i>	X	0.055	-0.037
	Y	-0.042	0.094
	Z	0.035	0.057
<i>po</i>	X	-0.243	0.315
	Y	0.016	-0.034
	Z	-0.382	-0.181

Appendix II

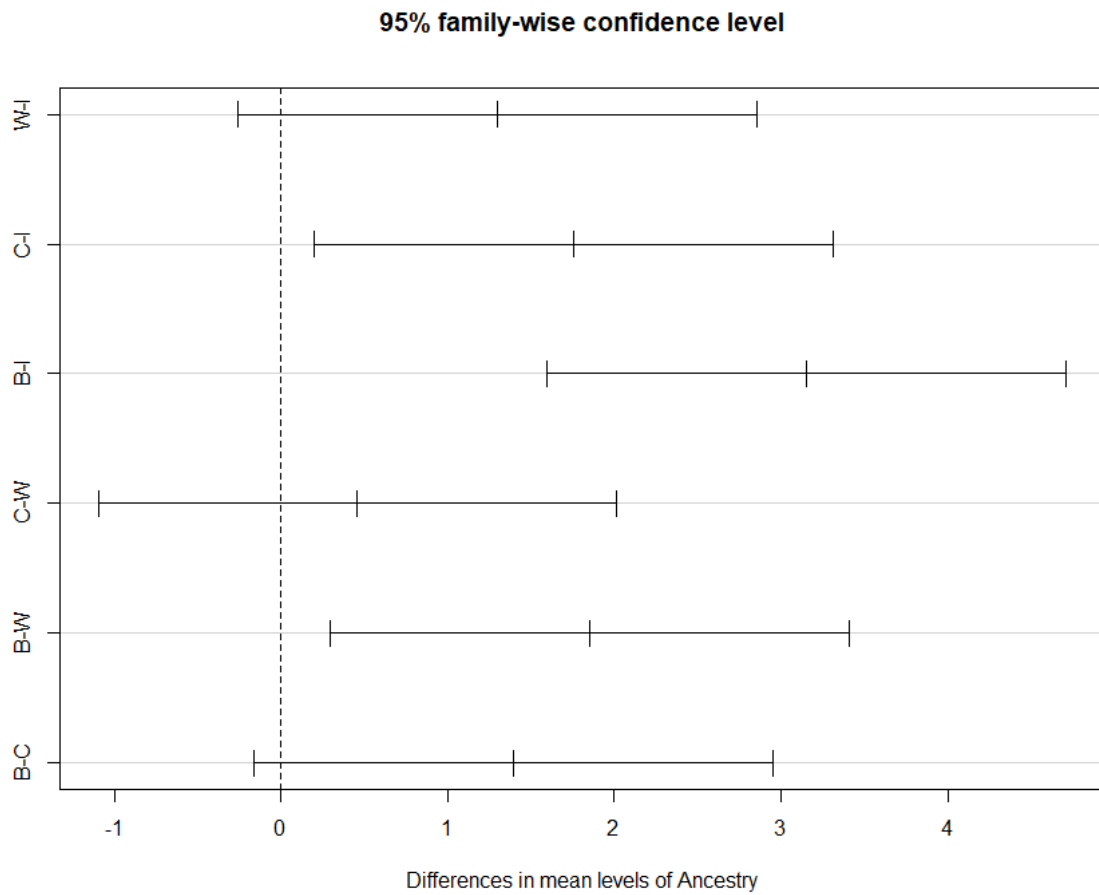


Figure A1. Tukey's HSD plots depicting statistically significant overlap between groups for ancestry when males and females were combined looking at PorZygoml (B = Black; C = Coloured; W = White; I = Indian).

95% family-wise confidence level

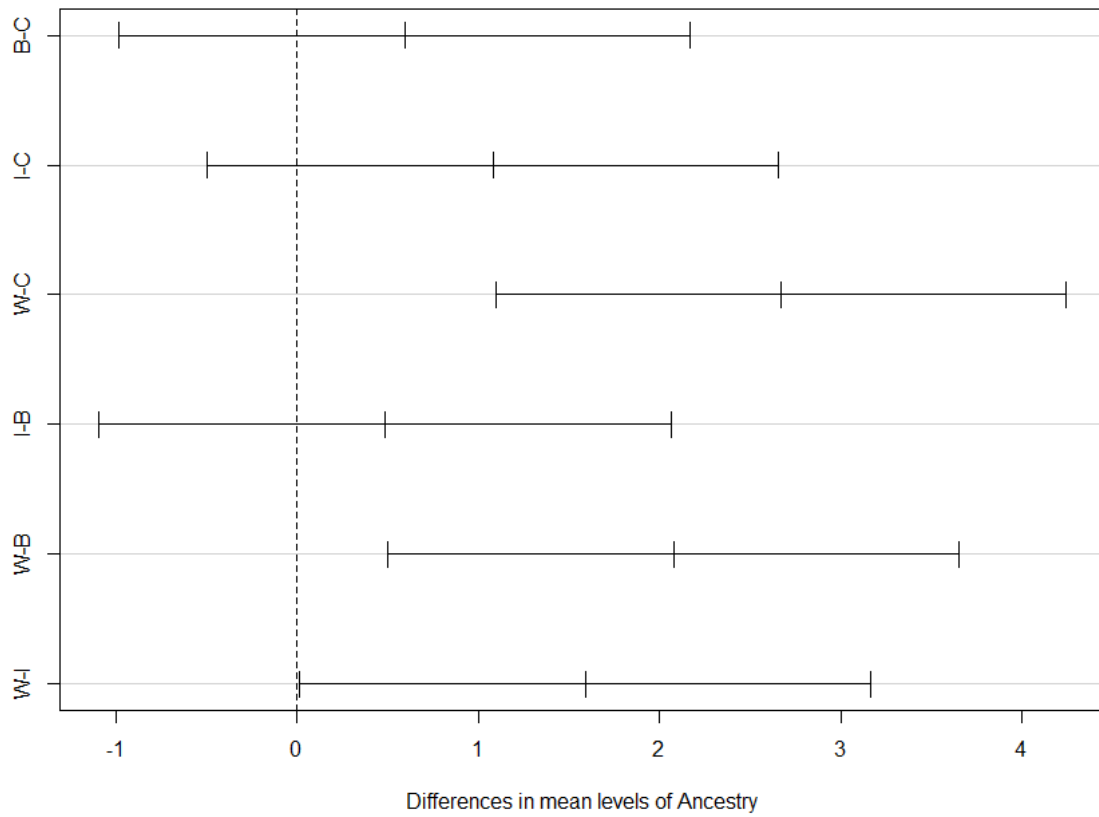


Figure A2. Tukey's HSD plots depicting statistically significant overlap between groups for ancestry when males and females were combined looking at ZML (B = Black; C = Coloured; W = White; I = Indian).

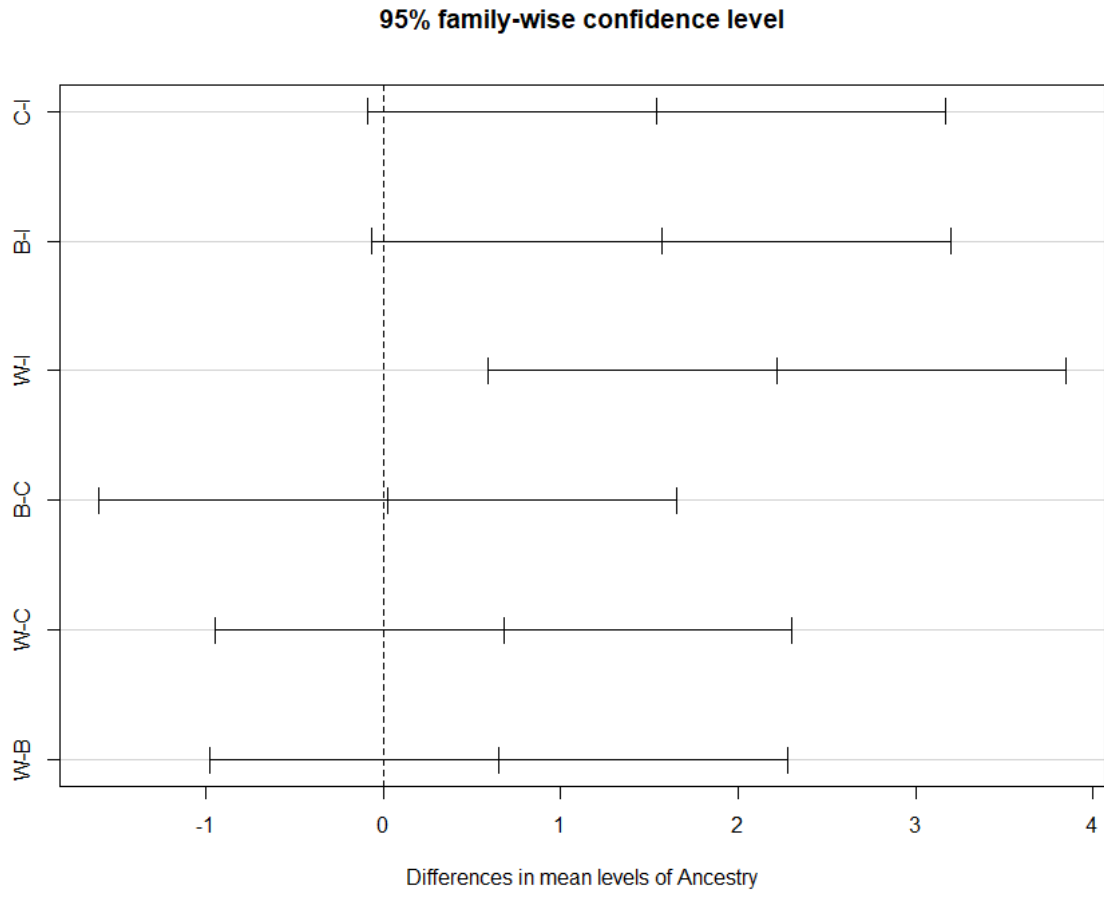


Figure A3. Tukey's HSD plots depicting statistically significant overlap between groups for ancestry when males and females were combined looking at PorZygool (B = Black; C = Coloured; W = White; I = Indian).

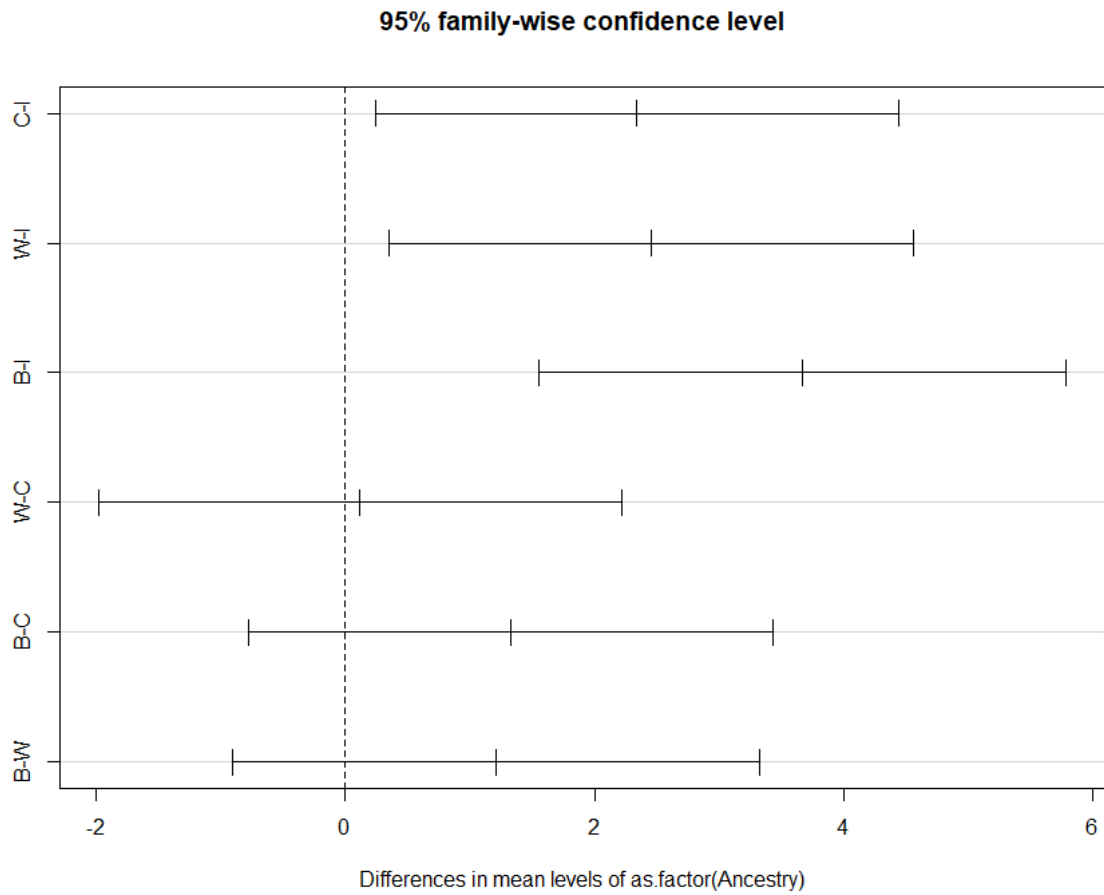


Figure A4. Tukey's HSD plots depicting statistically significant overlap between groups for ancestry of male South Africans looking at PorZygoml (B = Black; C = Coloured; W = White; I = Indian).

95% family-wise confidence level

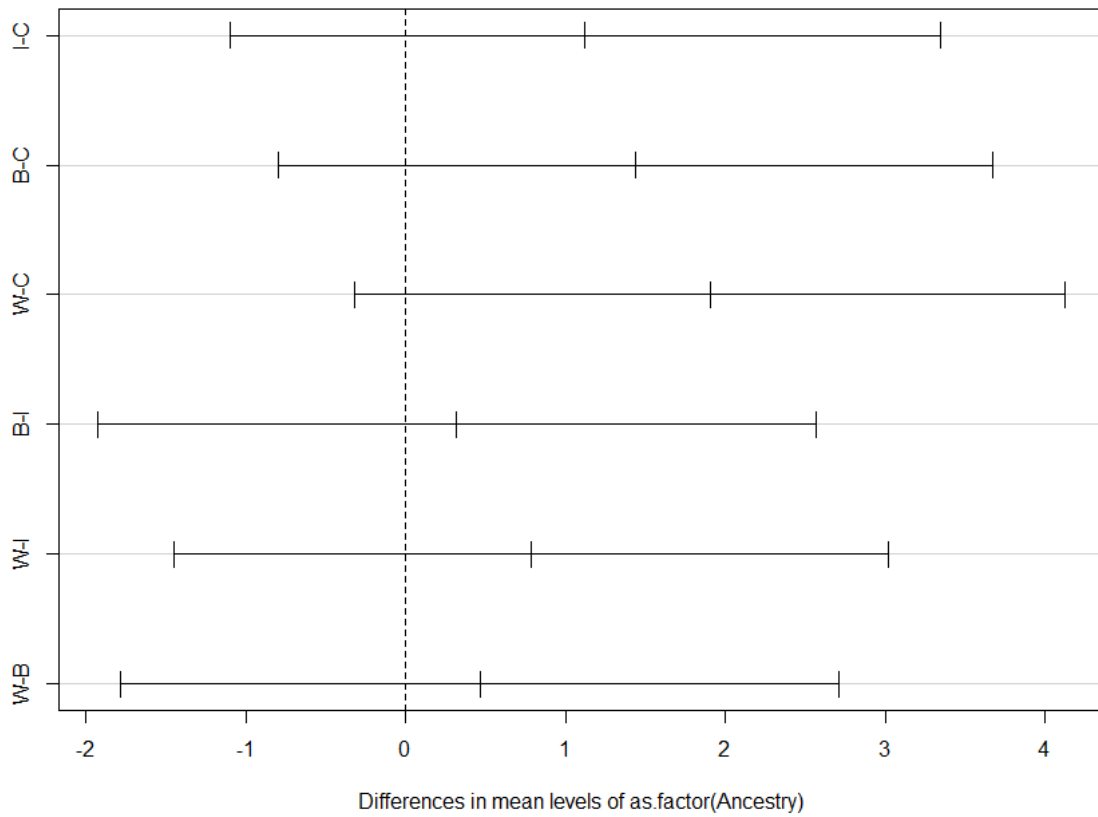


Figure A5. Tukey's HSD plots depicting statistically significant overlap between groups for ancestry of male South Africans looking at ZML (B = Black; C = Coloured; W = White; I = Indian).

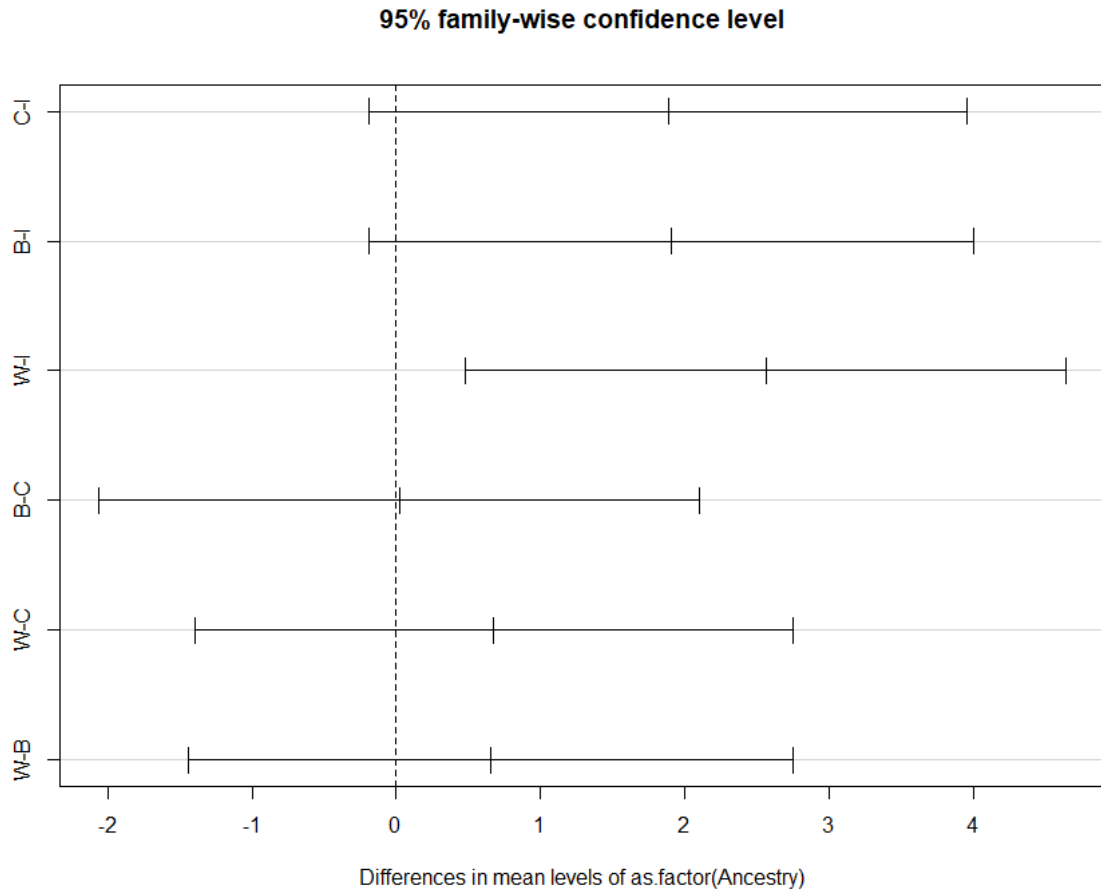


Figure A6. Tukey's HSD plots depicting statistically significant overlap between groups for ancestry of male South Africans looking at PorZygool (B = Black; C = Coloured; W = White; I = Indian).

95% family-wise confidence level

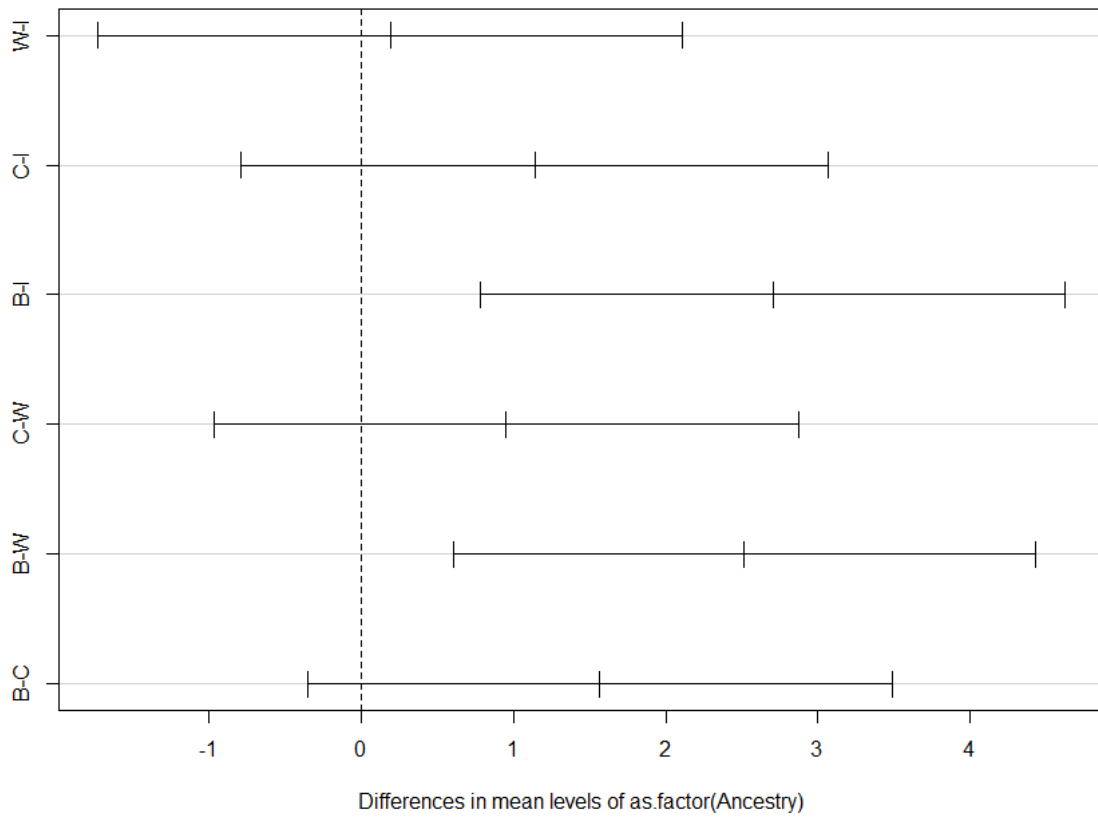


Figure A7. Tukey's HSD plots depicting statistically significant overlap between groups for ancestry of female South Africans looking at *PorZygoml* (*B* = Black; *C* = Coloured; *W* = White; *I* = Indian).

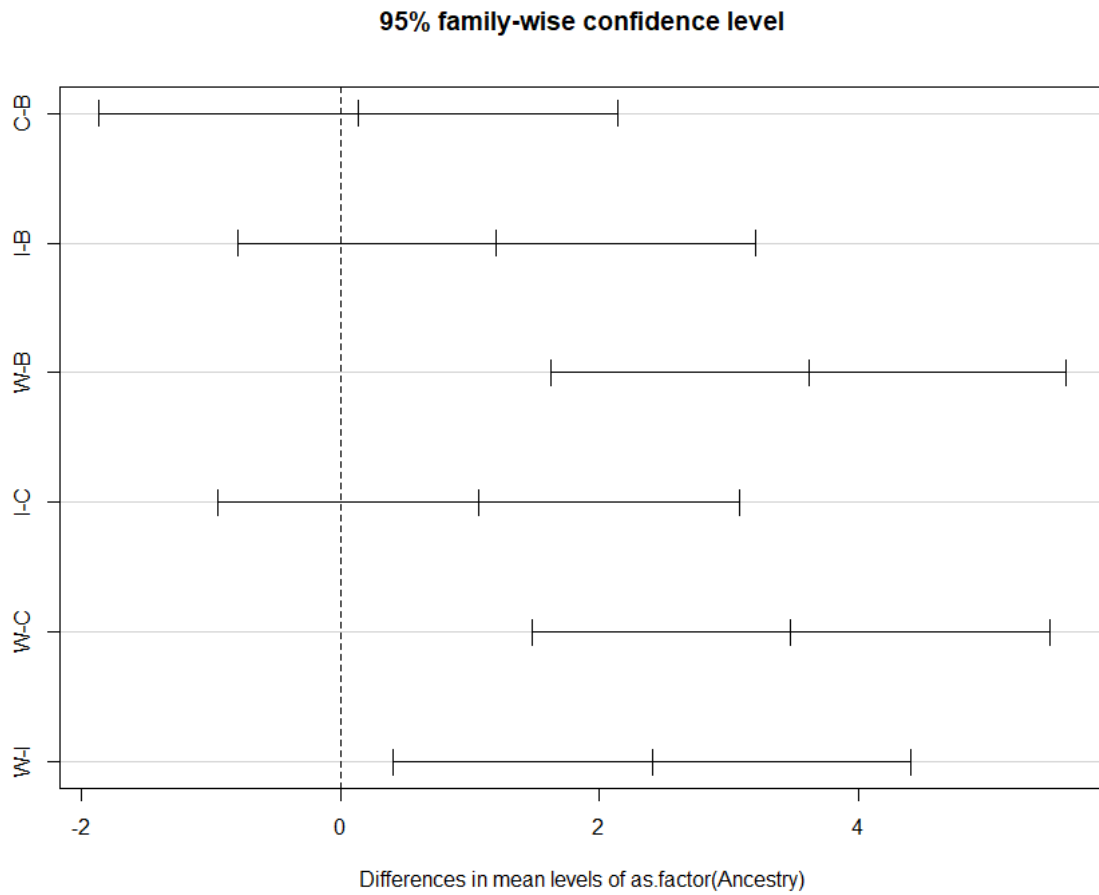


Figure A8. Tukey's HSD plots depicting statistically significant overlap between groups for ancestry of female South Africans looking at ZML (B = Black; C = Coloured; W = White; I = Indian).

95% family-wise confidence level

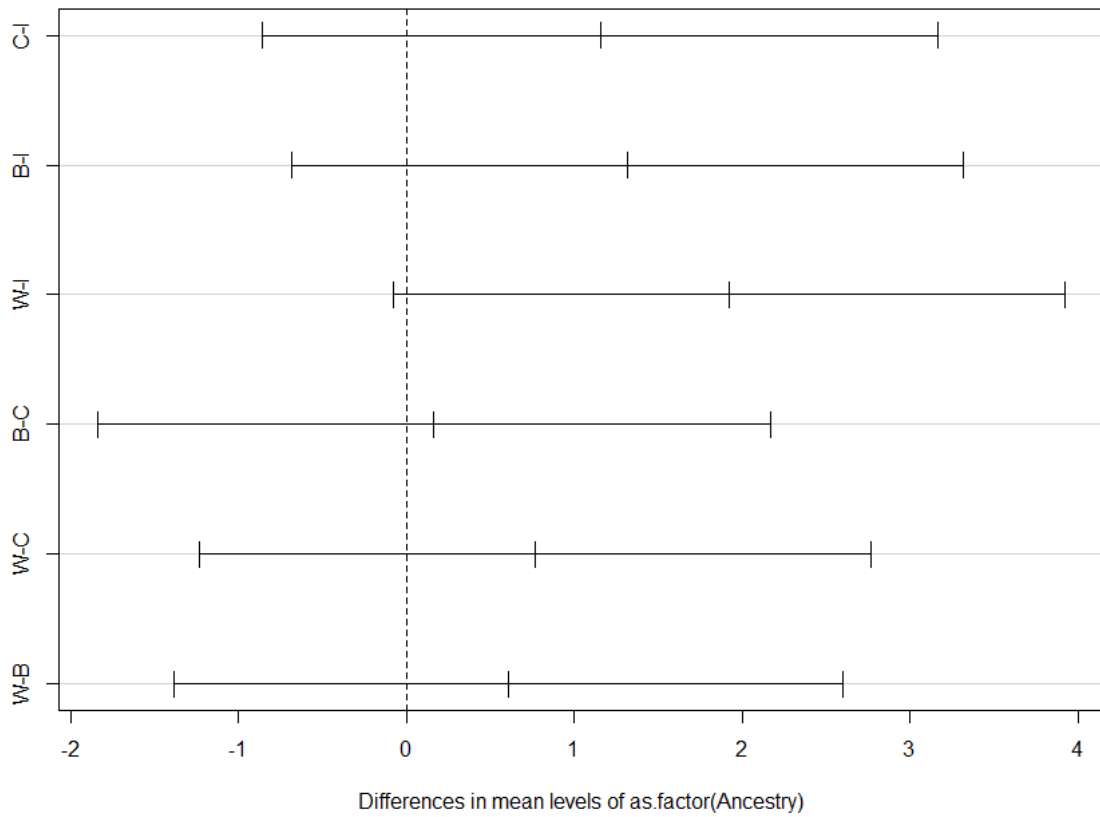


Figure A9. Tukey's HSD plots depicting statistically significant overlap between groups for ancestry of female South Africans looking at PorZygool (*B* = Black; *C* = Coloured; *W* = White; *I* = Indian).

95% family-wise confidence level

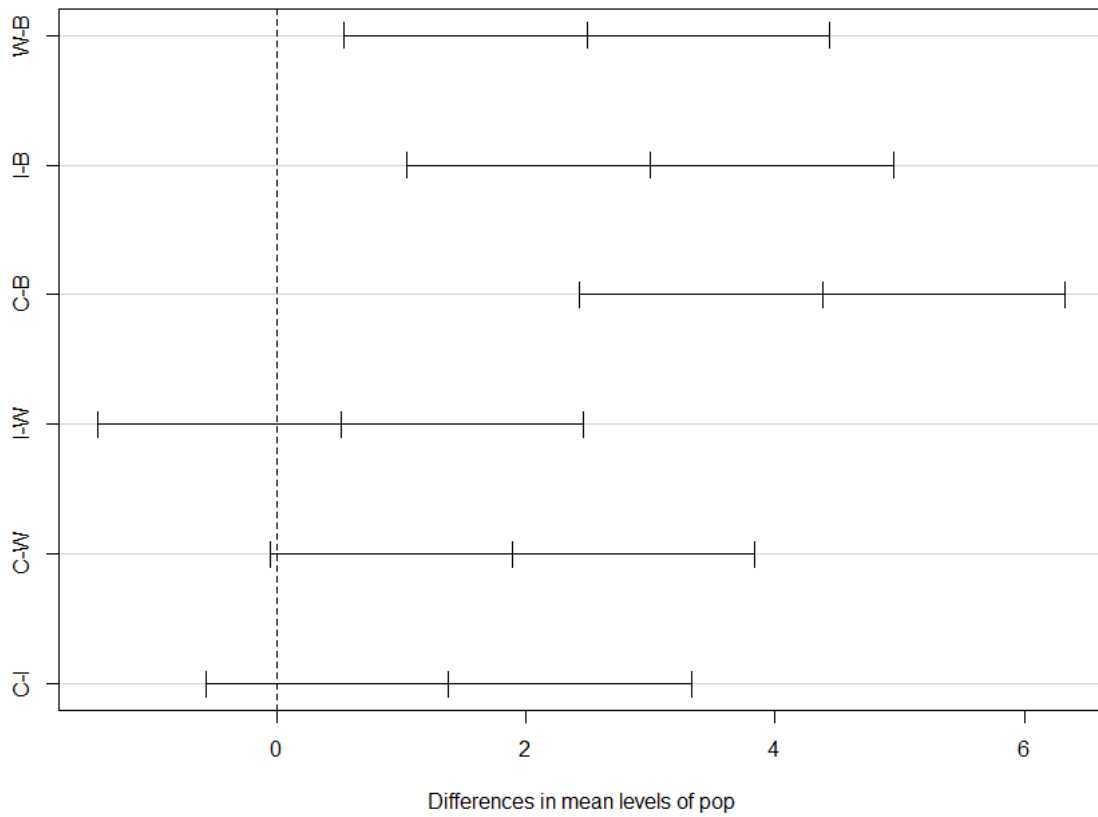


Figure A10. Tukey's HSD plots depicting statistically significant overlap between groups for ancestry when males and females were combined looking at Angle1 (B = Black; C = Coloured; W = White; I = Indian).

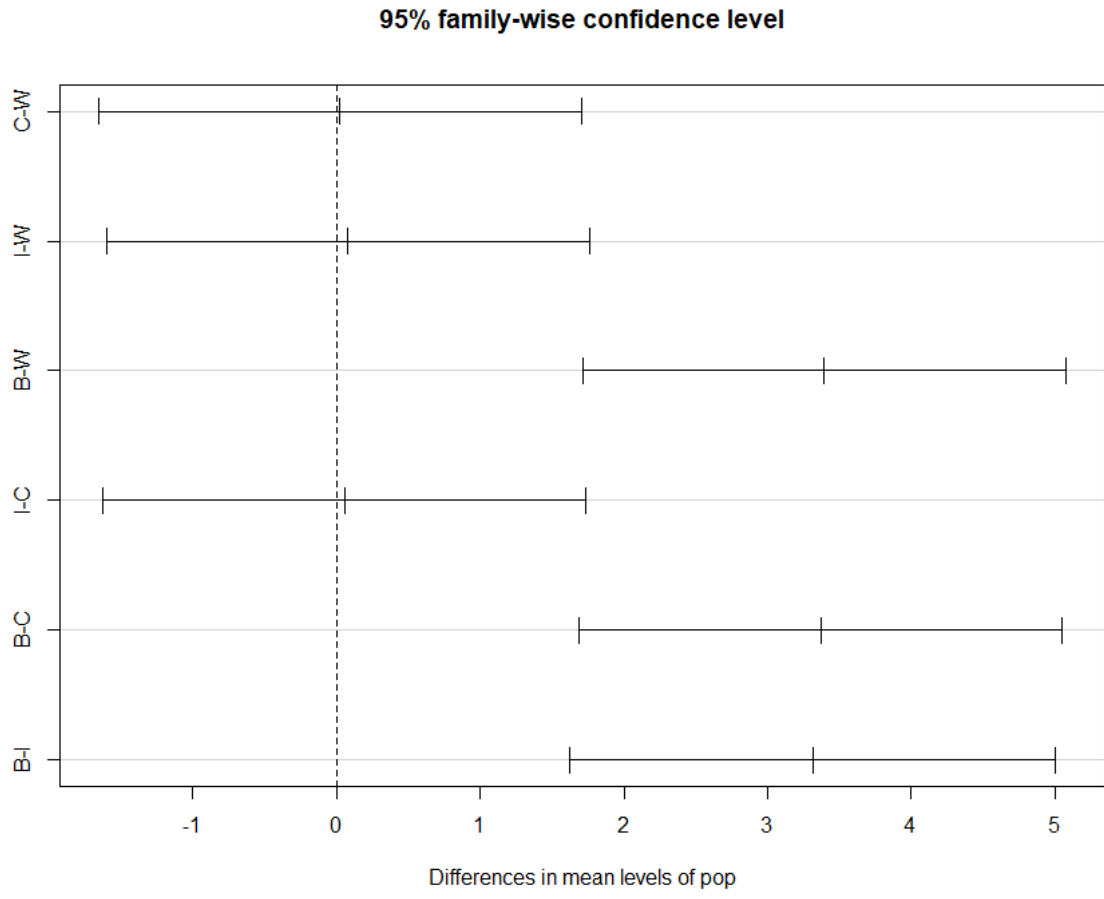


Figure A11. Tukey's HSD plots depicting statistically significant overlap between groups for ancestry when males and females were combined looking at Angle2 (B = Black; C = Coloured; W = White; I = Indian).

95% family-wise confidence level

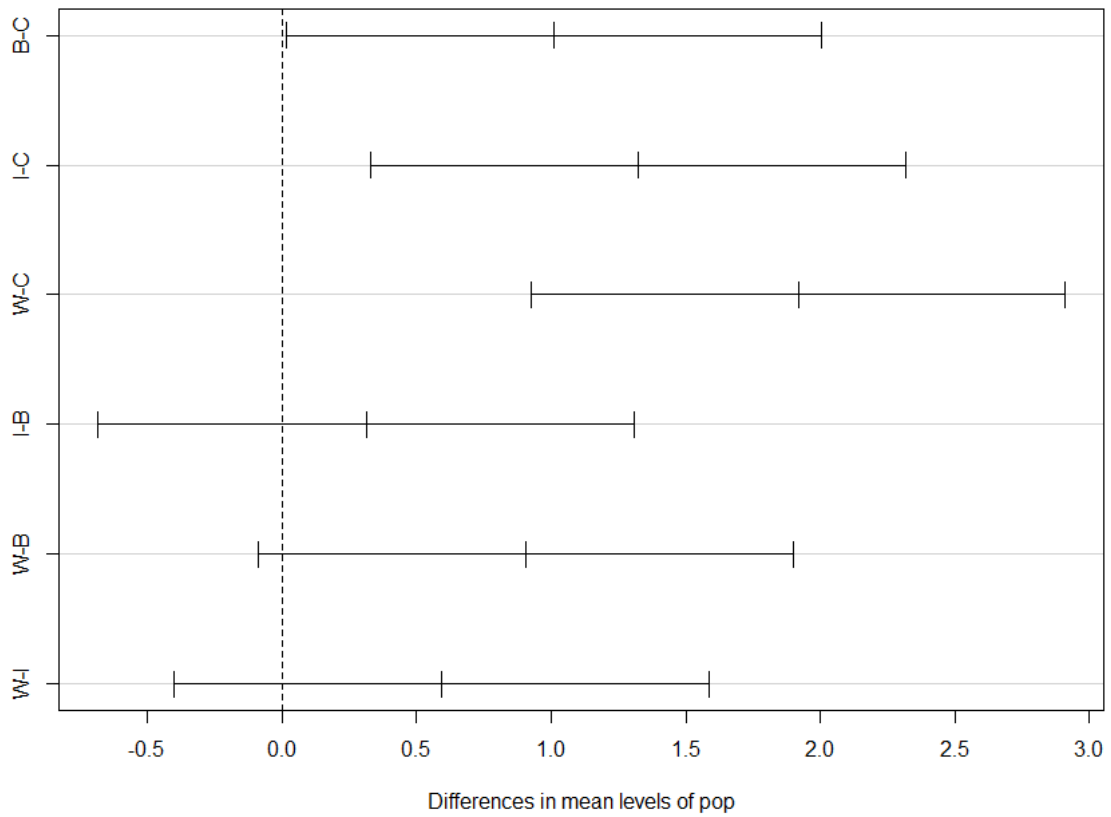


Figure A12. Tukey's HSD plots depicting statistically significant overlap between groups for ancestry when males and females were combined looking at Angle3 (B = Black; C = Coloured; W = White; I = Indian).

95% family-wise confidence level

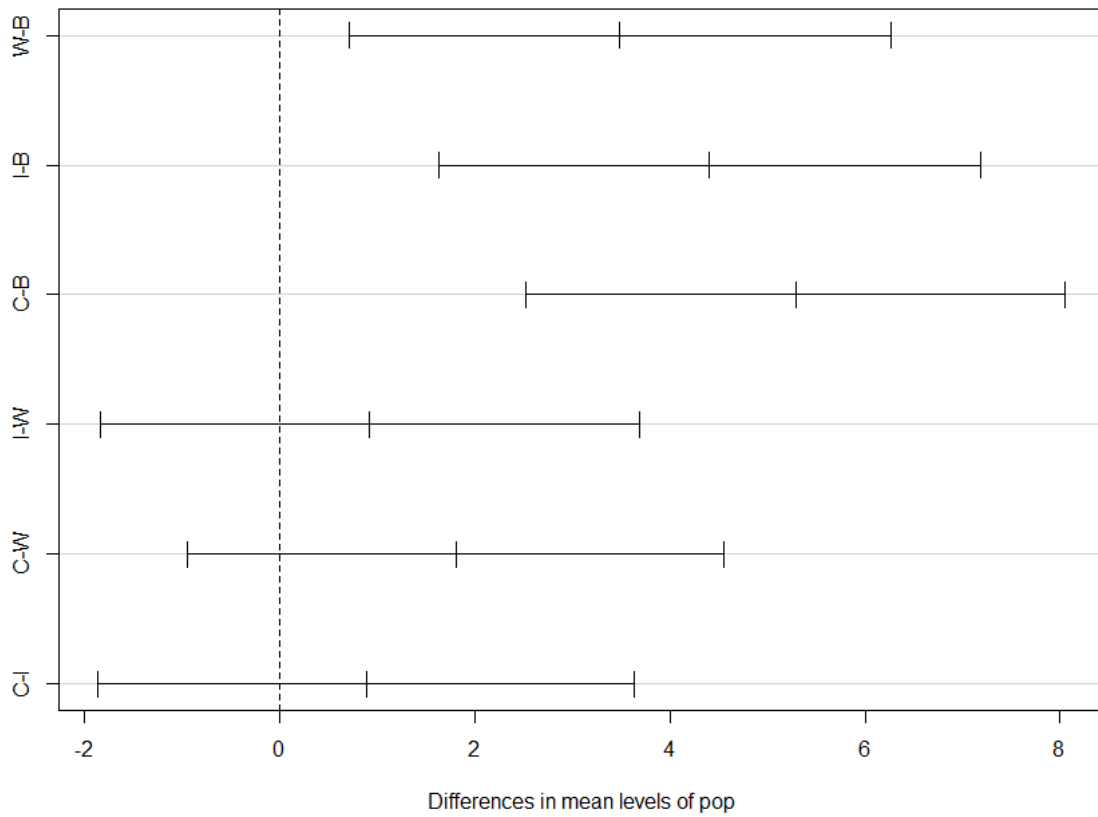


Figure A13. Tukey's HSD plots depicting statistically significant overlap between groups for male South Africans when looking at Angle1 (*B* = Black; *C* = Coloured; *W* = White; *I* = Indian).

95% family-wise confidence level

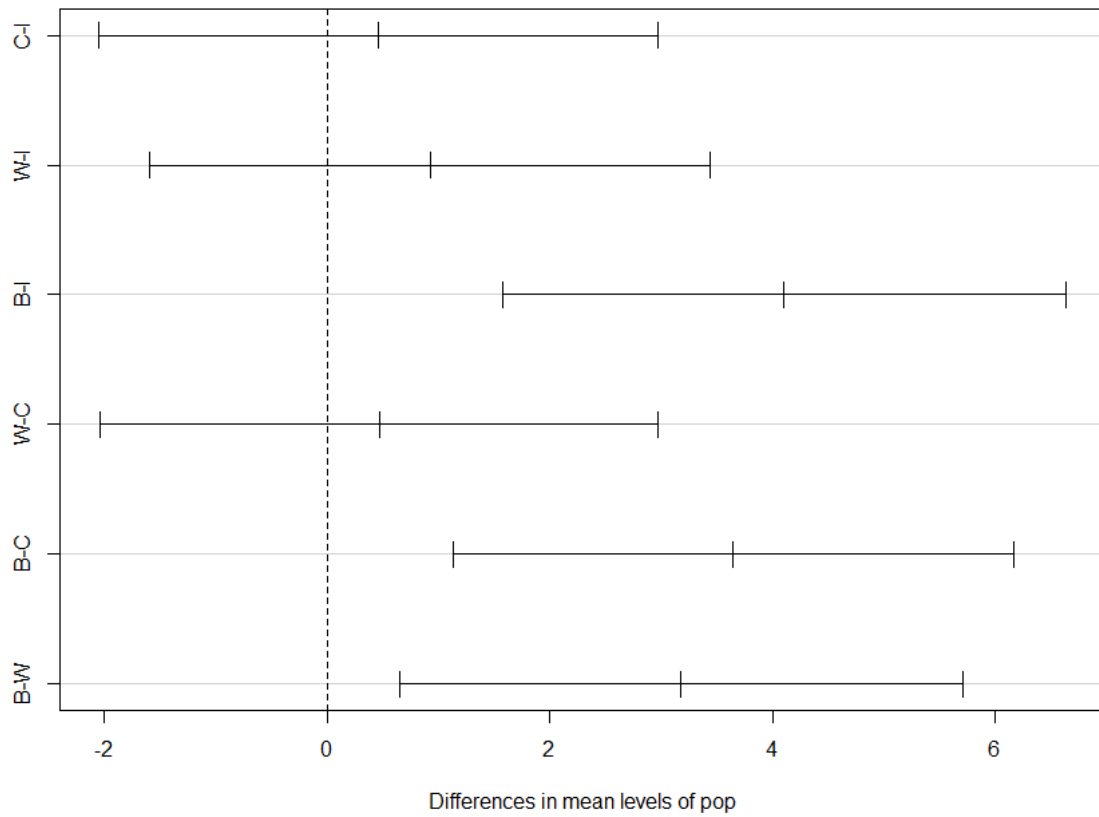


Figure A14. Tukey's HSD plots depicting statistically significant overlap between groups for male South Africans when looking at Angle2 (B = Black; C = Coloured; W = White; I = Indian).

95% family-wise confidence level

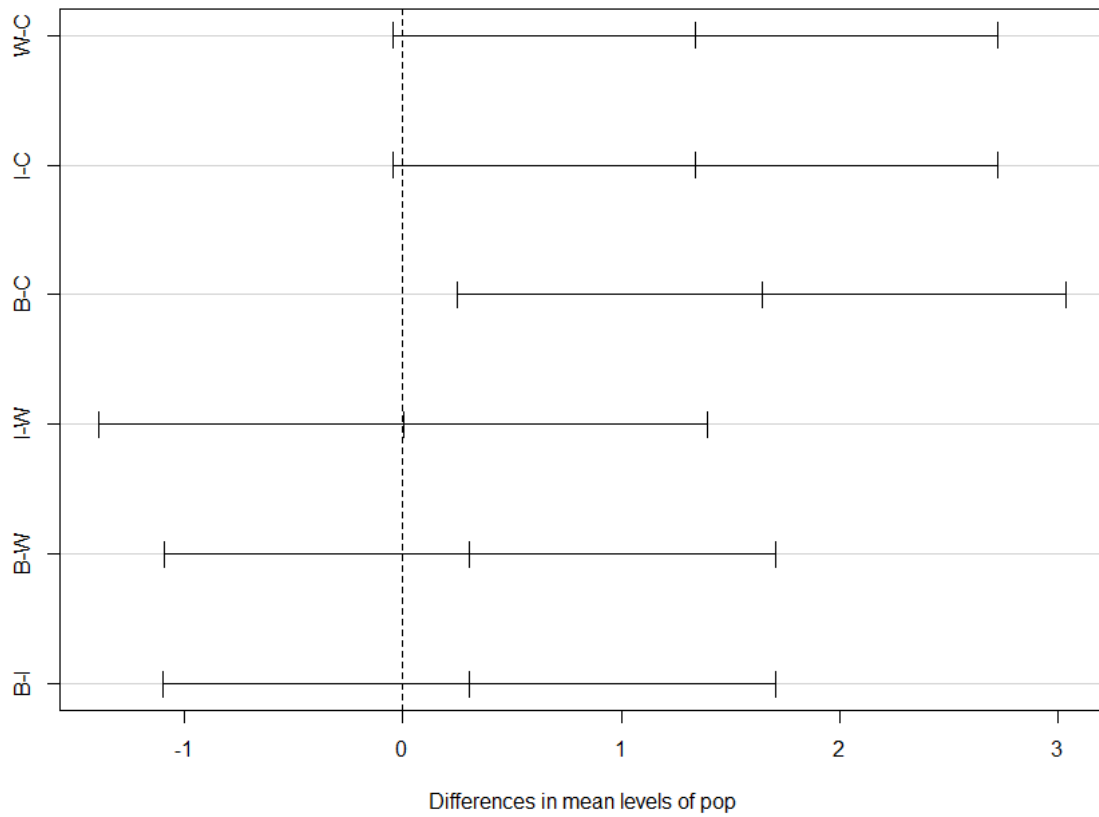


Figure A15. Tukey's HSD plots depicting statistically significant overlap between groups for male South Africans when looking at Angle3 (B = Black; C = Coloured; W = White; I = Indian).

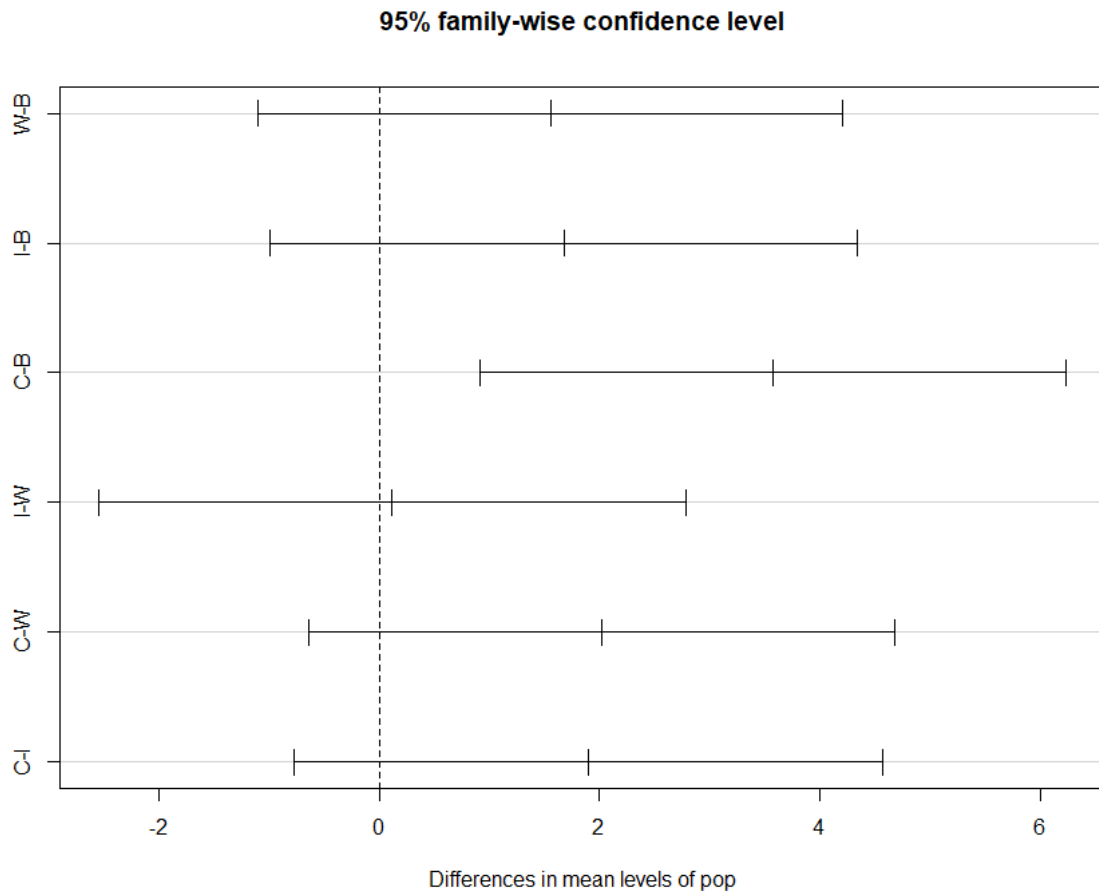


Figure A16. Tukey's HSD plots depicting statistically significant overlap between groups for female South Africans when looking at Angle1 (B = Black; C = Coloured; W = White; I = Indian).

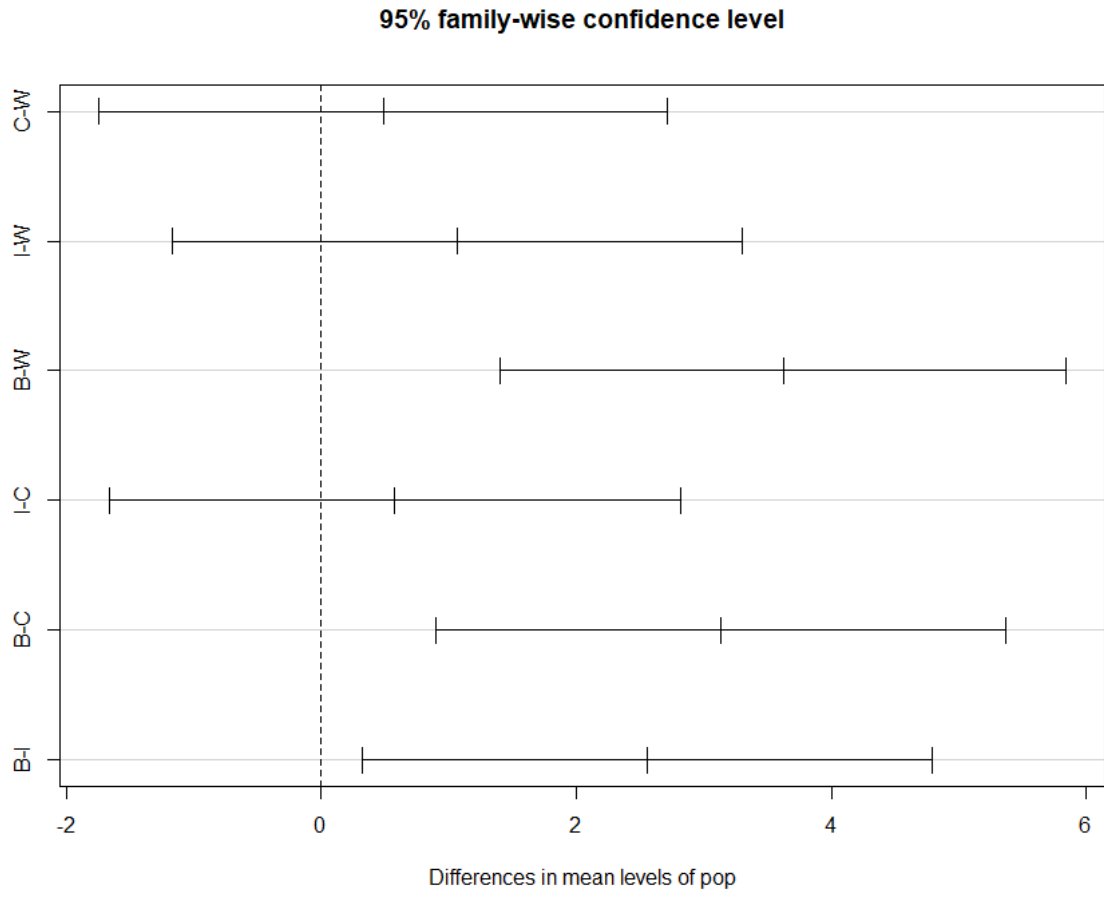


Figure A17. Tukey's HSD plots depicting statistically significant overlap between groups for female South Africans when looking at Angle2 (B = Black; C = Coloured; W = White; I = Indian).

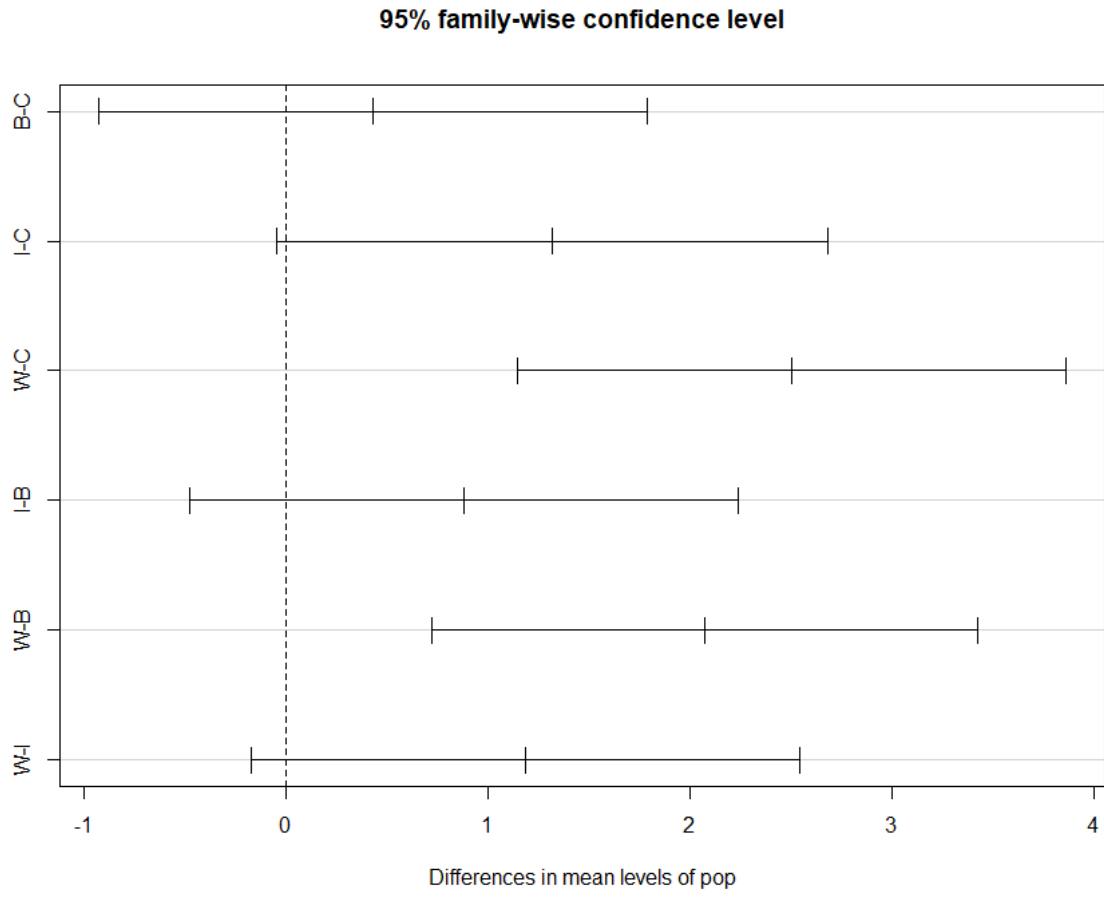


Figure A18. Tukey's HSD plots depicting statistically significant overlap between groups for female South Africans when looking at Angle3 (B = Black; C = Coloured; W = White; I = Indian).



Faculty of Health Sciences

Institution: The Research Ethics Committee, Faculty Health Sciences, University of Pretoria complies with ICH-GCP guidelines and has US Federal wide Assurance.
• FWA 00002587 Approved and 22 May 2000 and Expires 03/30/2022.
• ORG #: IORG002762 OMB No. 080 0279 Approved for use through February 20, 2022 and expires: 03/04/2023.

20 July 2020

Approval Certificate Annual Renewal

Ethics Reference No.: 432/2019

Title: Shape analysis of the zygoma to assess ancestry and sex variation in modern South Africans

Dear Miss S Muller

The Annual Renewal as supported by documents received between 2020-06-22 and 2020-07-15 for your research, was approved by the Faculty of Health Sciences Research Ethics Committee on its quorate meeting of 2020-07-15.

Please note the following about your ethics approval:

- Renewal of ethics approval is valid for 1 year, subsequent annual renewal will become due on 2021-07-20.
• Please remember to use your protocol number (432/2019) on any documents or correspondence with the Research Ethics Committee regarding your research.
• Please note that the Research Ethics Committee may ask further questions, seek additional information, require further modification, monitor the conduct of your research, or suspend or withdraw ethics approval.

Ethics approval is subject to the following:

- The ethics approval is conditional on the research being conducted as stipulated by the details of all documents submitted to the Committee. In the event that a further need arises to change who the investigators are, the methods or any other aspect, such changes must be submitted as an Amendment for approval by the Committee.

We wish you the best with your research.

Yours sincerely

Dr R Sommers
MBChB MMed (Int) MPharmMed PhD
Deputy Chairperson of the Faculty of Health Sciences Research Ethics Committee, University of Pretoria

The Faculty of Health Sciences Research Ethics Committee complies with the SA National Act 61 of 2003 as it pertains to health research and the United States Code of Federal Regulations Title 45 and 46. This committee abides by the ethical norms and principles for research, established by the Declaration of Helsinki, the South African Medical Research Council Guidelines as well as the Guidelines for Ethical Research: Principles Structures and Processes, Second Edition 2016 (Department of Health)